EARLY-STAGE ASSESSMENT OF OUTDOOR COMFORT, SOLAR POTENTIAL AND BUILDING FORM IN URBAN ENVIRONMENTS

- A CASE STUDY IN NEW YORK CITY -

POLO TERRITORIALE DI LECCO
SCHOOL OF ARCHITECTURE URBAN PLANNING CONSTRUCTION ENGINEERING
MASTER'S DEGREE IN ARCHITECTURAL ENGINEERING
ACADEMIC YEAR 2020-2021

SUPERVISOR:
GABRIELE MASERA

CO-SUPERVISORS:
SIMONE GIOSTRA
ANDREA GIOVANNI MAININI

CANDIDATE:
LUDOVICA ROSSI

Acknowledgements

I would like to give special thanks to Professor Gabriele Masera, supervisor of this thesis, for the help he gave me, with his constant friendly availability. I would also like to thank Professor Simone Giostra, co-supervisor of the work, without whom this whole collaboration would not have been possible: it was a pity not to be able to leave for New York, but I think that an interesting confrontation was born anyway. Lastly, thanks also to Prof. Andrea Giovanni Mainini, co-supervisor too, for all his precious advices, and to Rafaella, working on the complementary research project, that have been an example and constant source of ispirtation.

Lastly, a special mention is deserved by all my colleagues of the Arup Italy Office, in particular the "MEP and Sustainability" team, because, with their commitment and above all their passion for job, they provided me not only knowledge, but also the strength to continue researching.

Abstract (English)

In the coming decades, sustainable urban planning will face two major challenges: first, the impact of climate change and, second, that of urbanization and the necessity of balancing the various conflicting spatial demands. The urban setting, due to the presence of more asphalt than greenery, CO2 emissions from vehicles and climatization systems of buildings can exacerbate the impact of this exposure on a local scale. Therefore, the expansion of urban centers affects global warming. This phenomenon is called Urban Heat Island and can determinate an increase of temperature in the cities.

Having in mind the climate issue, the present study aims to propose a way to approach the theme of the urban Outdoor Comfort, especially related to summer conditions and so to high temperatures, focusing on Buildings Forms - to be intended as pure geometry - in the very early-stages of the architectural design. The main question is how the conformation of the urban built environment - under a purely geometrical point of view - can influence temperature fluctuations. To achieve this result, the focus will be on three main building typologies, namely: tower, bar, and courtyard (iterated in base dimensions and height) with the purpose to cover all possible variables of existing and new buildings. Typologies were compared based on the offered Outdoor Comfort according to a first indicator, called UTCI (Universal Thermal Climate Index), which takes into account, in addition to temperature, humidity, solar radiation, wind speed and solar radiation. It was observed that, in a summer scenario, solar radiation tends to be the determining factor, and, consequently, solutions with a greater presence of shade, are the favorites in terms of UTCI. To counterbalance this aspect and stress on the importance of solar energy (e.g., for heating, lighting, energy generation, DHW, etc.), Solar Potential (kWh/m2year), intended as the capability of the envelope to catch radiation, has been chosen as a proxy to also express the positive effects of a beneficial annual solar exposure.

These two will be combined to identify the winning typologies (the "Champions") and relative base dimensions. From the analysis was noticed that courtyards perform the best for both indicators. Worst performances, indeed, are obtained by the tower, while the bar has been identified as the more adaptable typology, showing the highest number of shape and dimensions variations in the selected indicators' ranges.

Abstract (Italian)

In futuro, lo sviluppo urbano sostenibile dovrà affrontare due importanti sfide: la prima, mitigare le conseguenze del cambiamento climatico; la seconda, dover soddisfare la crescente richiesta di urbanizzazione a scopi commerciali e residenziali. La maggioranza di superfici asfaltate rispetto alle verdi, le emissioni di CO2 di veicoli, impianti industriali, sistemi di riscaldamento e aria condizionata ad uso domestico sono le maggiori cause di accumulo termico urbano. Pertanto, l'espansione dei centri urbani incide notevolmente sull'entità del riscaldamento globale. Tale fenomeno è denominato Isola di Calore Urbana e determina l'aumento delle temperature.

Con l'obiettivo di trovare una soluzione al problema, il presente lavoro di ricerca propone un approccio nuovo al tema del Comfort esterno in ambito urbano, specialmente in merito alle condizioni estive e alla mitigazione di alte temperature, focalizzandosi sulla Forma, intesa in termini puramente geometrici, degli edifici. La principale domanda è: come può la conformazione del contesto urbano influenzare le fluttuazioni di temperatura?
Al fine di rispondere a questo interrogativo tre principali tipologie di edifici sono state identificate, propriamente: edifici a torre, in linea e a corte. Tali "prototipi", nonché le rispettive iterazioni in termini di dimensioni di base e altezza, sono stati selezionati al fine di coprire il più ampio spettro possibile di variabili edilizie. Esse sono state confrontate sulla base del comfort esterno offerto in base a un primo indicatore, definito UTCI (Universal Thermal Climate Index), tenente conto, oltre che della temperatura, anche di umidità, radiazione solare, velocità del vento e radiazione solare.
È stato osservato che, in uno scenario estivo, la radiazione solare tende ad essere il fattore determinante, e, di conseguenza, soluzioni con maggior presenza di ombra, sono le favorite in termini di UTCI. Al fine di controbilanciare questo aspetto e per sottolineare l'importanza dell'energia solare (per riscaldamento, produzione di energia elettrica rinnovabile, acqua calda sanitaria, etc.), il Potenziale Solare (in kWh/m2 anno) è stato selezionato come secondo indicatore. Esso fungerà quindi da "proxy" per gli effetti benefici dell'esposizione solare degli edifici.

I due parametri solo quindi stati combinati e ne è derivata una lista di tipologie "vincenti", e relative dimensioni di base. Dall'analisi è risultato che la forma a cortile è quella che offre maggiori benefici per entrambi gli indicatori. Al contrario, la torre ottiene risultati peggiori di tutti. La barra, infine, mostra di essere la tipologia più flessibile, mostrando il più alto numero di variabili dimensionali nei range considerati.

Table of Contents

Table of Figures

1 Introduction

Climate Change and Urban Heat Island

In the coming decades, sustainable urban planning faces two major challenges: first, the impact of climate change and the necessity for adaptation measures to mitigate the consequences, and second, that of urbanization and the necessity of balancing the various conflicting spatial demands. Climate change projections suggest that summer heatwaves will become more frequent and severe during this century, consistent with the observed trend of the past decades [1].

While rural areas will generally be exposed to the same change in regional climate as the surrounding area, the urban setting can exacerbate the impact of this exposure on a local scale. Besides this, urbanization will continue in the following decades [2]. Both factors can therefore be decisive in influencing the climatic conditions of the urban environment and consequently affect the comfort of citizens and the livability of the cities.

This type of phenomenon has been define as Urban Heat Island effect.

As stated before, the presence of many buildings and artificial surfaces at the expense of open ground, open water and vegetation creates unique local climates altering temperature, moisture, wind patterns, and radiation. Consequently, local climate may vary considerably within cities [5].

But what is Urban Heat Island in reality and why it is so important for urban outdoor comfort? This effect is simply defined as higher temperatures within urban areas compared to their surroundings [6] [7]. Generally, it is

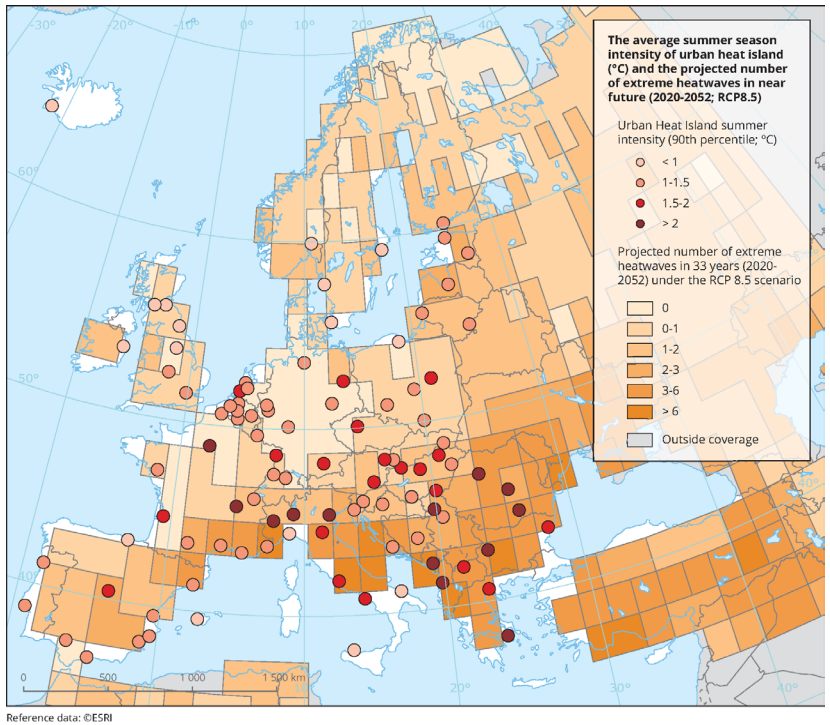

Fig. 85 Map presenting the projected number of extreme heatwaves in the near future across Europe and the summer intensity of the urban heat island effect in 100 European cities [4].

a result of urbanization that is most likely triggered by industrialization [8] causing structural and land cover changes in urban areas [9]. The UHI is induced by a combination of factors, including street canyon geometry, the amount of artificial surfaces with increased emissivity, and also anthropogenic heat production [6]. This phenomenon appears in almost every urban area, no matter whether the specific city is small or large, or whether it is situated in a warm or cold climate [9]. In the future the urban climate will likely be affected by additional summery heat load due to climate change, associated with the increase of heat waves of higher intensities and longer duration [10]. One major effect of UHIs is the increase of human discomfort, especially in the inner-cities well documented by urban heat stress studies [11]; [12]; [13].

Thermal comfort is defined by the ISO International Standard 7730 (1984, revided 1990) as "that condition of mind which expresses satisfaction with the thermal environment". Since the 1980s, studies of thermal comfort in the outdoor environment have grown in number because of increased attention for pedestrians in urban canyons, plazas and squares.

To ensure an effective and coherent development of adaptation strategies aimed at improvement of the urban thermal environment, a better understanding of the spatial and temporal variability in local climate (intra-urban variability), and the influence of urban features thereon is needed [5]. In fact, outdoor thermal comfort is often implicitly linked with the UHI phenomenon [14].

Human thermal comfort not only depends on air temperature but on the combined effect of air temperature, wind speed, air humidity and radiation [15].

Air temperature alone is not an appropriate measure to quantify the intra-urban spatial variability of climate concerning human thermal comfort. An increase of the built-up area at the expense of natural surfaces like vegetation, open ground or water causes a change in the surface energy balance

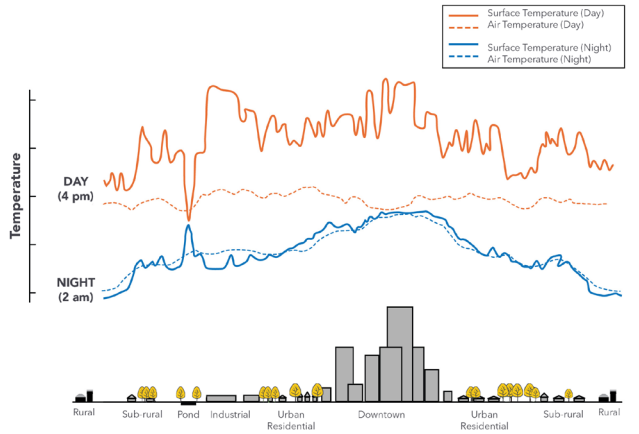

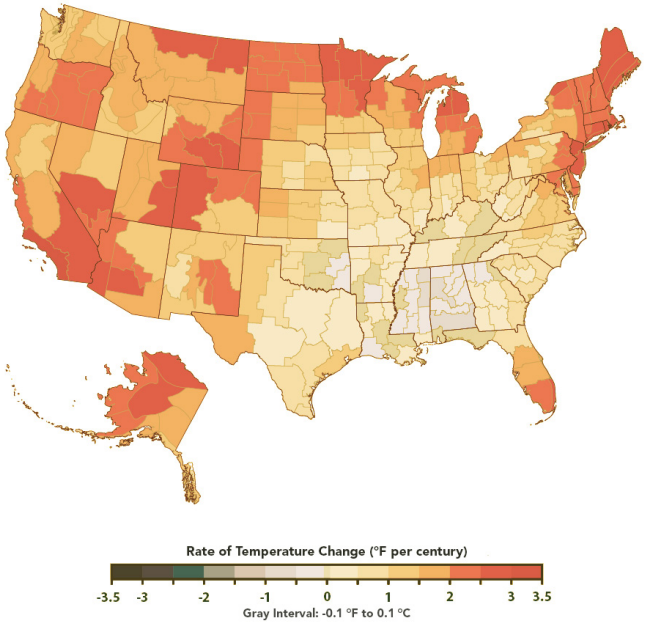

Fig. 86 An illustration from the U.S. Environmental Protection Agency highlighting the impact of different land uses to the air and surface temperatures of a city [3].
Fig. 87 Rate of temperature Change in the United States, 1901-2015 (Source: NOAA (National Oceanic and Atmospheric Administration) [17]

resulting into higher surface and air temperatures. Urban geometry relating to the height and spacing of buildings is considered to be another important feature determining local climate because of its effect on radiation and air flow. Important parameters are the surface albedo, mean building height, ratio between mean building height and mean street width (height-width ratio or aspect ratio), and the sky view factor [16].

In the past years, the impact of land cover buildings, impervious and green surfaces, on local air temperatures has been well documented. Similarly, the influence of the materials chosen for building envelopes and exterior surfaces has also been extensively tested. It is enough to see the conspicuous presence of published material on the greening of the urban fabric [18], or the studies conducted on the reflectivity of materials used for roofs, facades and urban surfaces in general.

Purpose of the study

Having in mind the climate issues expressed in the previous paragraph, the present study aims to propose a different way to approach the theme of the urban Outdoor Comfort, especially related to summer conditions and so to the UHI effect, throughout the analysis of buildings forms in the very early-stages of the architectural design.

The objective is rather to test how the conformation of the urban built environment, under a purely geometrical point of view, can influence temperature fluctuations and consequently mitigating the extreme weather conditions and foreseen heat waves.

The main research questions will rather be:

1. how large is the urban variability in outdoor thermal comfort, and to what extent are these two linked?
2. to what extent is this variability determined by the building form?
3. how much a specific typology could affect the surrounding outdoor comfort?

To achieve this result, the focus will be on three of the main typologies for the distribution of buildings on parcels of land, namely: tower typology, bar typology, and courtyard typology. The purpose is to try to cover all possible variables of residential (but not only) buildings, through iterations in floor plan and height of these three main proto-types.

The focus will be on the Form of the building itself, rather than on its constituent materials or their properties (e.g., albedo, reflectivity, color, % of greenery, ect.). In fact, it has been hypnotized a dichotomy between "permanent" and "transitory" elements in the urban environment, where the form of the building, the building "mass", is considered "permanent", i.e. once "installed" in the environment it stays to mark the context. Conversely, the component of materials is defined as "transitory", replaceable or modifiable in a relatively short time. The following assumption is made: once an architectural Form, capable of maximizing outdoor comfort, has been identified only through the selection of its geometrical features (i.e. height, base dimensions, orientation, etc.) - the "permanent" part - the subsequent measures taken for the choice of the "transitory" component can only be facilitated. The aim is to provide the designer early-stage design guidelines regarding the typologies, and then he/she will be free to choose the specific characterization, starting, however, from an early-stage optimized form.

Clearly, the model that will be created will be decidedly simplified if compared to the majority of commonly known urban contexts. This standardization is however intentional, aiming to create a potentially applicable model in every type of context and that can represent not only the simulated conditions but a wider range of situations. It is assumed that the simulated form-types are adaptable to a large sample of urban models and in the same way the final considerations that will be drawn. The three building typologies will be judged according to the selected indicators, trying to understand if the building mass has indeed an impact on the building performance, and if so, which typology or building dimensions shows to be

the more beneficial.

Lastly, since, together with comfort, the other parameter on which the analysis was calibrated is the mitigation of high temperatures due to the urban heat island, it was decided to reduce the spectrum of possible analyzed periods to the summer season, in particular, to the hottest week of the year (i.e. the worst case in terms of hot temperatures mitigation).

Evaluated Indicators

Once defined the main scope, the next required action is to choose possible indicators to judge the above-mentioned three categories of buildings and relative iterations. The first step is to find an indicator for the main parameter, namely the comfort. Over time, the choice of a possible standard capable of defining outdoor comfort has been one of the most discussed topics in the field of architecture and bio-climatology. Numerous attempts have been made, starting from the 1980s.

These topic is, still now, quite obscure. In fact, while there have been many studies on the thermal comfort of people staying indoors, relatively fewer researchers have investigated outdoor thermal comfort and its determinants. With the increase in urbanization and tourism, urban planners and architects are looking more closely on the effect of climatic on urban planning. What makes the assessment of outdoor thermal comfort different from the analysis of indoor thermal one, besides the scale of work, is the massive difference between the thermal needs of different individuals, which vary with the region and study conditions [25][26].

Moreover, other challenging obstacles could be the great variety of subjective characteristics and requirements and the lack of a defined level of comfort (easier to determine and control for indoor environments). Lastly, the more challenging issue is that it could definitely defned impossible to "mechanically" control climate conditions outdoor.

First Indicator: UTCI (Universal Thermal Climate Index)

Following the manifestation of the consequences of climate change, the subject of thermal comfort in outdoors has attracted the attention of many researchers, especially those working in the fields of climate, urban development, and environmental research [27]. Over the years, researchers have introduced various indexes for measuring outdoor thermal comfort, which include Predicted Mean Vote (PMV) [28], Standard Effective Temperature (SET), which was later developed into OUT-SET [29], Man-Environment heat Exchange (MENEX) [30], Physiological Equivalent Temperature (PET) [31].Comfort Formula (COMFA) [32], and Universal Thermal Climate Index (UTCI) among others. Unlike the indoor, air-conditioned environment, the urban micro-climate is dynamic. For example, in an open urban park, the changing nature of solar radiation, wind and shading from trees makes the environment non-steady. Whereas in an urban transport facility like a railway station, radiant heat and latent heat also influence thermal comfort. Moreover, owing to its temporal nature, a steady state approach to evaluate thermal comfort, as in indoors, is not suitable for outdoor and semi-outdoor conditions.

Within the recently completed European COST Action 730, the Universal Thermal Climate Index (UTCI) was made available as an operational procedure for assessing the outdoor thermal environment in the core fields of human bio-meteorology [33]. The aim of UTCI was to characterize the thermal stress defined by the combined influence of air temperature, radiation, humidity and wind on an equivalent temperature scale [33]. The simulated dynamic response of an integrated thermo-physiological and behavioral clothing model was used to derive this scale and to establish UTCI threshold values defining different categories of thermal stress [33]. The history of this index and the reasons behind the need of having a "universal" index to describe thermal outdoor comfort will be discussed in the

following paragraphs.

According to the researchers, a thermo-physiologically significant assessment of the atmospheric environment is one of the key issues in human bio-meteorology [34].

Starting from the fact that air temperature is not the only relevant variable, in the last 150 years more than 100 simple thermal indices, most of them two-parameter indices, have been developed to describe the complex conditions of heat exchange between the human body and its thermal environment. Excellent reviews have been made; see e.g. Fanger (1970), Landsberg (1972), Givoni (1976), Wenzel & Piekarski (1982), and Driscoll (1992). Heat load conditions have been mainly described by combinations of temperature and one of the measures for humidity to express the role of latent heat flux.

However, none of the formerly indices (e.g. SET), and to some extent still popular, take into account all mechanisms of heat exchange. Consequently, such simple indices are not able to meet the requirement for a thermo-physiologically significant assessment procedure. Therefore, they are not universally valid and cannot be applied to all climates, all regions, every season, every scale, and in general, every biometeorological task [34].

The heat exchange between the human body and its environment takes place by sensible and latent heat fluxes, radiation and (generally negligible) conduction. Consequently, dealing with the thermo-physiologically significant assessment of the thermal environment requires the application of a complete heat budget model that takes all mechanisms of heat exchange into account [35]. The European Union has funded within the COST (European Cooperation in Scientific and Technical Research) Action 730 the development of the Universal Thermal Climate Index UTCI. This enforced the efforts of ISB Commission 6 on UTCI which already started in 2000.

In 2006 Windsor conference, called "Windsor-Conference on Thermal

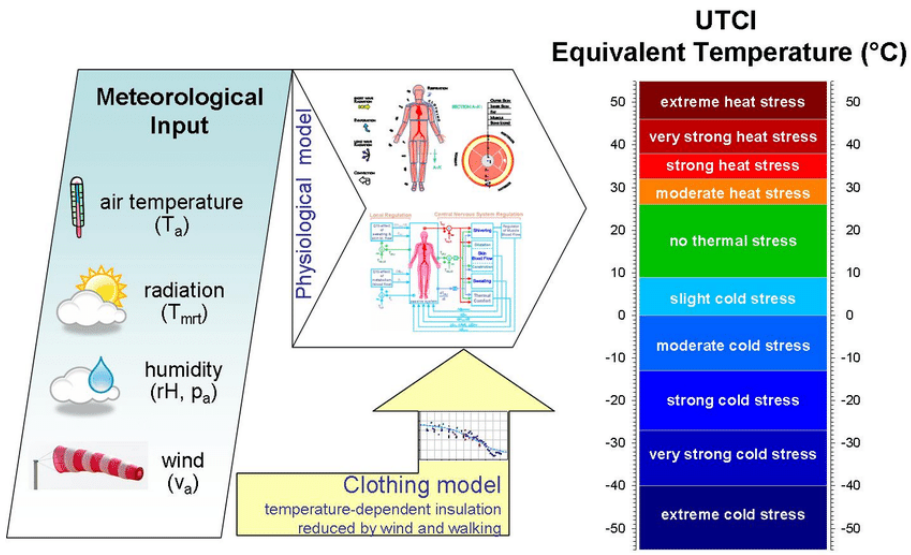

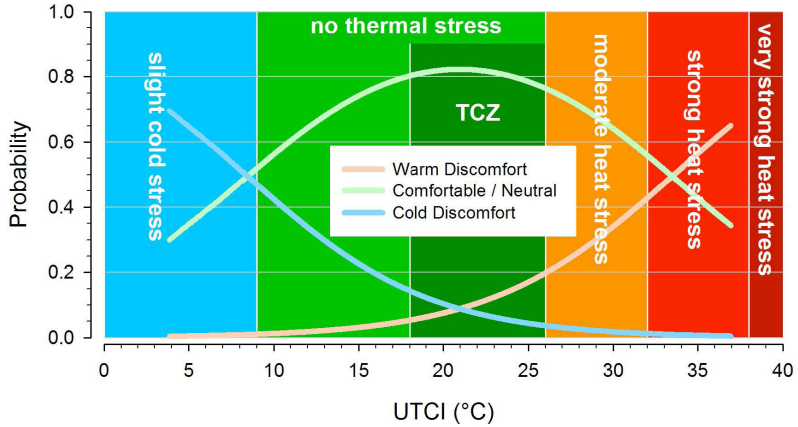

Fig. 88 Concept of UTCI as categorized equivalent temperature scale derived from the dynamic response of a thermo-physiological model coupled with a behavioral clothing model. [37]
Fig. 89 Probabilities of the individual categories of thermal comfort predicted by ordinal logistic regression analysis with UTCI as explanatory variable. Also shown are the boundaries of the thermal stress categories from the UTCI assessment scale and the sub range of UTCI values compliant to the definition of the 'Thermal Comfort Zone' (TCZ) by the Glossary of Terms for Thermal Physiology (2003). [37]

Standards" (April 5th - 8th, 2001, Windsor, UK) the Universal Thermal Climate Index has been discussed and defined to owe the following requirements:

- to be thermo-physiologically significant in the whole range of heat exchange;
- to be valid in all climates, seasons, and scales;
- to be useful for key applications in human biometeorology (e.g. daily forecasts in the public weather service, warnings, urban bioclimatology (design and engineering of outdoor spaces, outdoor recreation and climatotherapy, bioclimate maps in all scales from micro to global, epidemiological studies, climate impact research) [36].

After accessible models of human thermoregulation had been evaluated, the advanced multi-node 'Fiala' thermoregulation model was selected, extensively validated, and extended for purposes of the project. In the next step a state-of-the-art adaptive clothing model was developed and integrated. This model considers (i) the behavioral adaptation of clothing insulation observed for the general urban population in relation to the actual environmental temperature, (ii) the distribution of the clothing over different body parts providing local insulation values for the different model segments, and (iii) the reduction of thermal and evaporative clothing resistances caused by wind and the movement of the wearer, who was assumed walking 4 km/h on the level. UTCI was then developed following the concept of an equivalent temperature. This involved the definition of a reference environment with 50% relative humidity (but not exceeding 20 hPa), with still air and radiant temperature equalling air temperature, to which all other climatic conditions are compared. Equal physiological conditions are based on the equivalence of the dynamic physiological response predicted by the model for the actual and the reference environment. As this dynamic response is multidimensional (body core temperature, sweat rate, skin wittedness, etc. at different exposure times), a single-dimensional strain index was calculated by principal component analysis. The UTCI equivalent temperature for a given combination of wind, radiation, humidity and air temperature is then defined as the air temperature of the reference environment which produces the same strain index value [38].

The associated assessment scale was developed from the simulated physiological responses and comprises 10 categories that range from extreme cold stress – very strong cold stress – strong cold stress – moderate cold stress – slight cold stress – no thermal stress – moderate heat stress – strong heat stress – very strong heat stress – extreme heat stress. "Stress" is appropriate in this instance since it refers to the insult to the body; strain is the resultant consequence due to exposure [15], [34].

Second Indicator: Solar Potential

Since, due to the selection of the extreme hot week as a reference period, this choice will tend to favor those solutions that offer more shaded external situations, it was considered necessary to choose another parameter able to counterbalance the previous one. This indicator has been identified in the Solar annual irradiance, also called Solar Potential, in kWh/m^2.

Sunlight, or solar energy, can be used directly for heating and lighting, for generating electricity, and for hot water heating. Most critical, given the growing concern over climate change, is the fact that solar electricity generation represents a clean alternative to electricity from fossil fuels, with no air and water pollution, no global warming pollution, no risks of electricity price spikes, and no threats to our public health.

For these reason it was decided to use this parameter as a proxy to express also the positive effects of a beneficial annual solar exposure, such as energy production through Phovoltaic Panels and Solar Collectors. Resulting cases for the three typologies will in this way be a compromise between the two indicators and combine at the same time two relevant aspects of the early design.

2 Literature Review

Outdoor Comfort and Building Typologies

Several attempts to correlate building form with outdoor comfort have been already carried out among the researcher's community in this field. Studies of the effect of urban form on outdoor micro-climate are more recent than studies of the indoor climate. Among them, it is worth mentioning Olgyay that, with its study "Design with Climate" of 1963, together with Oke (Boundary layer climates, 1987), were the first scholars who discussed relationships between architects and urban designers from a climatologist point of view, focusing on the interactions between the building and micro-climate design. Givoni deliberates the impacts of urban typologies in different climates [19].

Steemers et al. proposed six archetypal generic urban forms for London and compared the incident of solar radiation, built potential and daylight admission. Their studies, for instance, lead to the conclusion that large courtyards are environmentally adequate in cold climates, where under certain geometrical conditions they can act as sun concentrators and retain their sheltering effect against cold winds [20].

Another comprehensive study on urban courtyards at a latitude of 26-34° N was done by Yezioro et al. They showed that, for cooling purposes, the best direction of a rectangular courtyard was North-South (NS, i.e., with the longer facades on East and West), followed by NW-SE, NE-SW, EW (in this order) [21].

Thorsson and Lindberg in a simulation study for a high latitude city in Sweden (Gothenburg) found out that open areas are warmer than adjacent narrow street canyons in summer, but cooler in winter. They also showed that a densely built structure mitigates extreme swings in Tmr and PET index, improving outdoor comfort conditions both in summer and in winter [22].

In the Netherlands (52 °N on average), few studies have addressed PET or other outdoor thermal comfort indices. Furthermore, van Esch et al. compared urban canyons with street widths of 10,15, 20 and 25 m and concluded that the E-W canyons do not receive sun on the 21st of December, whilst during summertime and in the morning and afternoon, they have direct sun. At noon the sun is blocked. On the shortest day, the N-S canyons get some sun for a short period (even the narrowest canyon) and are fully exposed to the sun in the mornings and afternoons [23].

According to Taleghani et al. in their study called "Outdoor thermal comfort within five different urban forms in the Netherlands", careful urban planning may be able to provide for cooler urban environments. Different urban forms provide different microclimates with different comfort situations for pedestrians. In their research they tried to compare singular East-West and North-South and courtyard form for the hottest day so far in the temperate climate of the Netherlands (19th June 2000 with the maximum 33 °C air temperature). The open spaces surround 8 blocks, these blocks are 10 x 10 m2 each with a height of 9 m (3 storeys). The receptor (the point considered for thermal comfort) is located in the center of the canyon or courtyard at a height of 1.40 m [24]. The five simulated urban forms are:

1. Singular blocks E-W; and b) Singular blocks N-S;
2. Linear blocks E-W; and d) Linear blocks N-S: these models are the same as form a and b but now the building blocks are connected to each other, forming a set of terraced houses;
3. A courtyard block: this block again consists of the same 8 modules forming an internal courtyard of 10 m2.

The conditions of person they used for the study were: Activity (80 W), Clothing (0.5 Clo) and personal data of the simulated human being (1.75 m, 75 kg, 35 years, male). The results of this paper showed that in the temperate climate of the Netherlands, the singular shapes provide a long duration of solar radiation for the outdoor environment. This causes the worst comfort situation among the models at the center of the canyon. In contrast, the courtyard provides a more protected micro-climate which has less solar radiation in summer. Considering the physiological equivalent temperature (PET), the courtyard has the most comfortable hours on a summer day. Since courtyards are not yet very common in temperate climates, the changing global climate, with an expected increase of temperature levels in Western Europe, advocates the usage of courtyards in (new or redeveloped) urban settings[24]. Regarding the different orientations of the models and their effect on outdoor thermal comfort, it is difficult to specify the differences between the singular E-W and N-S forms because they receive equal amounts of insulation and are equally exposed to wind. Nevertheless, the linear E-W and N-S forms are different in their thermal behavior. The center point at the linear E-W form receives sun for about 12 h a day. In contrast, this point at the linear N-S form receives 4 h of direct sunlight per day. Therefore, in comparison with the E-W orientation this N-S orientation provides a cooler micro-climate [24].

The main parameters for simulating were outdoor air temperature, mean radiant temperature, wind speed and relative humidity converted into Equivalent Temperature (PET), an indicator which is very similar to the UTCI

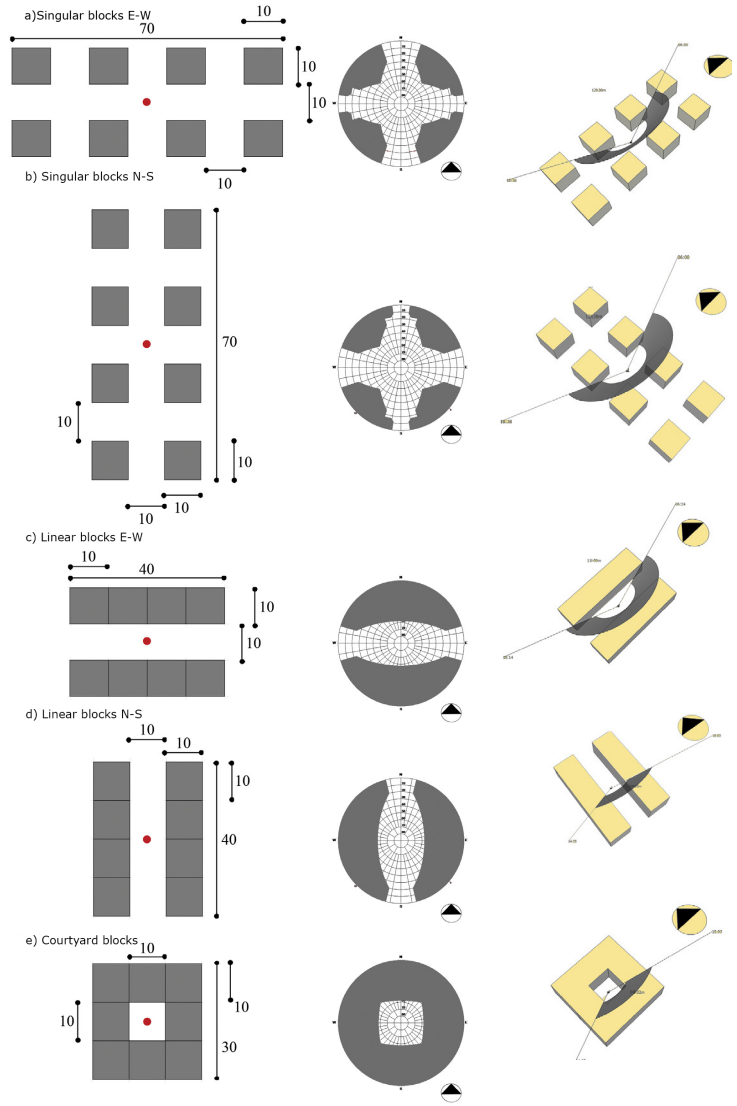

Fig. 90 Left: the five models and the positions of the reference points (the numbers are in meter); Right: the Sky View Factor (SVF) of all the forms, a) and b) 0.605, c) and d) 0.404 and e) 0.194) (calculated and produced by RayMan) [24]

that will be indeed used in this paper. The models with different compactness provided different thermal environments. The results demonstrate that duration of direct sun and mean radiant temperature, which are influenced by urban form, play the most important role in thermal comfort.

The study aims to show which of the urban forms can provide a more comfortable micro-climate on the hottest week of a year. Understanding the thermal behavior of these micro-climates would allow landscape and urban designers to have clear guidelines for planning and design at their proposal. Therefore, to perform the comparison it has been chosen as an indicator for the outdoor temperatures the thermal comfort index called UTCI (Universal Thermal Climate Index) which will be further discussed in the following paragraph.

Solar Potential and Building Arrangements

One of the studies in this field, conducted by Cheng et al., shows a pretty interesting methodology for Solar Potential evaluation. The study defines Solar Radiation as the percentage of building envelope which receives an amount of solar radiation greater than or equal to the preset thresholds, which is suitable for PV panels application. The study comprises solar simulation of eighteen generic models; each represents a particular combination of built form and density. The paper examines the relationships between built forms, density and solar potential, with reference to three design criteria i.e. openness at ground level, daylight factor on building façade and PV potential on building envelope. The result shows the different effects of horizontal and vertical randomness on urban solar potential and it also reveals the interrelation between randomness, plot ratio and site coverage, which can provide helpful insights for planning solar cities [20].

The study was initiated by a research project concerning the sustainable urban design for São Paulo, Brazil. The study is parametric in approach, with eighteen generic models representing a range of built forms and den-

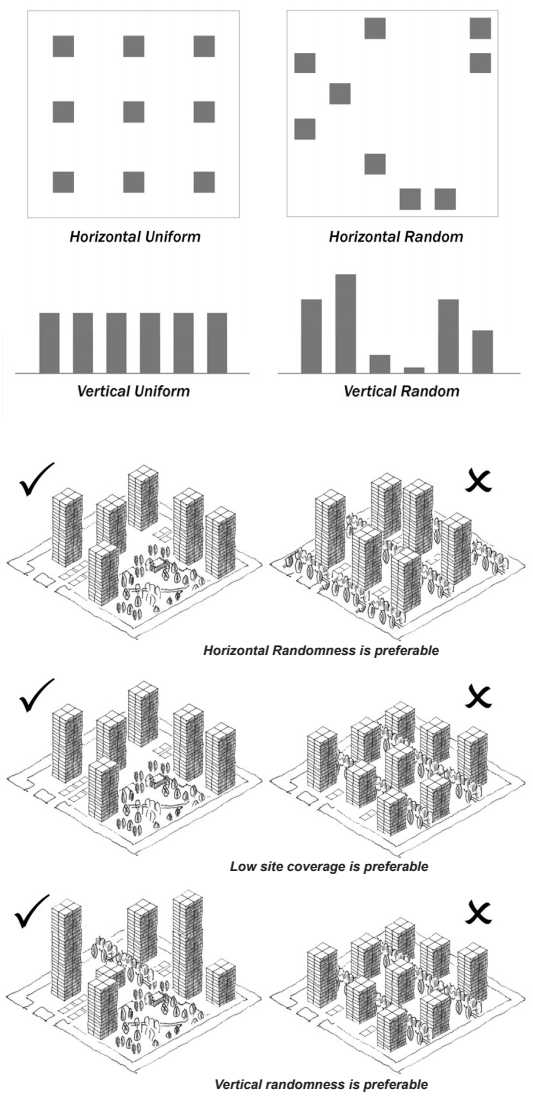

Fig. 91 Fig. X. Horizontal and vertical urban layouts [20]
Fig. 92 (a, b, c) Final considerations of Cheng et al. Study [20]

sities, compared for daylight performance and solar potential. These generic models can be categorized into four different built forms, three classes of plot ratio and two classes of site coverage. The four built forms correspond to different horizontal and vertical layouts, either uniform or random. The form of a model is denoted by an expression (H, V), where H represents the horizontal layout and V represents the vertical layout. Hence, the four categories of built forms are: (uniform, uniform), (uniform, random), (random, uniform) and (random, random).

In the simulation, building arrays were either uniformly or randomly laid out on a virtual site of 100m x 100m, as such models with the same plot ratio would provide the same amount of usable floor area.

Regarding the Solar Potential the study affirms that models with (uniform, uniform) layout and high site coverage perform significantly better than other models. This is mainly due to the fact that these models contain a large amount of unobstructed roof area which is highly suitable for PV application. The results suggest that high site coverage is favorable as it provides an extensive roof area which is a major source of high-level solar radiation. However, in such high coverage layout, random vertical layout is disadvantageous as it creates overshadowing of roof area which in turn, undermines the solar availability on roof surface.

Contrarily, in low site coverage development, random vertical layout is preferable. This is because in low site coverage layout, availability of roof surface is relatively limited and building façade becomes the major surface for PV application. Random vertical layout allows better solar access on façade, therefore results in higher solar potential. Horizontal randomness, on the other hand, does not affect the results very much.

In view of PV potential, the effect of vertical randomness depends more on-site coverage. It is favorable in low site coverage setting as it allows better solar access on façade. However, it would be disadvantageous in high site coverage setting as it creates overshadowing of roof area. Horizontal randomness, on the other hand, does not have significant influence on PV potential. High site coverage is in general not preferable as it undermines daylight and solar potential on ground and building façade, however, the extensive roof surface provided by high site coverage development is a major source for high level solar radiation which makes it advantageous for PV application.

The final findings of the mentioned study provide some helpful insights for the planning of high density solar cities. One of the most important recommendations is randomness in horizontal layout. Given the same amount of usable floor area, it is more desirable to arrange building blocks in scattered layouts than uniform arrays. Second, arrangements with higher buildings, less site coverage and more open space are more preferable than those with lower buildings and higher site coverage. Randomness in vertical layout should also be encouraged. In order to make this happen, building and planning regulations on building height would have to be made more flexible.

3 Methodology and Modeling

In the following section, it will be explained, at first, how the two selected indicators were calculated for the given iterations of buildings of each type and, secondly, how the whole geometry was modeled using mainly Rhino 3D + Grasshopper plugin.

First, the average UTCI at ground level (i.e., at the level of pedestrians in the outdoor environment) will be calculated. In fact, the simulations will iterate over the plot of land surrounding the buildings. This lot will be previously divided into a grid. From the intersection of such grate with the lot, a series of square sub-areas will be obtained, to which we will refer, from here on, with the name of "patches". Each of these "patches" will be provided with a sensor to record temperature, radiation, wind and humidity, obtaining an "equivalent" temperature, the UTCI, of that specific point over the selected period of time (Extreme Hot Week, in this case).

The second indicator, Solar Irradiance, will be calculated on the surface of the building envelope, also divided into a regular grid of 1 m² cells. Firstly, the total radiation in kWh/year will be calculated on an annual basis and, subsequently, it will be divided by the total surface of the external envelope in order to obtain a value in kWh/m²year. The latter value will be called indistinctly, during the dissertation, with the terms "Solar Potential" or "Solar Irradiance". On the right, it is possible to find a clearer summary of how both indicators have been calculated.

AVERAGE UTCI (°C) EVALUATION

PLOT DIMENSION=100X100 m
GRID DIMENSION=5X5 m
TOTAL N. OF PATCHES = 400

N. OF PATCHES
= 400 - (BULDING BASE DIM./5)

SELECTED PERIOD =
15 JUL 1:00- 21 JUL 24:00
(EXTREME HOT WEEK)

N. OF VALUES PER PATCH = 168
(HOURLY CALCULATION)

AVG. UTCI$_n$(°C) PER PATCH=
= AVARAGE OF 168 VALUES=

□ = 5 m² PATCH
[n.] = TEST POINT (SENSOR)

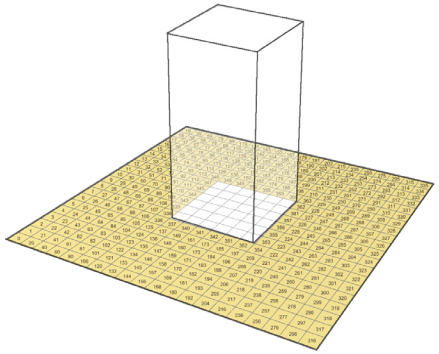

$$Avg.\ UTCI\ (°C) = \frac{\sum_{i=1}^{n} UTCI_i}{n} = \frac{UTCI_1 + UTCI_2 + \cdots + UTCI_n}{n}$$

SOLAR IRRADIANCE (kWh/m²year) EVALUATION

GRID DIMENSION=1x1 m
N. OF CELLS = BUILDING SURFACE (m²) /1

SELECTED PERIOD =
1 JAN 1:00 - 31 DEC 24:00
(FULL YEAR)

N. OF VALUES PER PATCH = 8760
(HOURLY CALCULATION)

□ = 1 m² CELL

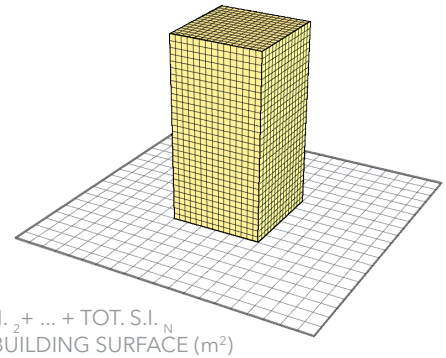

TOTAL S.I. (kWh/year) = TOT. S.I. $_1$ + TOT. S.I. $_2$ + ... + TOT. S.I. $_N$
SOLAR POTENTIAL = TOT. S.I. (kWh/year)/BUILDING SURFACE (m²)

Fig. 93 Indicators calculation methodology.

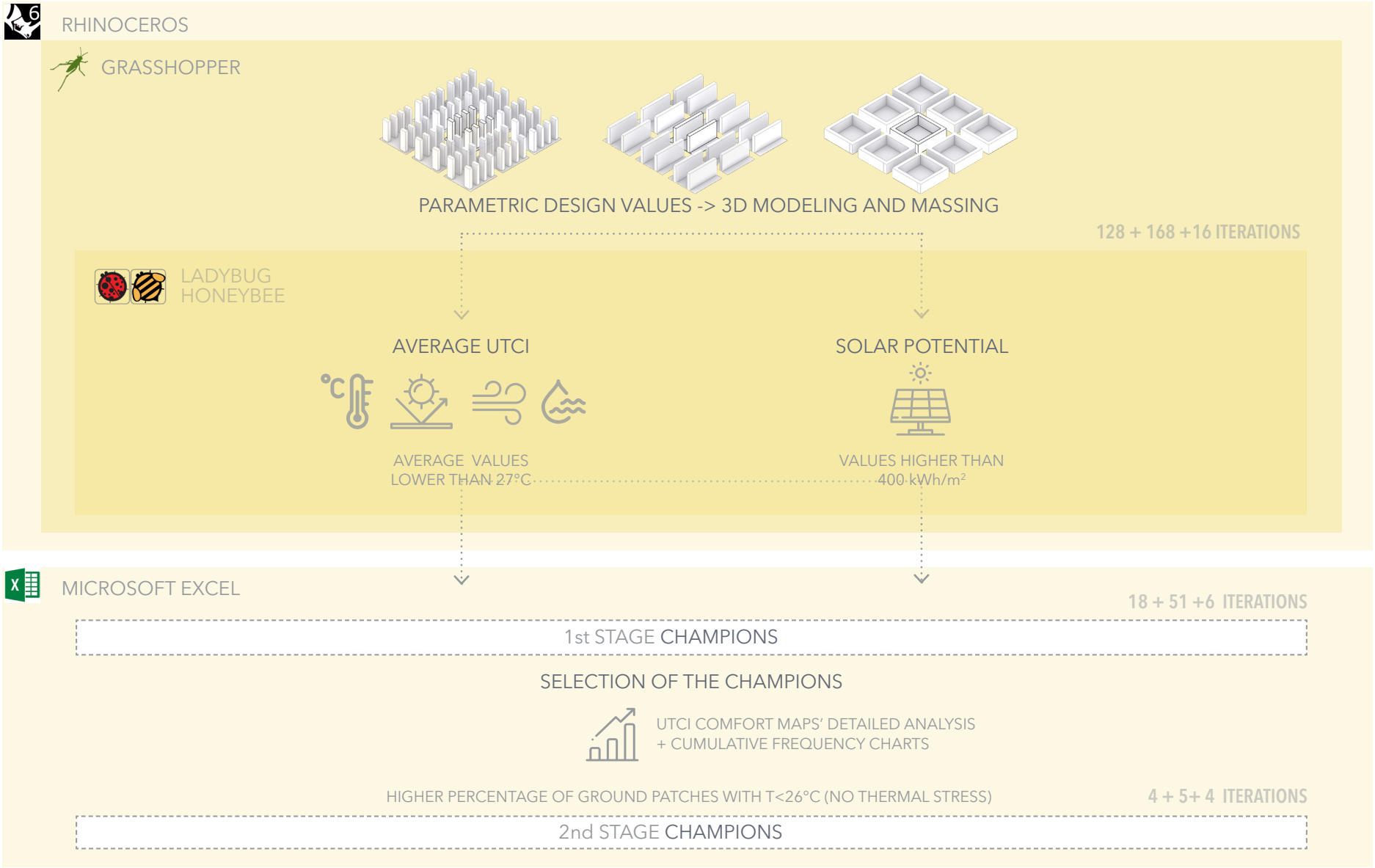

Fig. 94 General Methodology Flowchart (Process and Tools)

Building Modeling

The building modeling started from the definition of the plot of land on which the buildings will be placed. A squared parcel of land, measuring 100x100 m, has been selected as the central plot. Secondly, in order to facilitate the iterations of buildings, a grid 5x5 m has been overlapped to this base. The base dimensions' variation of the simulated buildings will follow this mentioned grid and incremented/decremented always of multiplies of 5 m.

In order to rule the iterations of the three typologies and limit the variability of the solutions to a common geometrical feature, all the cases studies have the same Floor-to-Area Ratio (FAR), equal to 3. This indicator is widely used in the related literature and represents the measurement of a building's floor area in relation to the size of the lot/parcel that the building is located on. FAR is expressed as a decimal number, and is derived by dividing the total area of the building by the total area of the parcel (building area ÷ lot area). FAR is an effective way to calculate the bulk or mass of building volume on a development site, and is often used in conjunction with other development standards such as building heights, lot coverage and lot area. It could be expressed with the following formula:

FAR = Gross Floor Area / Lot area

From the image on the right, which shows the effects of a FAR index common to different types, it is possible to understand the logic with which the building were sized for the three different building typologies.

Moreover, since the context in urban areas plays a very important role for outdoor comfort, especially with regard to over-shading effect, in this case has been introduced a context of a "fictitious" type. This context was built by distributing around the selected lot other 8 lots with the same size but shifted by 20 meters respect to the analyzed one. 20 m was chosen as the separation distance because it represents the average width of the streets of New York, generally consisting of four lanes for traffic and side lanes for pedestrians and cyclists.

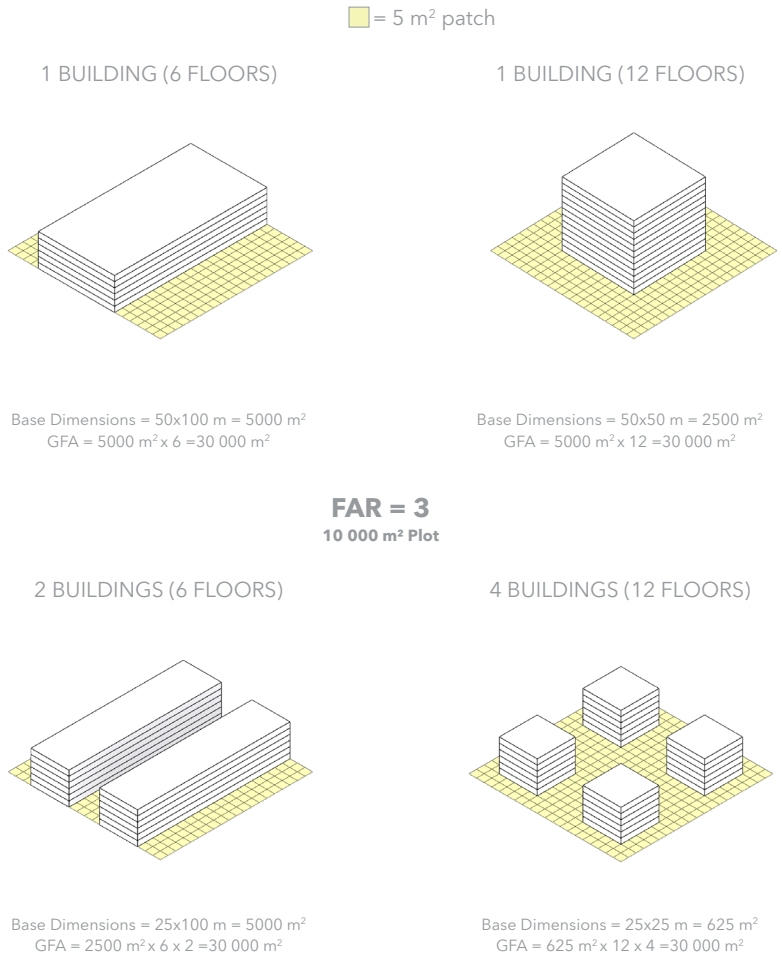

Fig. 95 Different building geometries sharing the same FAR ratio.

Context Buildings

The process of modeling has been carried out using the Grasshopper Plugin for Rhinoceros 3D. The three main simulation typologies will be positioned on the above mentioned plot area of 100x100 meters, subdivided into the 5x5 meters squares grid. Around this central plot area other 8 areas will be positioned presenting the same dimensions and the same number of equal-dimensions buildings in a kind of standardized neighborhood of equal building blocks. This precaution has been taken because of the necessity of taking into account the positive or negative effects of having context buildings that provide shading like in a normal urban environment. The process of modeling is shown in the picture.

The original 100x100 plot has been modeled starting from a fixed domain from 0 to 100 for both x and y dimensions and secondly the base grid has been added. In Grasshopper the y axis is set by default as the North direction indicator (gray navigator in the image). In a second stage, the plot has been copied from its central point with an offset of 120 m to create the surrounding bases. The use of Grasshopper has been very helpful not only in this first stage of the modeling, but also in the typologies one, because of the flexibility in managing the different input parameters that could be adjusted by moving the sliders on which the dimensions are calculated. In this way, it would be easier in a second moment to change them according the desirable dimensions and the whole model will simply self-adjust itself.

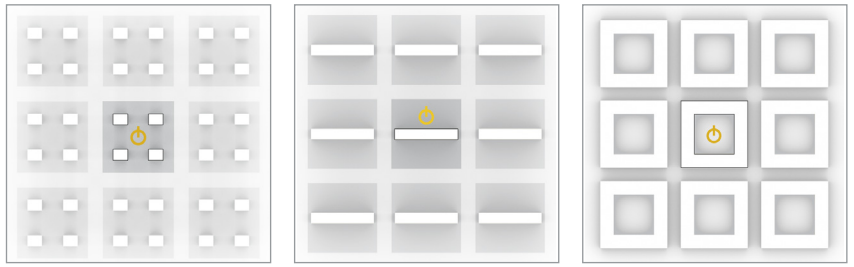

Fig. 97 Examples of context disposition for the three typologies: the central plot (black contour stroke) will be the analyzed one.

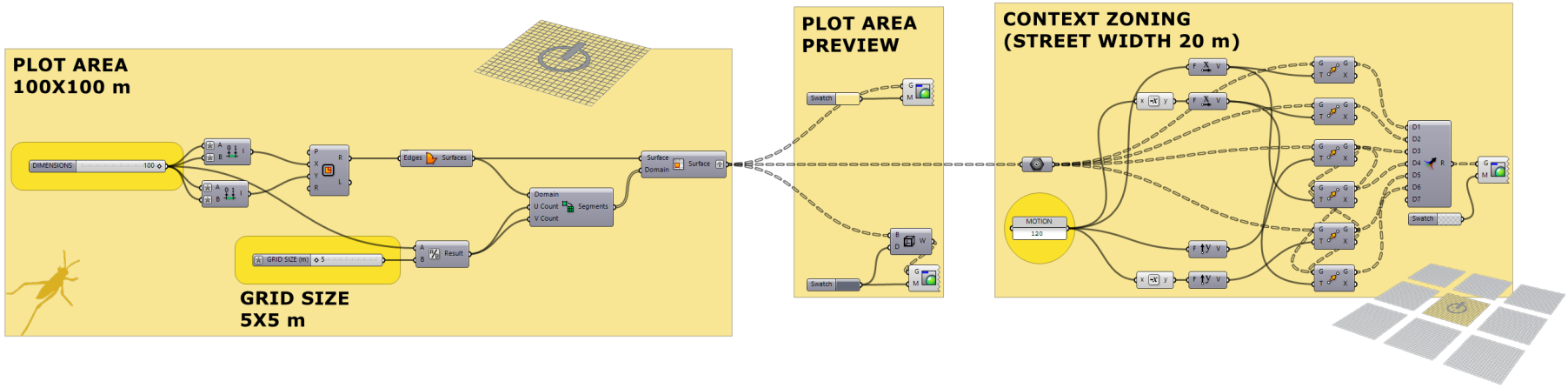

Fig. 96 Basic script from Grasshopper showing the script for the buildings' zoning lot.

Tower Geometry

The type of building structure that is tall in proportion to the size of its base, often by a considerable margin, is generally called tower. Also in this case, the tower typology shows the higher cases because in order to fulfill the 30000 m^2 of the Floor Area Ratio the building should be developed on several floors. The main aim of this paragraph is to present the logic on how the building geometries for Towers have been dimensioned and distributed on the zoning lot. Later on a deepening on the modeling script will be done.

In the present study four main types of towers' arrangements will be discussed. They have been divided into four main groups called "Clusters":

- Cluster One: 1x1, 1x2, 1x3 and 1x4
- Cluster Two: 2x1, 2x2, 2x3 and 2x4
- Cluster Three: 3x1, 3x2, 3x3 and 3x4
- Cluster Four: 4x1, 4x2 and 4x3.

The first number indicates how many lines of towers are present on the x axis and the second one how many on the y axis (e.g. type 1x1 has one tower, type 1x2 has 2 towers, 1x3 has three and so on).

Beside the arrangement, each type is also changing in size: base dimensions (both x and y) are varying from 10 m to 25 m in steps of 5 m increase. The smallest plan floor area of a single module is 10x15 m (or 15x10 m) and the largest is 25x25 m. A visual representation will be provided in the next page using the 10x15 m dimension, because, alongside with 15x10, taking in consideration the indoor spatial constraints for a residential building, is able to fit in all the distribution possibilities. Considering, for instance, the 25x25 m case is only possible for the cases with 2 towers in one axis (1x1, 1x2, 2x1, 2x2). In fact, another constraint applied to all the cases is that the minimum distance between one building and another is 17,5m.

From the figures of the next page it is easily understandable the effect of the constant FAR: this means that all the cases will have the same square footage but, since they are varying in base dimensions, smaller bases will result in taller towers. For instance, in the case with only one tower, the building will have double of the floors of the case with 2 towers (and same dimensions), and so on.

The following table lists the possible dimension combinations and the dot indicates whereas the combination of number of towers and base dimensions is possible despite the constraints.

Table a. Simulated cases for the Tower Typology

(x;y)	1x1	1x2	1x3	1x4	2x1	2x2	2x3	2x4	3x1	3x2	3x3	3x4	4x1	4x2	4x3
25x25	•	•			•	•									
25x20	•	•	•		•	•	•								
25x15	•	•	•		•	•	•								
25x10	•	•	•	•	•	•	•	•	•	•					
20x25	•	•			•	•			•	•					
20x20	•	•	•		•	•	•		•	•	•				
20x15	•	•	•		•	•	•		•	•	•				
20x10	•	•	•	•	•	•	•	•	•	•	•	•			
15x25	•	•			•	•			•	•					
15x20	•	•	•		•	•	•		•	•	•				
15x15	•	•	•		•	•	•		•	•	•				
15x10	•	•	•	•	•	•	•	•	•	•	•	•			
10x25	•	•			•	•			•	•			•	•	
10x20	•	•	•		•	•	•		•	•	•		•	•	•
10x15	•	•	•		•	•	•		•	•	•		•	•	•

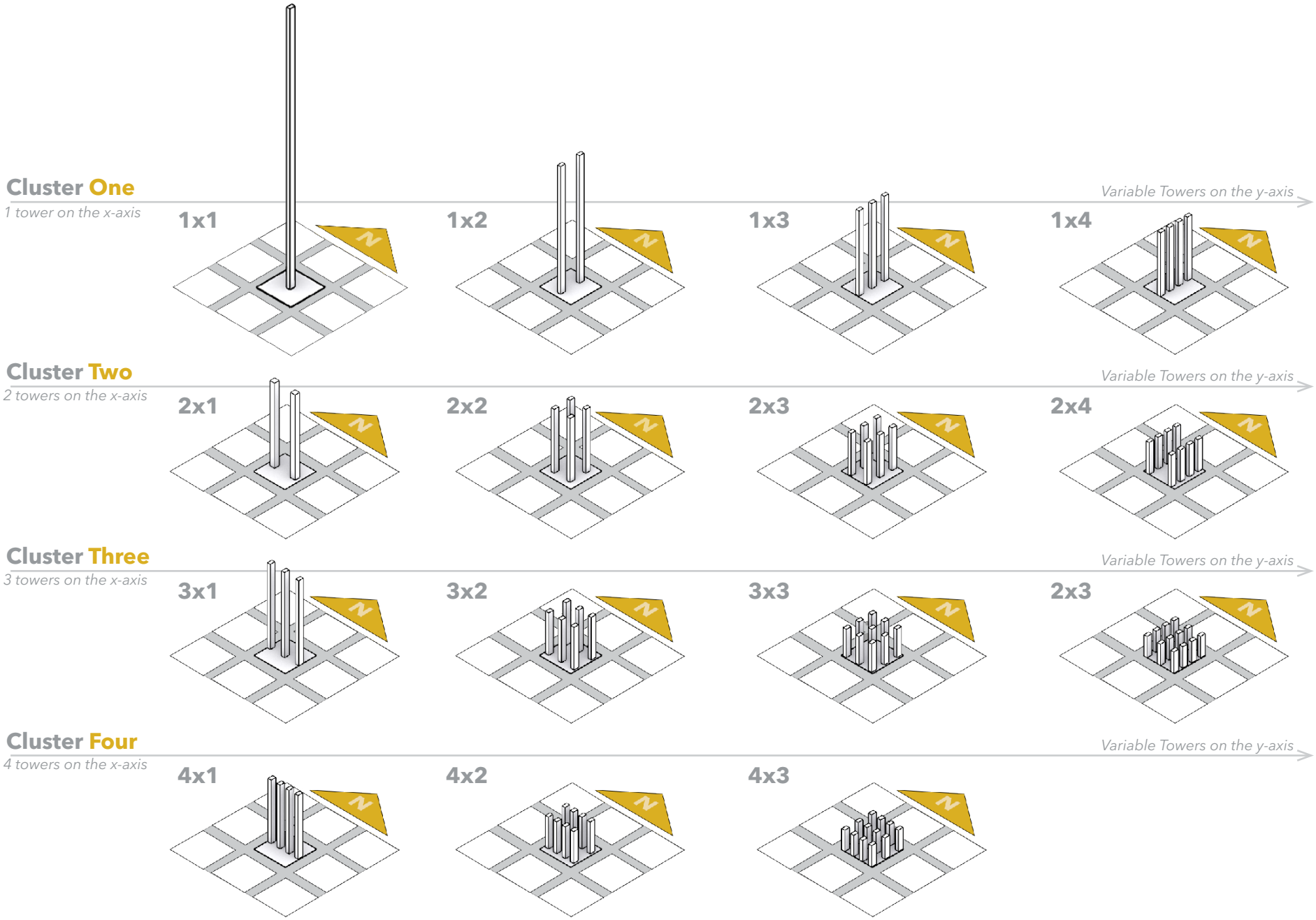

Fig. 98 Tower Typologies schemes for the common base dimensions 10x15 m.

Tower Script

In the image it is possible to see the Grasshopper script that have been used in order to model the Towers' geometries. The present script is referred to the 1x1 type in order to explain in a simple way the process; for types with an higher number of towers the same building is copied and distributed on the zoning lot.

First of all, the tower base dimensions (x and y) have been set. The two sliders to control the variations are inputted into the Colibri component in order to perform the iteration between all the possible combinations of base dimensions. Colibri is part of Grasshopper plugin TT Toolbox (by CORE Studio, 2017), that allows to iterate the geometry parameter and plot the results at the end. Secondly, a ground floor plan, located inside the original zoning lot, is originated from the combinations.

In a second stage, a fixed FAR (Floor Area Ratio) is set equal to three. If the zoning lot consists in a 10 000 m^2, the constant FAR determines that the buildings should have a common building floor area of 30 000 m^2 subdivided into floors. In fact, 30 000 m^2 divided by the 100x100 m plot area result in the initial FAR equal to three. The script, using some mathematical operators, automatically calculates the number of floors based on the FAR. Subsequently, the number of floors obtained is multiplied by 3,5 m, which consists in the standard height of a floor, resulting in the final height that will be used to extrude along the z-unit the base area created before obtaining the final building. Lastly, the contexts buildings have been placed on the previously created surrounding zoning lots in order to simulate the surrounding urban environment.

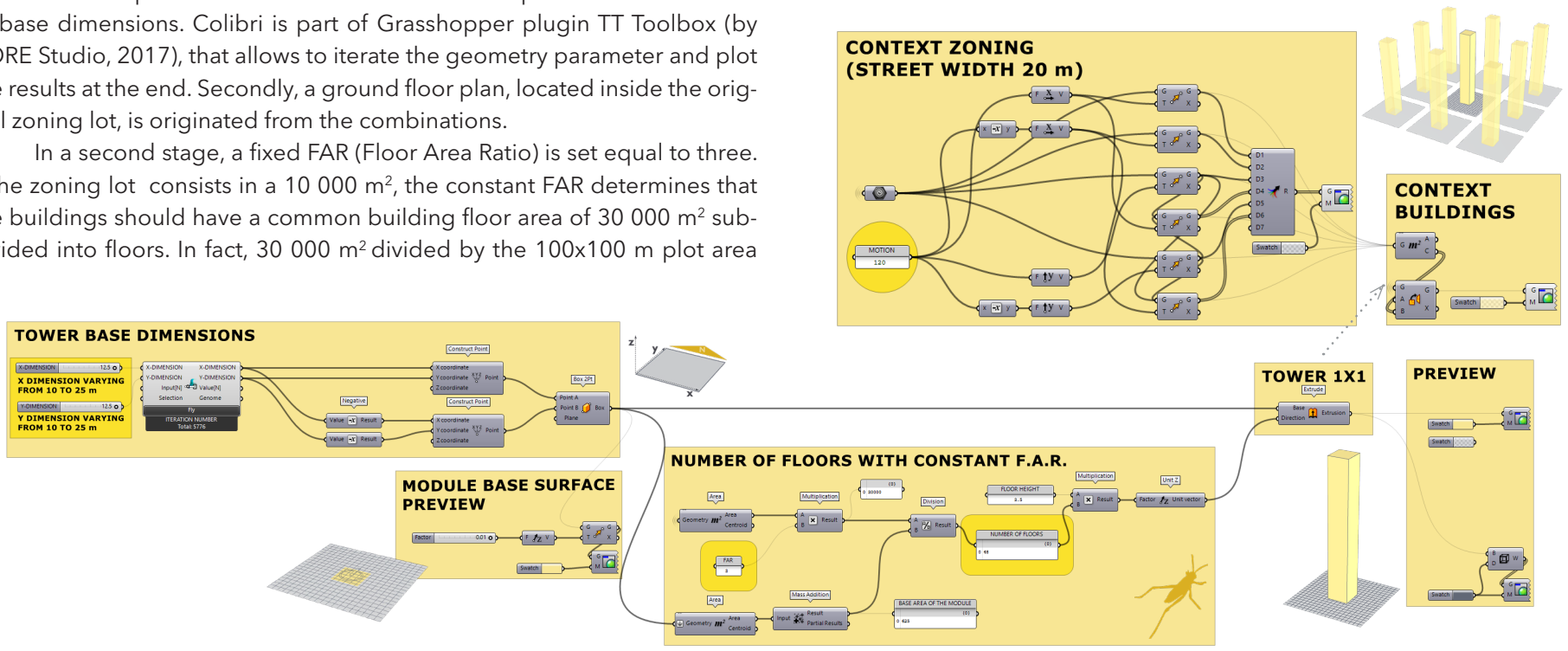

Fig. 99 Script from Grasshopper for Rhino, showing the modeling for the Tower case geometry (similar scripts have been used also for cases with more than 1 tower).

Bar Geometry

Is generally called "bar" the building with a preferable horizontal development presenting two facades significantly wider than the other two. This is a consequence of two base dimensions definitely bigger than the other two. For the sake of clariry, the longest dimension will be called "length" and the shortest "depth".

In the present research four main types of bar will be simulated, each one corresponding to a specific number of bars in the arrangement. We will have from 1 up to 4 bar arrangements on the former zoning lot. Besides the number of buildings, the bars' dimensions will vary in length from 40 to 100 m and in depth from 10 to 25 m (following the steps of the 5 m base grid). The bigger base dimensions are 25x100 m (or 100x25) while the smaller are 10x70 m (70 x10 m). The first case, with 100 m, it's the case where the longer facades are as wide as the plot side dimension, occupying it all.

Due to the big difference between the two main base dimensions it is inevitable for the typology to develop a specific orientation, which will be identified by orientation of the longer dimension. In view of this situation, two main orientations have been simulated:

- The N-S orientation where the longer sides of the bars are North-South oriented. This means that the y dimension is going to be the length (and consequently the x will be the depth);
- The E-W orientation where the longer sides of the bars are East-West oriented. This means that the x dimension is going to be the length (and consequently the y will be the depth);

The table on the right lists all the possible dimensions' combinations and the dot indicates whereas the combination of number of bars and base dimensions is possible despite the already mentioned constraints. In the following page a visual representation of the bars' iterations will be presented using base dimensions equal to 40x10 m and 100x10 m.

Table b. Simulated cases for the Bar Typology

(length;depth)	1 BAR E-W	2 BARS E-W	3 BARS E-W	4 BARS E-W	1 BAR N-S	2 BARS N-S	2 BARS N-S	4 BARS N.S
10X40	•	•	•	•	•	•	•	•
10X50	•	•	•	•	•	•	•	•
10X60	•	•	•	•	•	•	•	•
10X70	•	•	•	•	•	•	•	•
10X80	•	•	•	•	•	•	•	•
10X90	•	•	•	•	•	•	•	•
10X100	•	•	•	•	•	•	•	•
15X40	•	•	•		•	•	•	
15X50	•	•	•		•	•	•	
15X60	•	•	•		•	•	•	
15X70	•	•	•		•	•	•	
15X80	•	•	•		•	•	•	
15X90	•	•	•		•	•	•	
15X100	•	•	•		•	•	•	
20X40	•	•	•		•	•	•	
20X50	•	•	•		•	•	•	
20X60	•	•	•		•	•	•	
20X70	•	•	•		•	•	•	
20X80	•	•	•		•	•	•	
20X90	•	•	•		•	•	•	
20X100	•	•	•		•	•	•	
25X40	•	•			•	•		
25X50	•	•			•	•		
25X60	•	•			•	•		
25X70	•	•			•	•		
25X80	•	•			•	•		
25X90	•	•			•	•		
25X100	•	•			•	•		

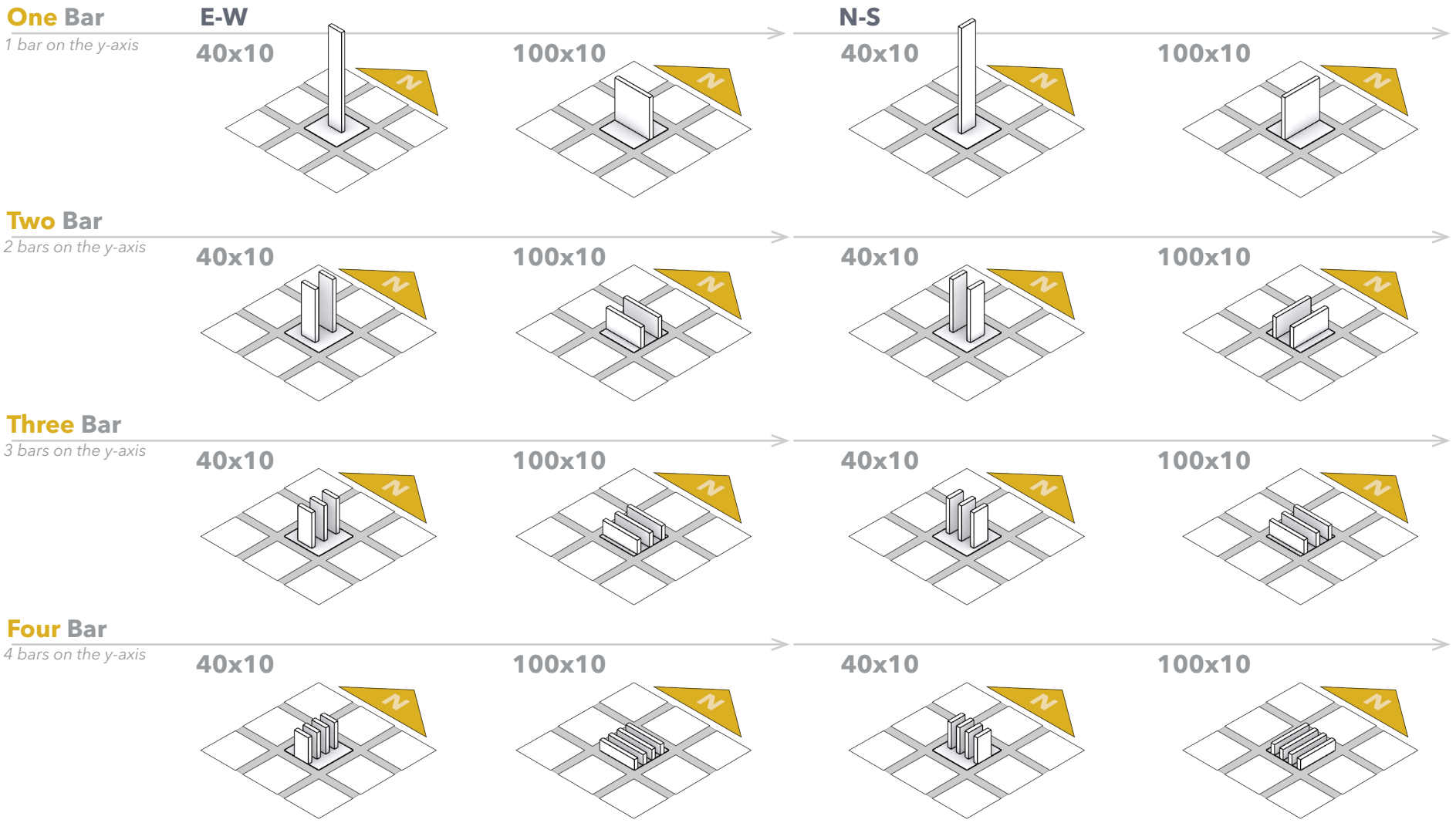

Fig. 100 Bar Typologies schemes for the common base dimensions 10x40 m, smaller base, and 10x100, bigger base.

Bar Script

In the image below it is possible to see the Grasshopper script that have been used in order to model the Bars' geometries. The present script is referred to the 1 bar type in order to explain in a simple way the process; for types 2, 3 and 4 bars the same building is copied and distributed in the zoning lot.

The procedure carried out for the bar dimensioning is very similar to the one presented for the Tower type. At first, the bar base dimensions (x and y) have been set. The only difference among this type and the tower one is that in the bar type one dimension is definitely bigger than the other one. For the E-W oriented cases the x dimension will be the bigger (lenght) and the y dimension the smaller (depth); viceversa for the N-S orientation. Again, the ground floor plan, located inside the original zoning lot, is originated from the combinations of base dimensions. The final height have been calculated considering the constant FAR multiplied by the avarage floor height of 3.5 m. To conclude, also in this case the urban context has been created by coping the building of the central zoning lot in the surrounding ones.

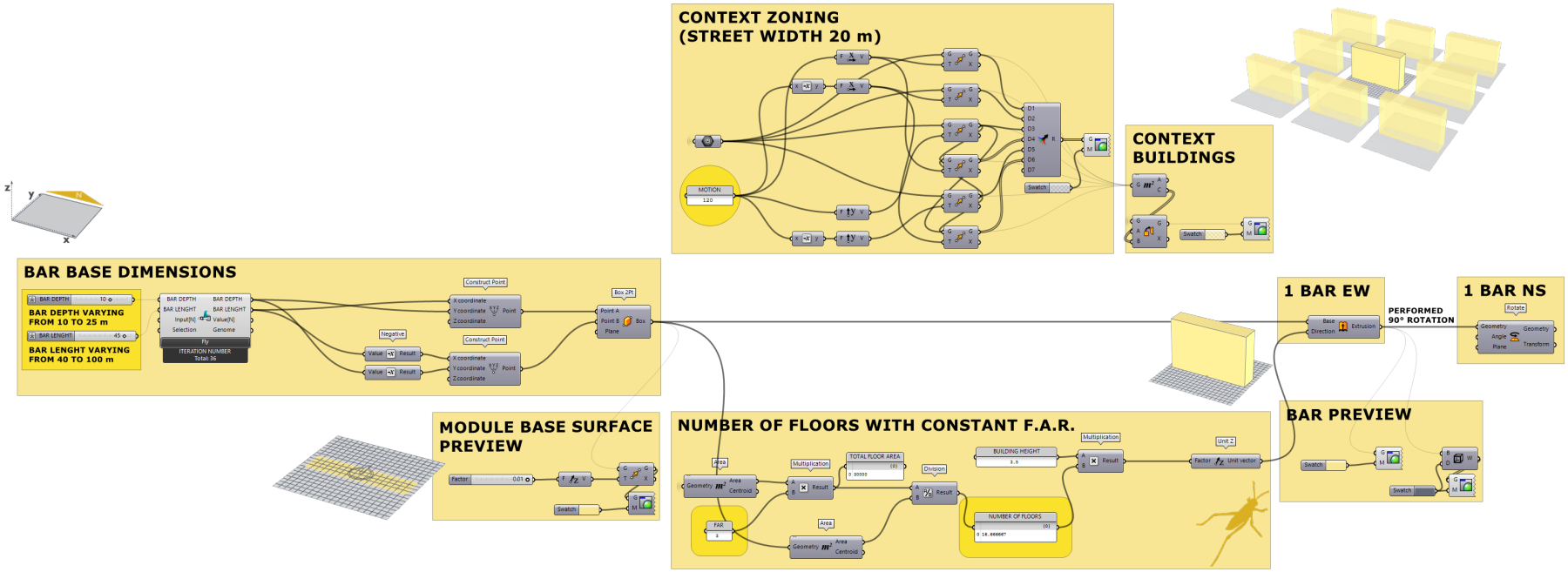

Fig. 101 Script from Grasshopper for Rhino showing the modeling for the Bar case geometry (similar scripts have been used also for cases with more than 1 bar).

Coutyard Geometry

The courtyard typology is composed by a building, or a complex of buildings, surrounding one or more circumscribed areas which are open to the sky (patios). The distribution options analyzed for this typology will be the followings:

- No internal division (No Div): the perimeter of the building is fixed and is equal to the zoning lot, with variable inner patio dimensions according to the building depth (which could vary from 10 to 25 m).
- No internal division with variable dimension of the setback from the plot boundary (NoDiv_FC, where "F.C." stays for Fixed Courtyard) the inner patio dimension is fixed to a square of 30 m side but the distance from the street will be changing according to the building depth).
- 1 division of the inner patio oriented E-W and N-S (1 Div EW/NS): the outer perimeter of the building corresponds to the dimension of the zoning lot and two internal courtyard are resulting from the division.
- 2 divisions of the inner patio oriented E/W and N-S (2 Div EW/NS): the outer perimeter of the building corresponds to the dimension of the zoning lot and three internal courtyard are resulting from the division.

The orientation (either E-W or N-S) is decided according to the longer dimension of the division. For this reason, when the courtyard building has one division E-W, it means that the loger side of the inner court is oriented pointing East and West and viceversa for the N-S case. Besides the distribution, the buildings also vary in depth. Following the adopted methodology, the depth vary from 10 m to 25 m in four main steps following the 5 m grid.

Differently, from the case of the towers or the bars where the combination between distribution and dimension created, respectively, 128 and 168 cases, in the case of courtyards the number of case studies is more limited for the 100x100 m plot. The only possible combinations of the above mentioned cases are 16 in total and are listed in the following table.

Moreover in the next page, a visual representation of the courtyard cases is provided. It is immediately clear the effect of the common FAR which results in buildings with different heights and an equal square footage. In this typology, as it happened with the previous one, the plot area also presents constraints and not all the combinations are possible, respecting the minimum distance between constructions of 17,5 m.

Table c. Simulated cases for the Courtyard Typology

	No Division (variable courtyard)	*No Division (Variable sidewalk)*	*1 Division E-W*	*1 Division N-S*	*2 Divisions E-W*	*2 Divisions E-W*
Depth 10 m	•	•	•	•	•	•
Depth 15 m	•	•	•	•		
Depth 20 m	•	•	•	•		
Depth 25 m	•	•				

Fig. 102 Courtyard Typologies schemes (1 Division E-W and 2 Division N-S cases are not here represented. Should kept in mind that they resemble the N-S ones but mirrored).

Courtyard Script

In the image below it is possible to see the Grasshopper script that have been used in order to model the Courtyards' geometries. The present script is referred to the No Division type in order to explain in a simple way the process, which will be adapted, without major variations, for the other courtyard typologies.

The modeling process starts from the usual 100x100 m plot where is initially modelled a simple bar, whose bigger dimension is the same as the plot side. This "bar" will be one of the four modular element which combined are forming the courtyard. It is immediately evident that the building depth increase leads to a decrease in the inner court dimensions. Later on, as it has been already seen for the other typologies the extrusion of the base (and so the building height) is calculated exploting the constant FAR of 3, which make sure that the floor area exactly correspond to 30000 m^2. In the last stage the same building is copied around the main one to create

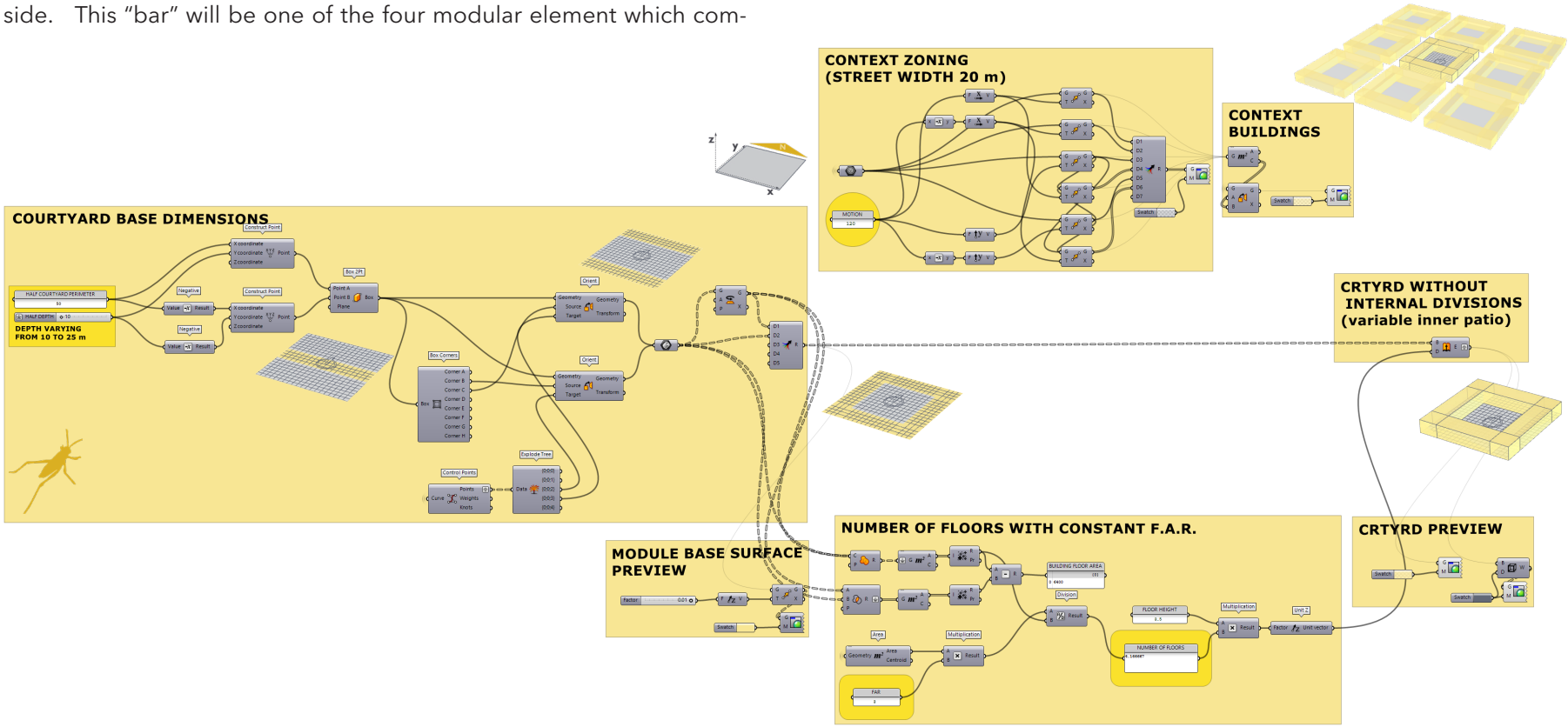

Fig. 103 Script from Grasshopper for Rhino showing the modeling for the Courtyard case geometry (similar scripts have been used also for cases with 1 or more divisions).

Indicators Simulations' Scripts

First Indicator: Avarage UTCI

The UTCI simulations have been carried out using the Ladybug and Honeybeed plugins for Grasshopper. The geometry of the ground surface is plugged to the "generate mesh" component which defines the grid size for the sensors and the height that they will be. Because the 100x100 m ground surface area 5 meters has been chosen and a distance of 0.001 m to be as close as possible to the grade level. The most smaller the grid is, the more accurate the analysis will be. The generated mesh consists in multiple surface area 5x5, each one having in the center a sensor for the UTCI in that point. In the final mesh, each 5x5 m square will be colored with according to the UTCI registered in that point according to a predefined color scale. The test mesh is plugged to the "body location" input of the "spacial solar adjusted temperature" component together with the context shading which consists in the surrounding buildings and the buildings of the arrangement itself.

This last component has the task to adjust an existing Mean Radiant Temperature for shortwave solar radiation. This component uses Radiance functions in order to determine the amount of direct and diffuse solar radiation falling on a comfort mannequin. The portion reflected off of the ground to the comfort mannequin is derived from these values of direct and diffuse radiation. The computation of the MRT is performed by the component based on the weather input parameters from the epw-file, not depending from human body, which are:

- Direct Normal Radiation (kWh/m^2)
- Diffuse Horizontal Radiation (kWh/m^2)
- Dry Bulb Temperature (°C)

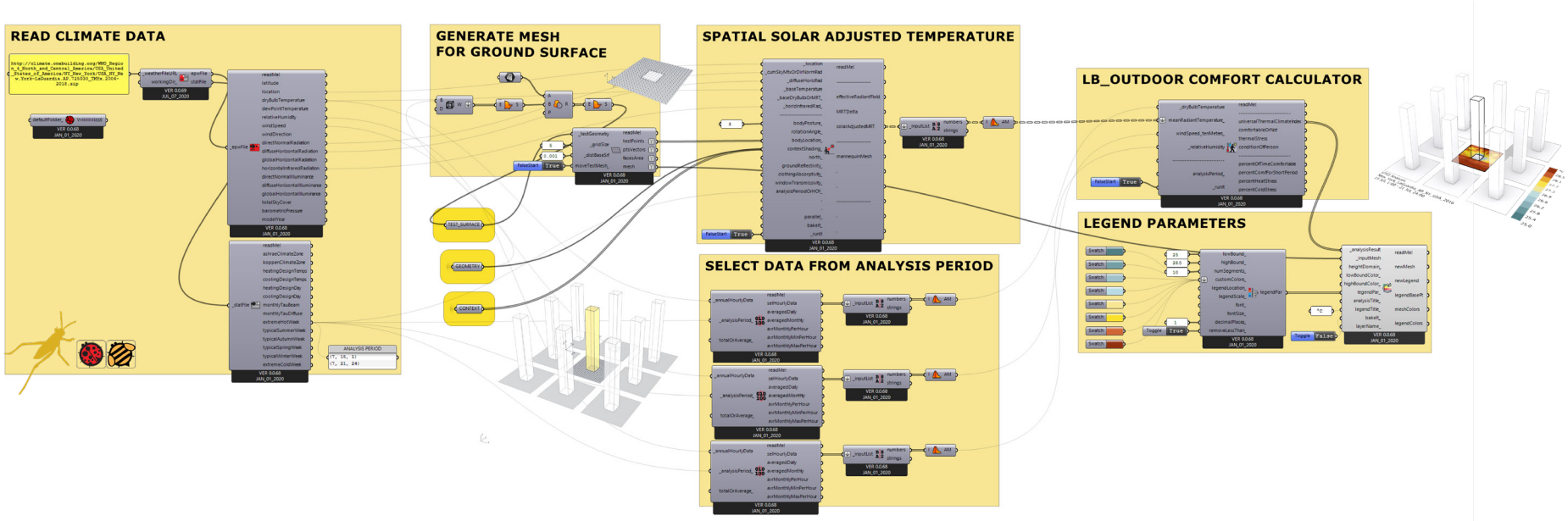

Fig. 104 Basic algorithm of Grasshopper for Rhino used to calculate the UTCI for the Extreme Hot Week for all the Typologies' iterations.

- Horizontal Infrared Radiation=down-welling long wave infrared radiation from the sky (kWh/m^2)
- Ground reflectivity (fraction of solar radiation reflected off of the ground) equal to 0.25, which is the characteristics of outdoor bare soil;

Other relevant "subjective" inputs related to human perception of the outdoor comfort are:

- Body Posture, which is set to "Low Resistance Standing" and so the normal condition of a person walking in the urban environment without performing physical activity;
- Clothing Absorptivity (decimal value between 0 and 1 that represents the fraction of solar radiation absorbed by the human body) which is set by default to 0.7 for (average/brown) skin and average clothing.

The output parameter is the estimated solar adjusted mean radiant temperature for each hour of the analysis period. This is essentially the change in mean radiant temperature added to the dry bulb temperature after inputting the above mentioned parameters.

The adjusted Mean Radiant Temperature is after used as an input for the "Outdoor Comfort Calculator" together with the other three main parameters used for computing the UTCI final value which are:

- Dry Bulb Temperature (°C)
- Relative Humidity (%)
- Wind speed (m/sec)

These three parameters were selected from the epw-file (EnergyPlus weather file) by means of the "Average Data" component on the basis of the selected analysis period (Extreme Hot Week) from the stat-file (EnergyPlus weather data statistics).

The output from the "Outdoor Comfort Calculator" will be a list of data expressing the UTCI value for each of the sensors located in each sub-area of the test mesh previously mentioned (e.g. if the mesh accounts 400 sub-area of 5x5 meters, the "Outdoor Comfort Calculator" will return 400 UTCI values centered in each 5x5 meters face of the grid). The "Re-color mesh" component is later used re-color a mesh with new a numerical data set whose length corresponds to the number of faces in the input mesh.

Being the analysis period the Extreme Hot Week the resulting temperatures will be generally high and for this reason the boundaries of the legend are ranging from <25 to >28.5 °C. For the bar charts representing the average UTCI of each building typology, the UTCI resulting from the "Outdoor Comfort Calculator" have been averaged using the appropriate component. This means that all values obtained for each sensor will be averaged to obtain a single values representative of the typology. This value could be useful to define a general tendency of the simulated typology but is not an exhaustive metrics for the comparison if used alone, because the UTCI is strongly varying from one point to another.

Second Indicator: Solar Potential

The second main parameter on which the present analysis is based is the solar potential (radiation falling on the envelope). The analysis has been carried out considering building surfaces like seamless object (without window's perforations). Firstly, because this is a very preliminary stage of the design and so the window/wall ratio is an aspect that should be considered later in the design process. Secondly, this parameter will be definitely relevant in an Indoor Comfort/Daylight study but this is not the main aim of this study, which is more focused on evaluating the real solar potential of the building form itself and using it like a contrasting value to the UTCI's results. Anyway, it is important to keep in mind that this values of Solar Radiation would get smaller after adding to the buildings the windows' opening due to the decrease of available surface.

In order to measure the radiation on the buildings, it was chosen to use the Grasshopper's plugin Ladybug and the relative homonyms component "Radiation Analysis". This component, in order to compute the solar radiation refers to the well known ray-tracing program "Radiance".

In fact, first of all, the analysis period is defined as the entire year and the proper sky matrix is created by means of the "Select Sky Matrix" component. Secondly, the "Generate Cumulative Sky Matrix" component uses Radiance's "gendaymtx function" to calculate the sky's radiation for each hour of the year in the location of the weather file. This is a necessary pre-step before doing radiation analysis with Rhino geometry or generating a radiation rose. The "Gendaymtx" takes a weather tape as input and produces a matrix of sky patch values using the Perez all-weather model. Perez Model uses are delta (representing sky brightness) and epsilon (representing sky clearness). These parameters are determined from the measured diffuse

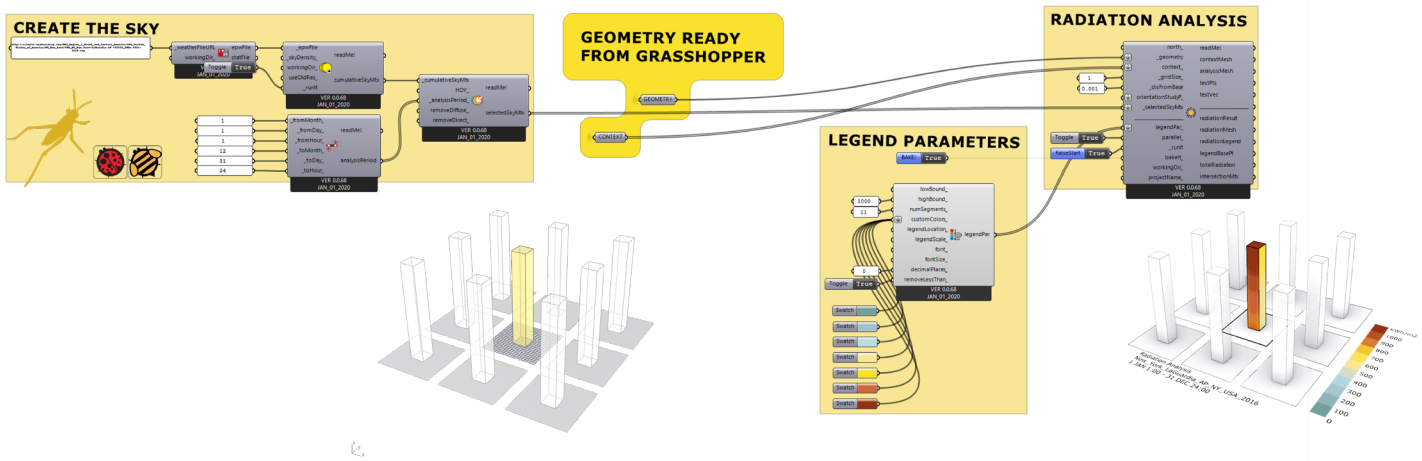

Fig. 105 Basic algorithm of Grasshopper for Rhino used to calculate the Solar Radiation on an annual basis for all the Typologies' iterations.

horizontal and direct normal irradiance values for specific sites and date/time combinations, which can be obtained from, for example, EnergyPlus. Diffuse Horizontal Irradiance is from the sky alone, measured horizontally. The units are watts per square meter. Direct Normal Irradiance is from the sun alone, measured by an irradiance meter aimed directly at the sun. Its units are also watts per square meter.

In a second stage, the Sky Matrix is plugged to the "Radiation Analysis component". This component allows to calculate the radiation falling on input geometry. This type of radiation study is useful for building surfaces, where the designer must be interested in solar heat gains, or solar panels and the amount of energy that can be collected. This component is also good for surfaces representing outdoor open spaces (such as parks or seating areas) where radiation could affect thermal comfort.

The way in which the solar radiation is computed in also supplied by Radiance. In fact, for the studied geometry it is asked to define grid dimension, which has been set to 1 meter. This means that the surface of the buildings has been subdivided into several cells, each of them having a surface area of 1 meter. In order to choose this value, it must be considered that it should be

smaller than the smallest dimension of the test geometry for precise results. The process is shown in the following image.

The distribution of the grid-points on the building surfaces should be as uniform as possible. Th e irradiation is considered constant on each small area, therefore, the number of points (and small areas) is adapted to the precision we want in the total irradiation calculation.

From the Radiation Analysis component different outputs could be extracted. At first, the Radiation Result (kWh/m^2) which represents the amount of radiation in kWh/m^2 falling on the input test geometry at each of the test points. This means, for example, if a 1000 m^2 testing surface has been sub-divided into a grid of 1 m^2 cells for each of the test points (or sensors) located in the middle of each cell (1000) it will be accounted the irradiance that hourly input on the test point for the whole year for a total number of 8760 results for each test point and so 8.8-E6 results.

The values which has been taken into consideration in this case is the total radiation in kWh falling on the input test geometry. This value is computed through a mass addition of results at each of the test points in kWh/m^2 multiplied by the area of the face that the test point is representing and so could be more representative of the solar potential of the building, representing the amount of the solar radiation collected by the building envelope on an annual basis. This values has been in a second time multiplied by the exposed area of the whole building in order to obtain a result in kWh/m^2 which allows the designer to be immediately aware about amount of energy collected by 1 square meter and use this value to calculate the number of potential PV panels that might be installed.

4 Performance Assessment

Introduction

This chapter is devoted to the evaluation of the three building typologies according to the selected indicators: UTCI and Solar Irradiance. Regarding the first one, the UTCI distribution on the ground will be firstly evaluated. As described in the chapter regarding methodology, massing and algorithms of the evaluated parameters, the UTCI is calculated on the 100x100 m plot (deprived from base areas of the buildings). The lot has been divided into "patches" each one having the same area dimensions of the base grid (25 m^2). As specified in the same chapter, the average UTCI for each building has been calculated for the hottest week of the year (Extreme Hot Week), statistically defined on the basis of temperatures measured over a sufficiently large sample of calendar years. For the case of New York City, this week has been defined as the one between the 15th and 21st of July, and in which the highest peak of dry build temperatures are recorded.

Since the UTCI of each ground "patch" is taken hour-by-hour during the designated week, it was necessary first to average all temperatures of each patch, and, in a second step, to average again all of the aforementioned patches, to obtain an average data for each iteration of each type. In a first stage, therefore, the data were collected iteration by iteration and represented in bar graphs where highlighting for each iteration the corresponding UTCI on the ground. From here, an attempt was made to draw conclusions based on the data found. Secondly, special cases of iterations for each type were selected based on variable criteria (that will be described later) and the recorded UTCIs were mapped on floor plans according to a color gradient to define UTCI temperature zones.

The second criterion evaluated, aimed at counterbalancing the values of UTCI, is the Solar annual Irradiance (often called Solar Potential) or the amount of solar energy in kWh/m2 year potentially collectable by the envelope. Also in this case, data have been gathered for each iteration of the three types and evaluated. Considerations have been formulated regarding the differences between the base sizes of each iteration.

Finally, for each typology the data of UTCI and Solar Potential will be combined together and represented in scattered chart showing on the y-axis the values of UTCI and on the x-axis those of Solar Irradiance, in relationship with modular base dimensions of each iteration. Specific ranges of both indicators will be defined and then a selection of the best cases for each type will be made. The following chapter will provide a separate evaluations of each typology. A combination of the data and the overall comparison will be performed later on in Chapter 6.

Tower Typology

Average UTCI (Extreme Hot Week)

All the obtained results for the selected period (July, 15th-21st) belong to the "Moderate Heat Stress" Range of the UTCI's Assessment Scale, which ranges from 26°C to 29°C, but, since in human perception of heat stress even smaller variations of temperature can be relevant, it is interesting to further comment and analyze the variation among data. In fact, even a small change of 1°C degree could be crucial in determining the personal sensation of outdoor comfort. Lastly,it should be pointed out that every time that in the following paragraph the word "UTCI" will be mentioned, reference is made to the average value of it on the whole plot of land.

The bar charts on the right are displaying the UTCI values dividing the iterations into 4 main clusters, according to the number of building that are present on the x-axis. Graphs can be read in two different ways. The first approach consists of a left-to-right reading of each "group". Each cluster is divided into as many "groups" as the iterations of dimension x (X equals 25, 20, 15, and 10 m). Within each group the base dimensions of each building composing the arrangement decrease as the y-axis decreases. The second type of reading, on the other hand, is the approach by number of buildings. Each iteration counts 1 to 4 bars corresponding to the type of arrangement (1 to 4 towers). For the reasons mentioned in the chapter on modeling procedures, not all iterations consist of the same number of types due to the building constraints previously exposed.

Referring to "Cluster One" it is possible to see a greater dependence of the oscillation of the values from the number of buildings rather than on the base dimensions. In fact, it is evident the remarkable difference between the 1-tower case (1x1) and the following ones. Generally, the value of the average UTCI on the ground seems to decrease as the number of buildings in the arrangement increases. The UTCI decrease progressively as the num-

Fig. 106 Cluster One: UTCI values for the Extreme Hot Week.

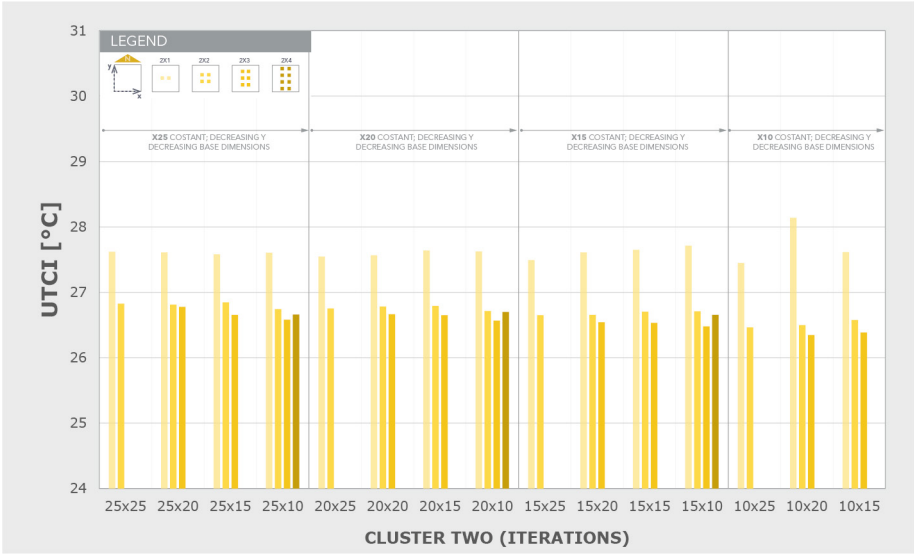

Fig. 107 Cluster Two: UTCI values for the Extreme Hot Week.

ber of buildings increases from 1 to 3. An exception should be made for the 4-building case, which has median values between the 2-building and 3-building arrangements. Base size, on the other hand, plays a decidedly less important role in determining UTCI, but still merits some consideration. Still for Cluster One, it is possible to see a slight increase in the values of the average UTCI of the arrangements, for each group, parallel to the decrease of the size y for the types 1x1 and 1x2. As far as the 1x3 and 1x4 cases are concerned, the variations as the y decreases can be considered negligible.

Similar considerations to those formulated for "Cluster One" can also be applied to the other three Clusters. In all of them, in fact, it is possible to see the same relationship of interdependence between decrease in the value of average UTCI and increase in the number of buildings. In cluster two, if compared with cluster one, is not possible to identify a clear trend of the results. In fact, it presents a less standardized behavior.

For these three other Clusters, the relationship between UTCI and base size can be considered even more instabile, when compared to Cluster One. Although specific trends of decreasing/increasing values are present, their effect can be considered significantly less important than that of increasing the number of buildings. In fact, it is assumed that, since the value of the UTCI is linearly dependent on the solar radiation on the ground, in cases where there is greater shading determined by the increase of shielding bodies, lower values of UTCI are detected and consequently higher comfort conditions are created for a summer scenario.

UTCI Comfort Maps

Since the bar charts presented above were displaying for each type the average value of the UTCI on the zoning lot, a more punctual analysis could be performed in order to evaluate how temperatures are distributed on the ground. In fact, even if a type has a low UTCI compared to other cases, this does not necessarily mean that the type represents the best scenar-

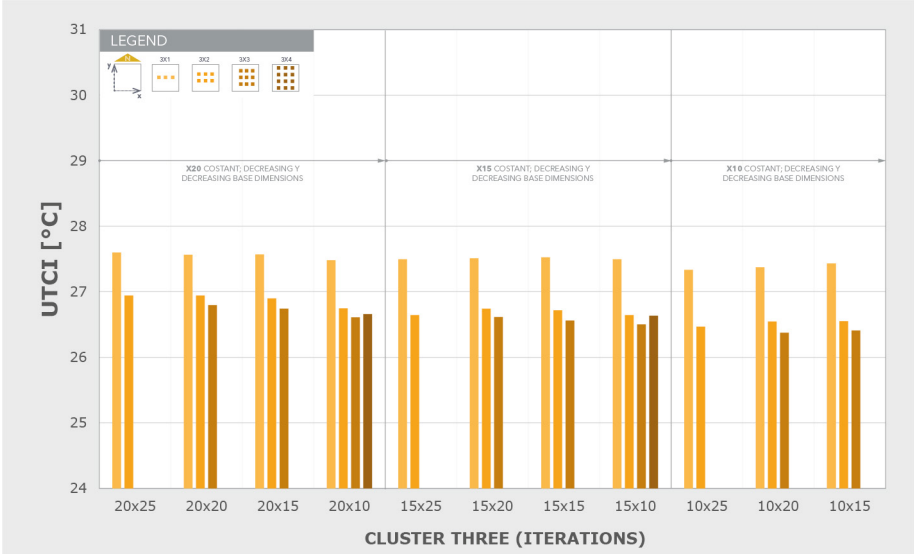

Fig. 108 Cluster Three: average UTCI values for the Extreme Hot Week.

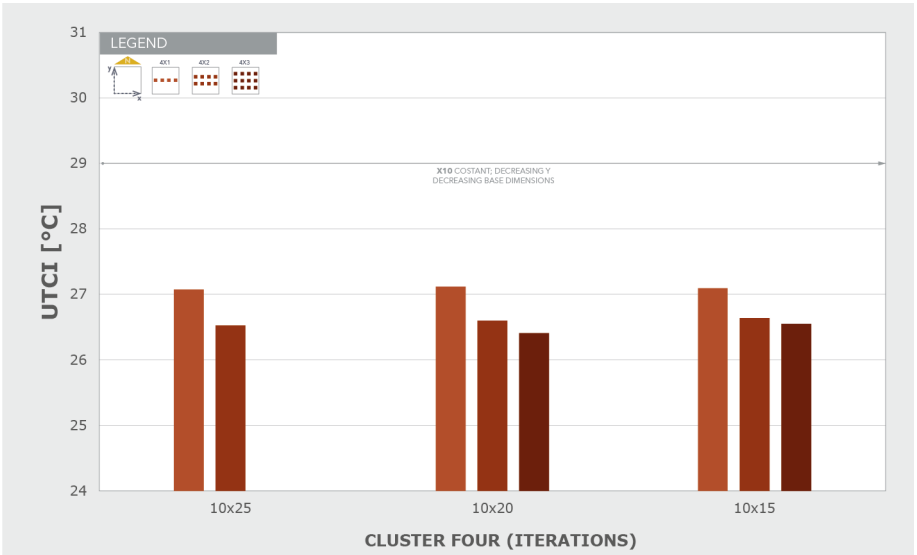

Fig. 109 Cluster Four: average UTCI values for the Extreme Hot Week .

io; thus, the average temperature could be low but big thermal asymmetries could be still present. In order to provide a visual representation, on the right of this page and of the following one, the UTCI maps for each type, with fixed base dimensions 15x10 m and 10x15 m (the smaller ones), are provided. Those base dimensions have been chosen cause they are able to give and exaustive representation of all the typologies. The main aim consists in understanding how the different geometries could be affecting the UTCI distribution on the ground. From these maps, It is very evident that fewer buildings in the arrangement (e.g., type 1x1, 1x2 and 2x1) result in higher UTCI due to the lack of the over-shading effect of the context buildings and the contribution of those of the arrangement itself. Conversely, denser arrangements show more uniform pattern of temperature values on the ground.

The UTCI pattern of those arrangements consisting in only one row of buildings (such as 4x1 or 3x1) can be considered the more interesting because, differently from the others, show clear thermal assymmetries in temperatures' distribution. In type 4x1, for example, the zoning area is divided into two neat temperature zone: one facing South and the other one facing North, separated by the buildings' row in the middle. In fact, the proximity of the four buildings is causing a strong over-shading effect in the Northern zone; this happens because the buildings are working as a shield preventing the stronger solar radiation coming from South to reach the North.

In type 4x2 the two lines of buildings are very far from each other and they are not able to provide enough shading in the central part and this is causing an hotter "stripe" in the middle of them.

After the previous observations, it is possible to affirm that, in general, the best types for outdoor thermal comfort are those which are presenting a more uniform distribution of buildings on the zoning lot, such as 2x2, 2x3, 2x4 and 3x2, 3x3 and 3x4. Among the other types, two main variation are present: buildings presenting a preferable N-S orientation, such as types

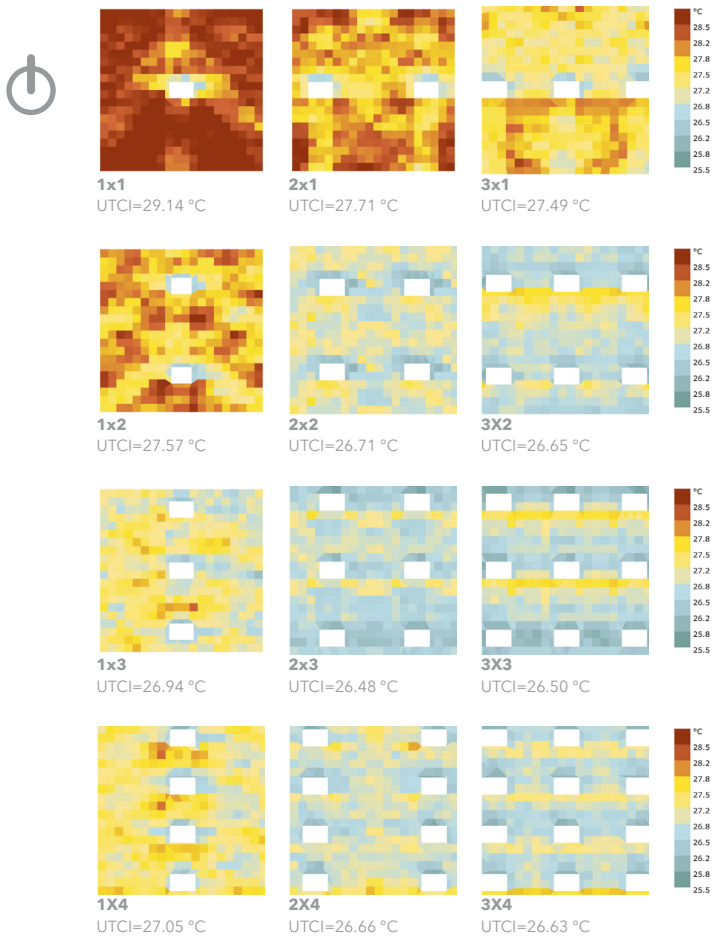

Fig. 110 UTCI comfort maps for all the Tower types with equal base dimensions 15x10 m (Weather Station: New York; LaGuardia AP_NY_USA; Period:1 JAN 1:00 - 31 DEC 24:00).

1x2, 1x3 and 1x4, and a E-W one, like 2x1, 3x1 and 3x4 (with N-S orientation it is intended an alignment of buildings along the y-axis from North to South; conversely, E-W considers buildings aligned along the x-axis from East to West). From the it is clear that the N-S orientation returns a more homogeneous distribution of the UTCI, against the asymmetries displayed by the E-W. A final consideration can be made, instead, about the orientation of individual buildings. Also in this case the direction of the longest side of each building is considered. Based on this it can be said that thermal asymmetries are higher for cases where buildings show a preferential E-W orientation. It is , for example, the 1x4, 2x4, 3x4 cases compared to the opposite 4x1, 4x2, and 4x3. In the latter, in fact, the bands of colors tending to red (and therefore warmer) are considerably more extensive than in the former.

Lastly, the following graph was included for the purpose of corroborating the previous statement regarding the effect of solar radiation on the ground. In fact, it is one of the most decisive components of the UTCI value. It is possible to notice here a linear dependence of the values of mean UTCI at ground level and annual solar radiation. The cases with high values of average UTCI, such as those with buildings in line (such as 1x2, 2x1, and so on), also have high values of solar radiation. The opposite is true for cases with more homogeneous arrangements, located lower in both values.

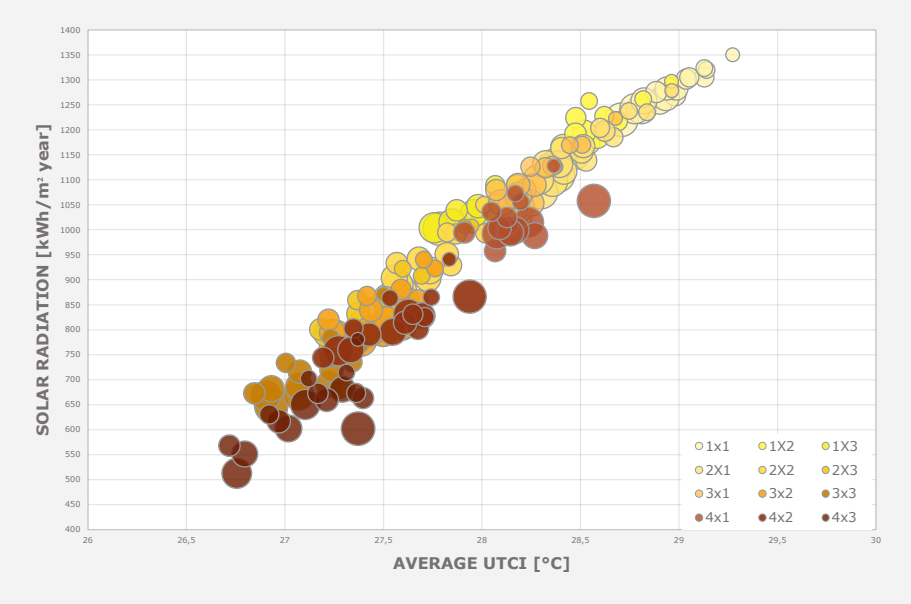

Fig. 112 Solar Radiation on the ground in kWh/m² year for different Tower types.

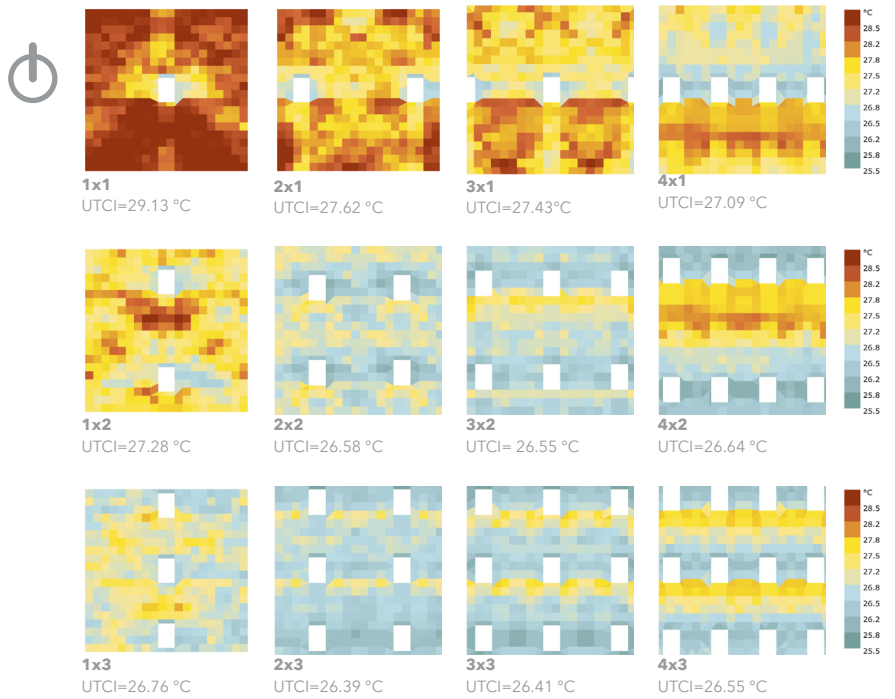

Fig. 111 UTCI comfort maps for all the Tower types with equal base dimensions 10x15 m (Weather Station: New York; LaGuardia AP_NY_USA; Period:1 JAN 1:00 - 31 DEC 24:00).

Please note that the graph on the left refers to the solar radiation on the ground; on the contrary, the next chapter will be dedicated to the solar radiation related to the envelope (facades and roofs).

Solar potential of the envelope

The main aim of this second stage is to identify common behavior in the Solar Irradiance trends for the Tower Typology. This time all the data have been combined into a unique chart to give to the reader a better overall view of the Clusters.

Also in the case of solar irradiance, the most interesting indicator to be evaluated is definitely the number of buildings. The colors given in the chart could be in this case helpful: arrangements with fewer buildings are identified with lighter shades of yellow, starting from case 1x1 with 1 building, up to a more brownish tone of red for the 12 building case. Having this is mind, it is possible to see how the increase in the number of buildings is parallel to a decrease in solar radiation per square meter. The only exception is constituted for each cluster by the 4-buildings types along the y-axis, which are registering higher values compared to the previous 3-buildings types.

The bar graph's information can be corroborated by the 3D diagrams on the next page that show the mapping of Solar Potential on the building envelopes. Also in this circumstance, the cases 10x15 and 15x10 have been selected to cover all possible iterations for each type. Since the 10x15 case, due to dimensional constraints, is not owing data for the 1x4, 2x4, 3x4 typologies, the opposite orientation has been used to provide greater completeness to the representation.

As it is possible to see, the main role in solar radiation collection is played by the roofs and by the higher parts of the South-facing facades of the buildings. It would therefore be logical to think that the cases with the highest number of roofs available are also those with the highest solar potential. From the data found, however, the less compact arrangements are at an advantage. This can certainly be explained by the fact that, given the con-

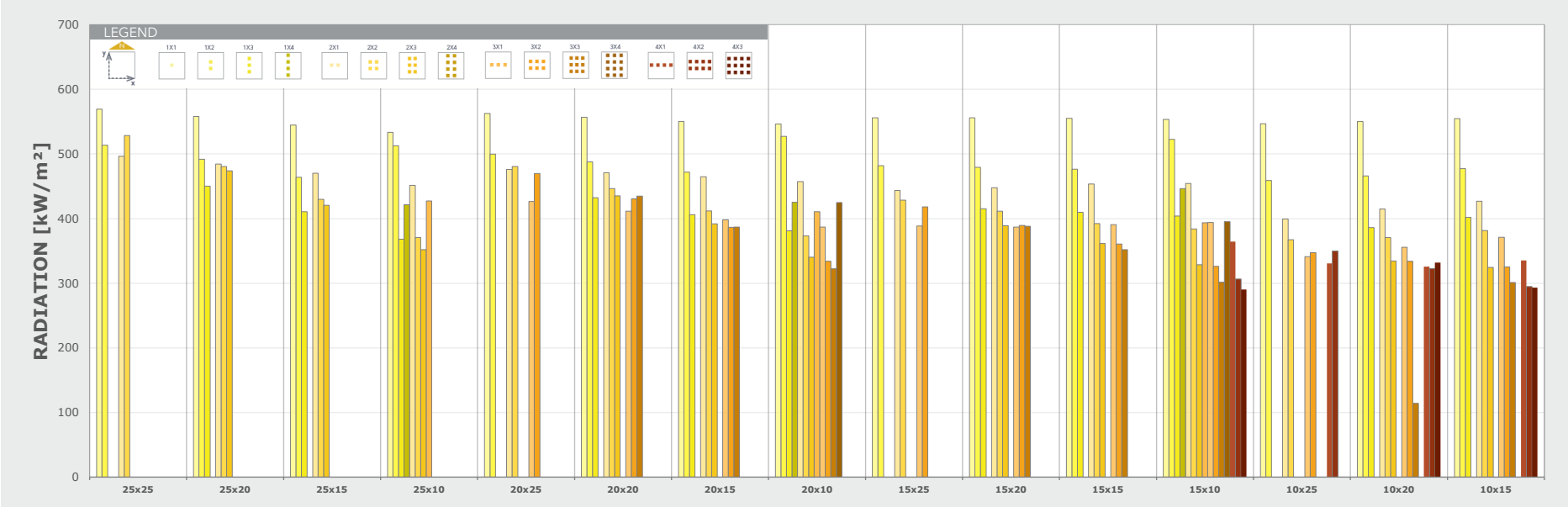

Fig. 113 Solar Potential (kWh/m²year) of the envelope for the Full Year: all the Clusters combined (Weather Station: New York; LaGuardia AP_NY_USA; Period:1 JAN 1:00 - 31 DEC 24:00).

stant nature of the FAR ratio, as buildings increase in number, their height also decreases. This leads to lower Solar Potential values. The presence of dense arrangements of buildings, increases the shielding potential on each other and the only available surface is that of the roof. Suffice it to see the difference detected both in terms of Total irradiance (in kWh/year) and in terms of Solar Potential (in kWh/m^2 year), between the case of 1 building and that of 12. There is in fact an increase of the total radiation of the 72% passing from the 1x1 case to the 4x3 one.

Nevertheless, a possible comparison is the one which can be perfored among types 2x1 and 3x1, arranged according to a preferable E-W orientatiom, and 1x1and 1x2, N-S arranged. It is interesting to notice from the data that in general the most efficient orientation is the N-S one. Looking at the bar chart of the above page to double check this observation, it is clear that the N-S oriented are collecting more radiation. For these reason, even if the number of buildings is the same (and so the number of floors and BCR are) the values of the radiation are very different. This peculiarity derives from the fact that in E-W orientations (e.g. 3x1) the upper surfaces of the envelope (aligned with the y axis), being very close to each other, shield each other. On the contrary, for cases oriented N-S (e.g. 1x3), these surfaces are exposed during the entire solar path, contributing more to the overall potential. It has been estimated, for the case 10x15 an increase of the Total Radiation of almost the 10% passing from case 2x1 to 1x2 and from the 3x1 to 1x3

Lastly, similar considerations can be formulated concerning cases 1x4, 2x4 and 3x4 (15x10) if compared to 4x1, 4x2 and 4x3 (10x15). It is possible to notice an increase of the 30-35% passing from the latters to the formers.

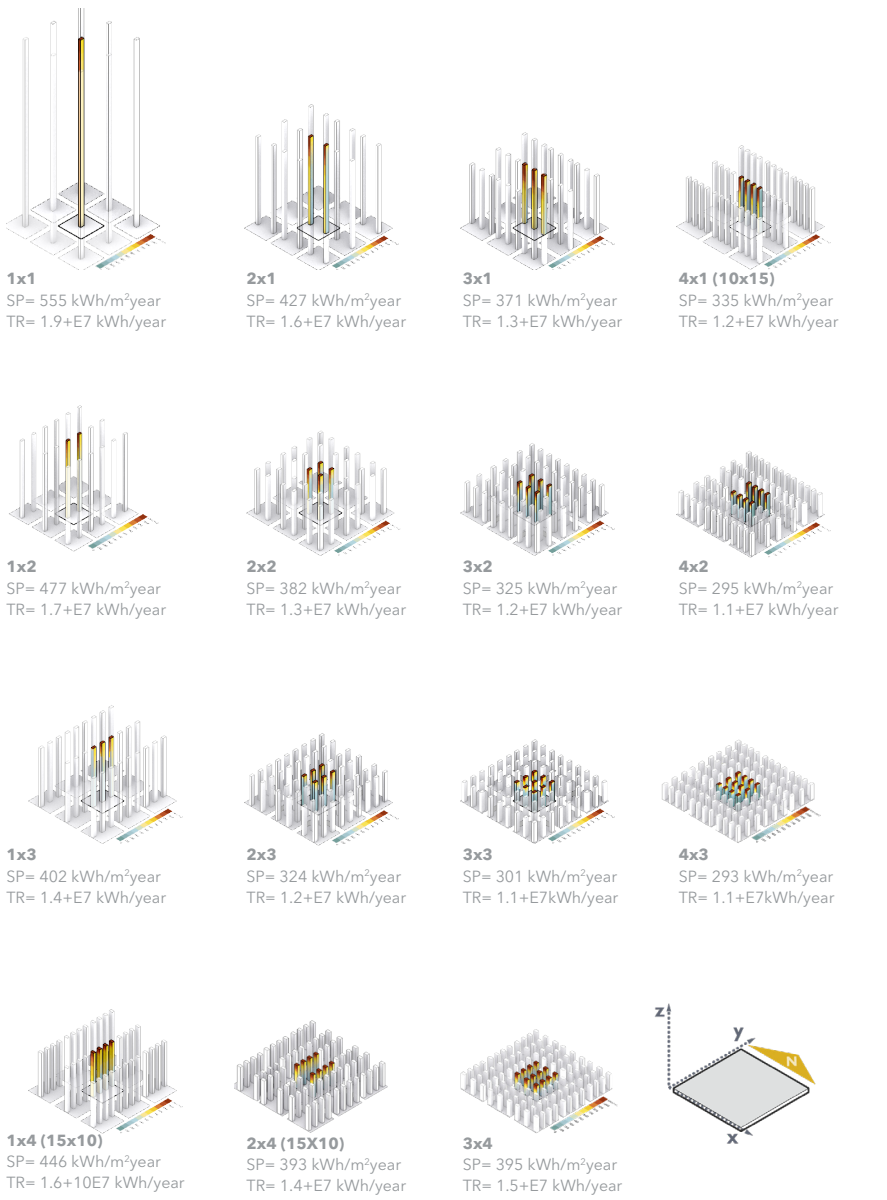

Fig. 114 3D schemes of the Solar Irradiance on the envelope for all the Tower Types showing the same base dimensions 10x15 and or 15x10 for Cluster Four (Weather Station: New York; LaGuardia AP_NY_USA; Period:1 JAN 1:00 - 31 DEC 24:00).

UTCI (Extreme Hot Week) vs Solar Potential (Full Year)

In following dispersion charts data UTCI and Solar Potential for all the iterations have been plotted in order to compare the behavior of all the Tower Types together. In a second moment, they have been subdivided into different UTCI and Solar Radiation ranges (Fig.34-35). By looking at Fig. 34 it is possible to see that only type 1x1 (top right corner) and the 2x1_10x20 belong to the very high UTCI range. For this reason this cases (16 in total) could be definitely excluded from the choice of the best performing cases.

The second range , the "High" one, includes 40 cases and represented the second more populated after the "Medium" one, with 63 cases in total. Lastly, only 9 cases belong to the "Optimal" UTCI range, which represents the best summer scenario for the UTCI. It is not surprising to find in the high range zone the type, such as 2x1, 3x1, 4x1, 1x2 and 1x4, with a row of buildings showing a preferable orientation, because of the assumptions made in UTCI paragraph. Therefore, some more consideration could be formulated by comparing the different orientations in terms of UTCI and Solar Radiation combined: considering the graph it is possible to understand the N-S orientation is generally the one which displays the higher solar potential, but the E-W one is generally showing lower UTCI values and so works better in preserving the outdoor comfort. On the other side, the more homogeneous arrangements, instead, are located in the Medium-Low ranges of UTCI.

Moving to the Solar Radiation, the preferable cases should be those which are collecting the higher amount of energy and so being located either in the Medium or High ranges. In the graph, it is very evident the relationship between number of buildings and Solar Radiation mentioned

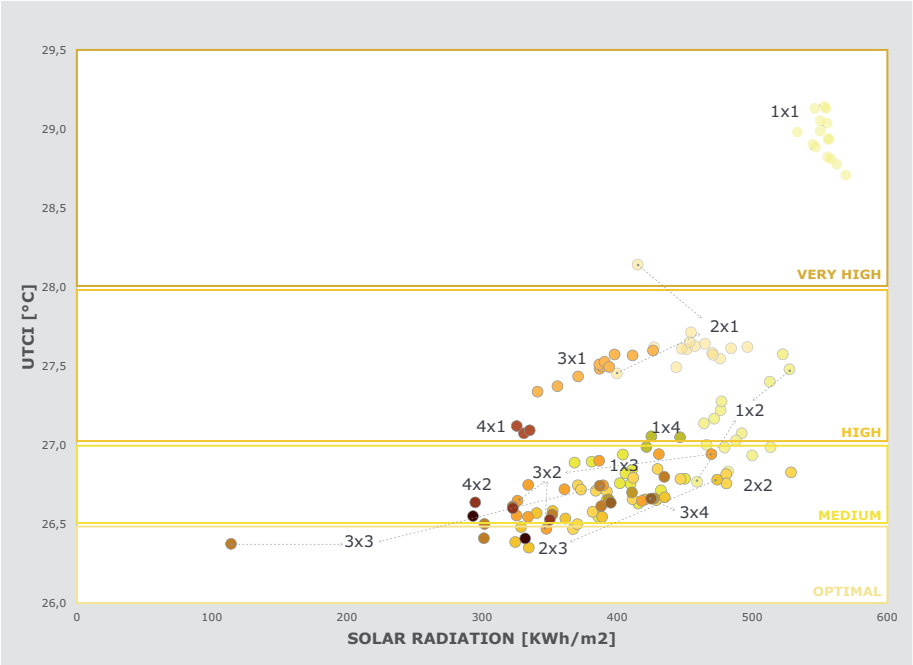

Fig. 115 Scattered Chart comparing Solar Radiation (Horizontal Axis) and average UTCI (Vertical Axis), with horizontal subdivision in average UTCI's bands.

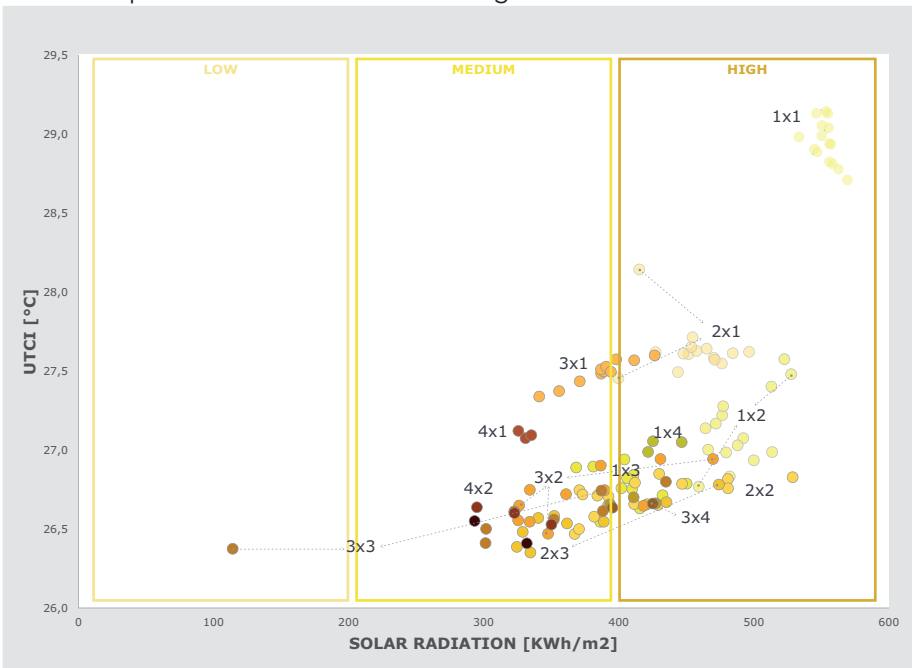

Fig. 116 Scattered Chart comparing Solar Radiation (Horizontal Axis) and average UTCI (Vertical Axis), with vertical subdivision in average Solar Radiation's bands.

above. In fact, the Medium range contains generally those types with more than 6 buildings, starting from 6 (type 3x2) to 12 (3x4 or 4x3), oppositely from those with a number of buildings from 1 to 4 (with the exception of types 3x4 and 3x3 which are values belonging to both ranges).

The selection of the best "area" where the "champions" should be located has been performed by merging the Medium-Low/Low UTCI areas included between 27 and 26 °C and the High Range Solar Radiation area. In the below graph (left) it is possible to differentiate three different zones that will be described in the following table, that can be used to classify the different cases according to the zone they belong to:

Table d. Identification of UTCI and Radiation Zones

Color	*Solar Potential*	*UTCI*	*Result*
White	High	Medium-Low/Low	Good summer outdoor comfort and high yearly solar potential
Lower Light Grey	Medium-Low	Medium-Low/Low	Good summer outdoor comfort and medium-low yearly solar potential
Upper Light Grey	High	High/Very High	Poor summer outdoor comfort and high yearly solar potential
Dark Grey	Medium-Low	High/Very High	Poor summer outdoor comfort and low solar potential

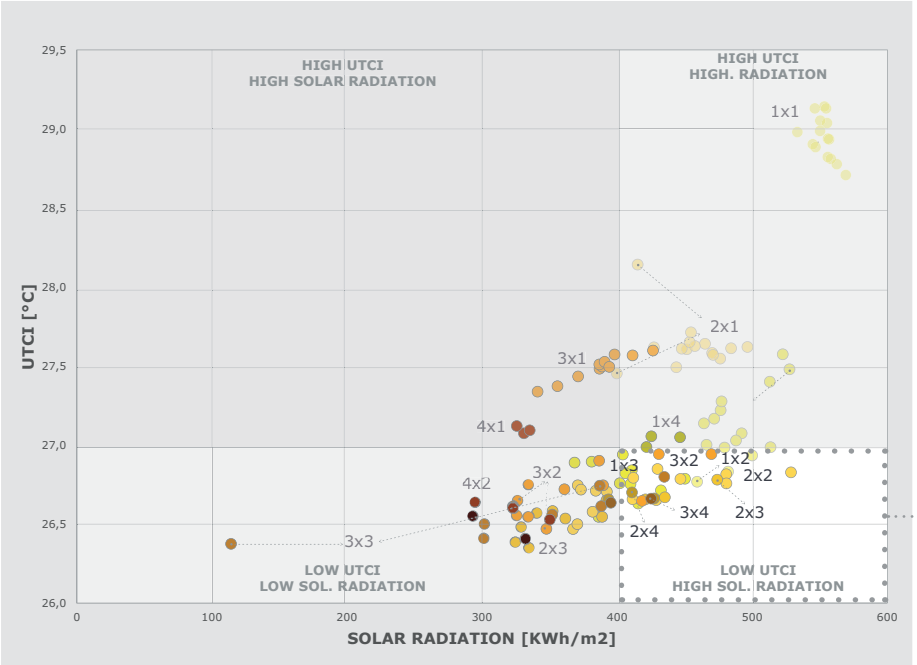

Fig. 117 Scattered Chart comparing Solar Irradiance (Horizontal Axis) and average UTCI (Vertical Axis), with further subdivision into 4 color zones representing different levels of the parameters.

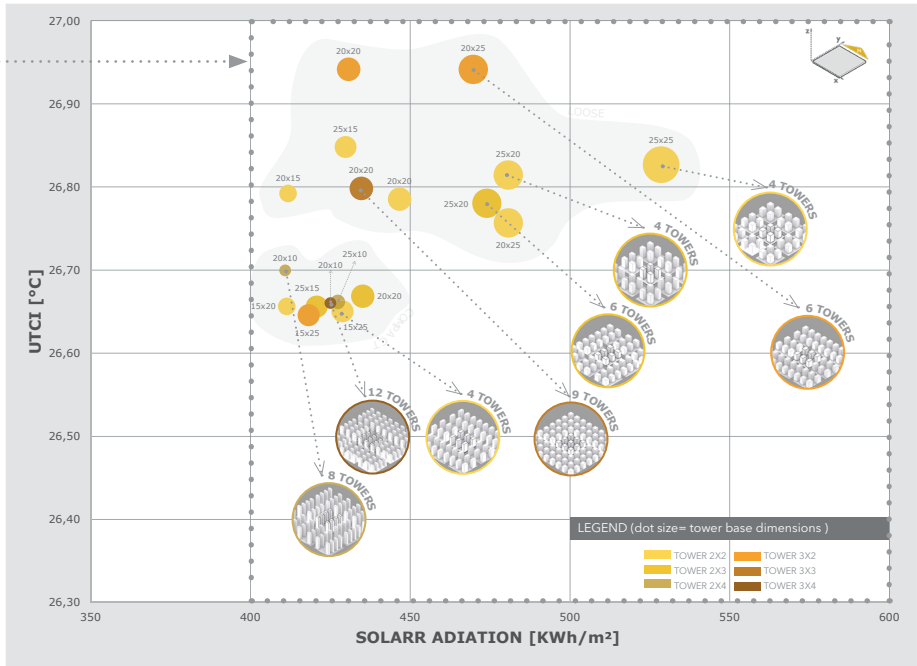

Fig. 118 Scattered Chart comparing Solar Irradiance (Horizontal Axis) and average UTCI (Vertical Axis) focused on the "white area" (26°C<UTCI<27°C; S.R.>400 kWh/m²) and identification of the relevant cases.

Bar Typology

Average UTCI (Extreme Hot Week)

In general, all the obtained results for the Extreme Hot Week scenario, like for the Tower type, belong to the "Moderate Heat Stress" Range of the UTCI's Assessment Scale, which ranges from 26°C to >29°C. Also in this case, since in human perception of heat stress even smaller variations of temperature are relevant, it is interesting to further analyze and comment the variations among the data.

The two bar charts below correspond to the two orientations. In each chart data have been divided into 4 main groups corresponding to the number of buildings of the arrangement, which will be generally called "types".

What is immediately evident is the presence of two very different trends characterizing the two orientation: the N-S one shows a more "standard" behavior, where it is possible to see a neat increase in the UTCI values of each group with the same x dimension as far as the y dimension (the longer) is decreasing from 100 to 40 m. Moreover, while the x dimension is decreasing from 25 to 10 m the values are also getting lower. In fact, the group where x is equal to 10 m and, as a consequence, the one with smaller base dimensions is also the one which is showing the lowest temperatures.

Furthermore, also the number of buildings is affecting in a strong way the data: the higher values overall are registered for the 3 bars type, followed by the 1 bar, the 2 and the 4 bars types. The reason behind this differences in the number of buildings deserves a further analysis which will be carried out later on in this chapter.

It is very evident that, the E-W orientation presents a completely different behavior from N-S one. In this case, it is not possible to define a specific trend to be followed like in the previous case, despite temperature levels of both orientations are comparable. So, for this case the UTCI'svariation is less dependent by changes in the base dimensions. It is rather still valid the effect of the number of buildings showed by the N-S orientation, with higher values for the 3 bars type, followed by the others.

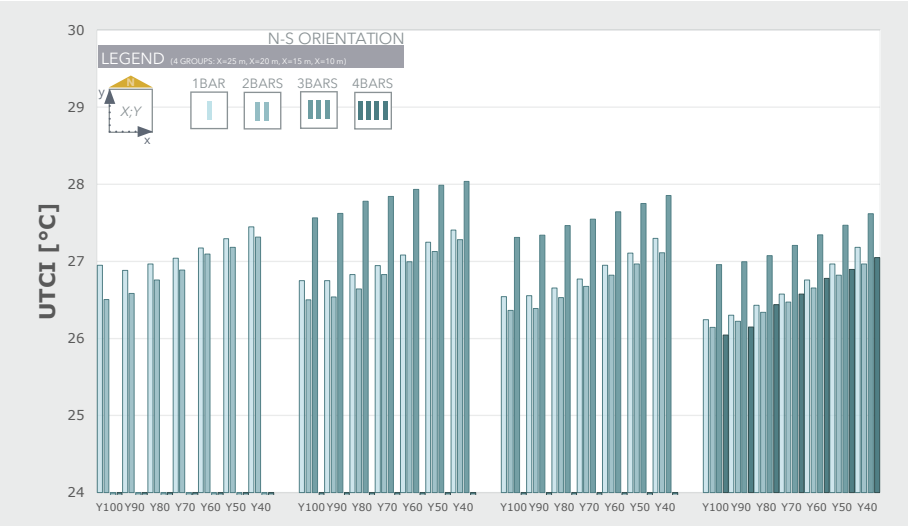

Fig. 119 Avarage UTCI values for all the iterations of the Bar Typology showing a N-S Orientation.

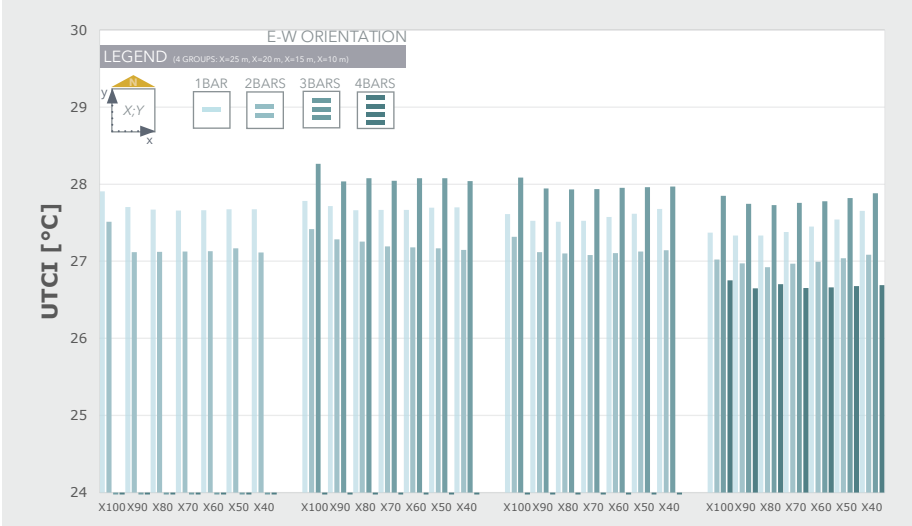

Fig. 120 Avarage UTCI values for all the iterations of the Bar Typology showing a E-W Orientation.

By looking at the 1 bar type it is interesting to notice that, as far as the x-dimension is changing from 100 to 40 m the UTCI's values have the tendency to be higher for x equal to 100m, then lower for y equal to 90 or 80 m and then to raise toward the 10 m dimension. The same behavior is also characterizing the 3 bars type and the 2 bars one only for the y equal to 10 m. In the other three cases (Y equal to 25, 20 and 15 m) the values for the 2 bars type are generally decreasing as far as the x dimension is decreasing. Lastly, for the 4 bars type, differently from the N-S orientation, the UTCI values could be considered constant for all the variations.

UTCI Comfort Maps

Since the bar charts presented above are displaying for each type the average value of the UTCI on the zoning lot, a more punctual analysis could be performed in order to evaluate how temperatures are distributed on the ground. In fact, even if a type has a very low UTCI, this does not necessarily mean that the type in question represents the best scenario; in fact, the average temperature could be low but big thermal asymmetries could be still present.

In order to provide a visual representation, on the right the UTCI maps for each type, with fixed base dimensions equal to 10x90m and 10x50m (N-S orientation) and 90x10 m and 50x10 m (E-W orientation), are provided. The main aim consists in understanding how changes in base dimensions and number of building are affecting the UTCI distribution on the ground surface. It is immediately clear the reason why, in general, the N-S orientation is showing lower results: the sun-path follows a West-East direction and for this reason, when buildings are N-S oriented they provide more shading benefits to the zones between them. On the contrary, when buildings result

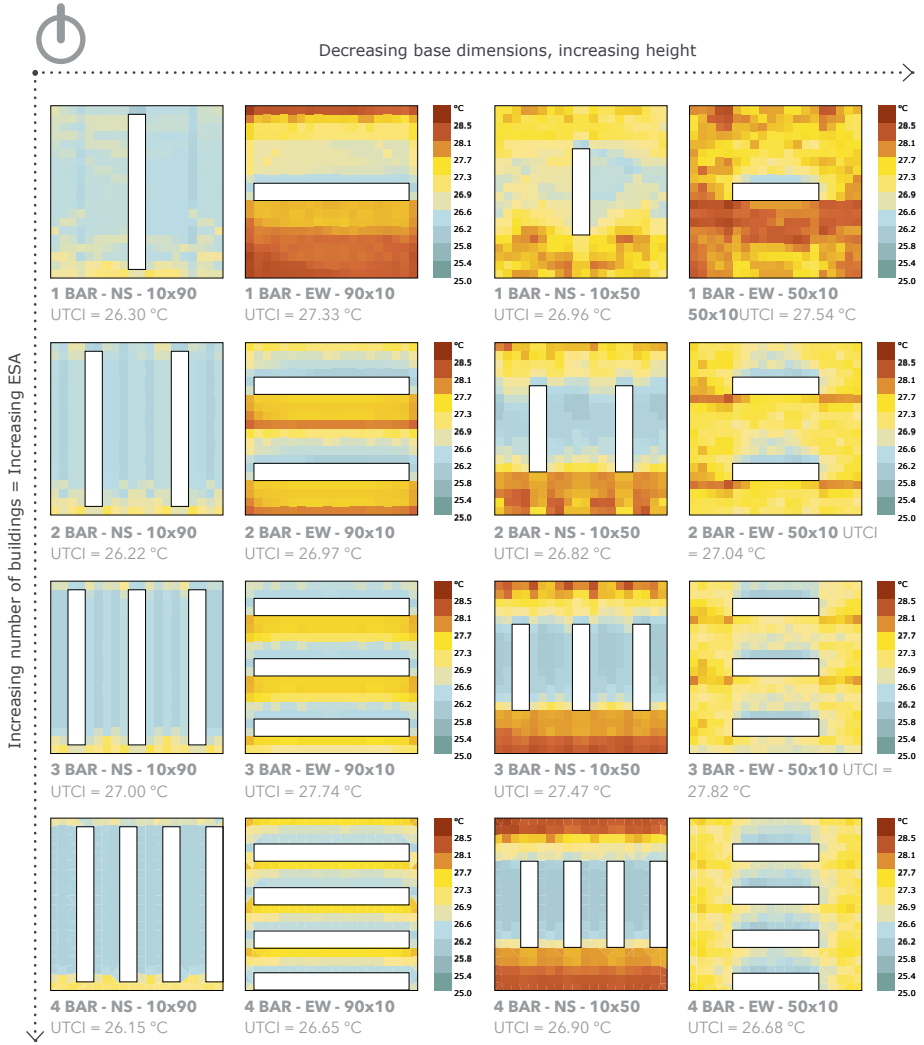

Fig. 121 UTCI comfort maps for all the Bar types with equal bigger base dimensions 10x90 m (N-S) or 90x10 (E-W) and smaller base dimensions10x50 m or 50x10 m (Weather Station: New York; LaGuardia AP_NY_USA; Period:1 JAN 1:00 - 31 DEC 24:00).

aligned with the sun path in the space in the middle of them the shading effect is no longer effective resulting in big thermal asymmetries. These thermal asymmetries are concentrated on the base of the buildings South-oriented due to the stronger solar radiation coming from this side.

Furthermore, by means of comparison of different base dimensions, for both orientations, when the longest dimension of the buildings is almost occupying the entire extension of the plot (x or y equal to 90 m) the average temperature is generally lower. This happens because, as far as the longer dimension of the bar decreases, more space could be affected by the radiation without adequate shading. In this case, even if temperature levels are comparable the N-S orientation is the one showing less asymmetries.

Solar Potential

In the following section the bars' typologies will be evaluated according to the Solar Irradiance on the envelope of the buildings. Reference is made to the amount of radiation falling on the building geometry on each of the test points. In fact, being Solar Energy use, alongside with Outdoor Comfort, the main focus of the present paper, this kind of study could be useful to the designer in order to identify solar heat gains (and so the amount of energy that could be collected), and eventually foreseen the installation of Solar Collectors or PV Panels on the roof/facades.

By looking at the image on the right it is possible to see that the orientation is not playing a big role in the solar potential. In fact, N-S and E-W cases of the same type with the same base dimensions do not show strong differences in the amount of solar irradiance annually collected. The only noteworthy aspect is that the E-W orientation is always showing slightly higher values of solar irradince if compared to the N-S one. In fact, in the first case the wider facade of buildings is South exposed and so is gathering more energy not only on the roofs but also on the top part of the South-ex-

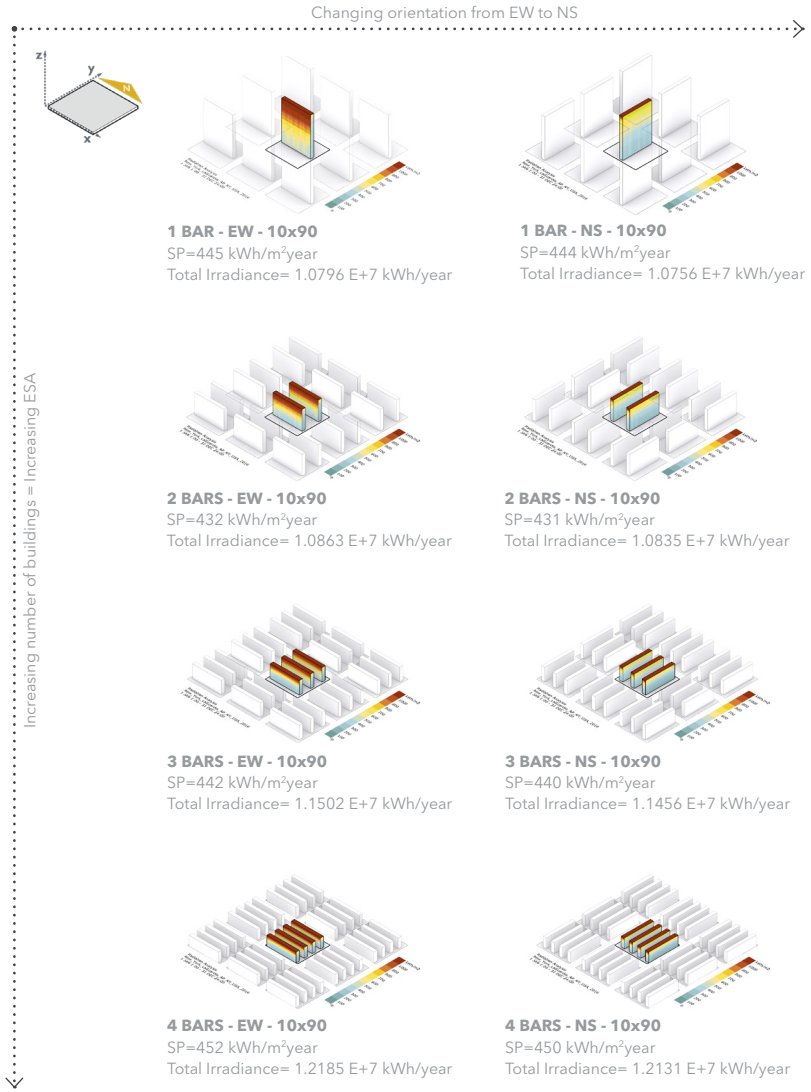

Fig. 122 3D Schemes for Solar Radiation on the envelope for all the Bar types with equal bigger base dimensions 10x90 m (N-S) or 90x10 (Weather Station: New York; LaGuardia AP_NY_USA; Period:1 JAN 1:00 - 31 DEC 24:00).

posed walls. Conversely, in the N-S orientation the smaller surface of the blocks is facing South, and so is less capable of collecting energy.

Other interesting observations could be done referring to changes in the number of buildings. From the bar charts on the right it is possible to see that, in both orientations:

- For the type with 2, 3 and 4 bars the solar irradiance is generally decreasing as far as also base dimensions are (i.e. x from 25 to10 m and y from 100 m to 40 m for the N-S orientation; x from 100 to 40 m and y from 25 m to 10 m for the N-S orientation).
- The 1 bar type needs a more careful analysis; in fact, its values of solar irradiance are decreasing parallel to base dimensions, when the shortest dimension (either x or y) is equal to 25 and 20 m but, then, for 15 and 10 m, the solar radiation is increasing as far also base dimensions are decreasing.

Regarding the variations in the number of buildings, it is remarkable to point out that their variation are related to changes in the base dimensions, in particular to those of the shortest dimension. This fact could be understand by looking at the bar chart down on the right. Here the trends of each bar type are highlighted trough dotted lines (tendency lines). Generally, in every group of data with the same x-dimensions when base dimensions are bigger (Y100) the types with more buildings present higher solar radiation, but, in each group, there is always a "trend inversion" which happens when y dimension reaches a specific values. This value is changing in a predictable way and is moving, as far as the x is changing from 25 to 10 m, towards the Y100. The "trend inversion" happens at Y50 for X25, at Y70 for X20, at Y80 for X15 and at Y90 for X10m.

The same applies for the E-W orientation, but, in avoid repetitiveness, the data weren't plotted because very similar to the N-S ones.

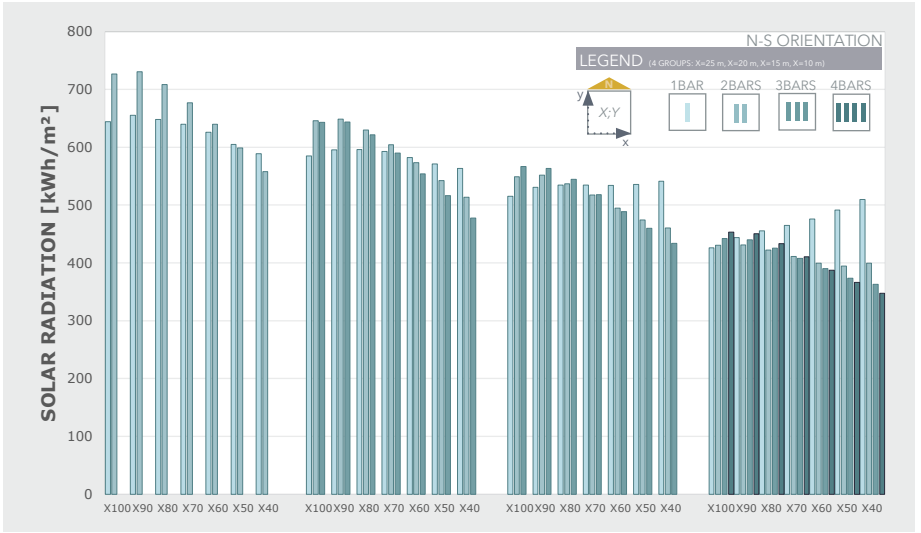

Fig. 123 N-S orientation, yearly solar radiation (kWh/m²) on the envelope.

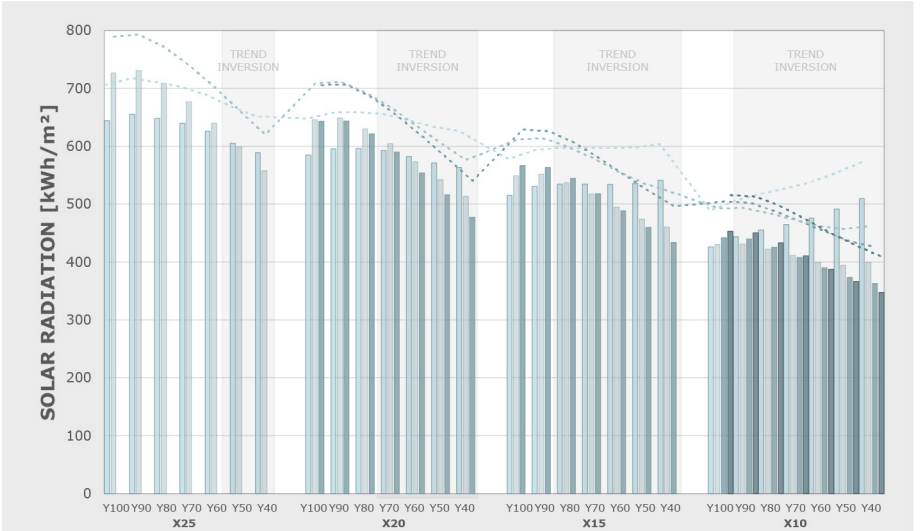

Fig. 124 N-S orientation, analysis of the yearly solar radiation (kWh/m²) on the envelope.

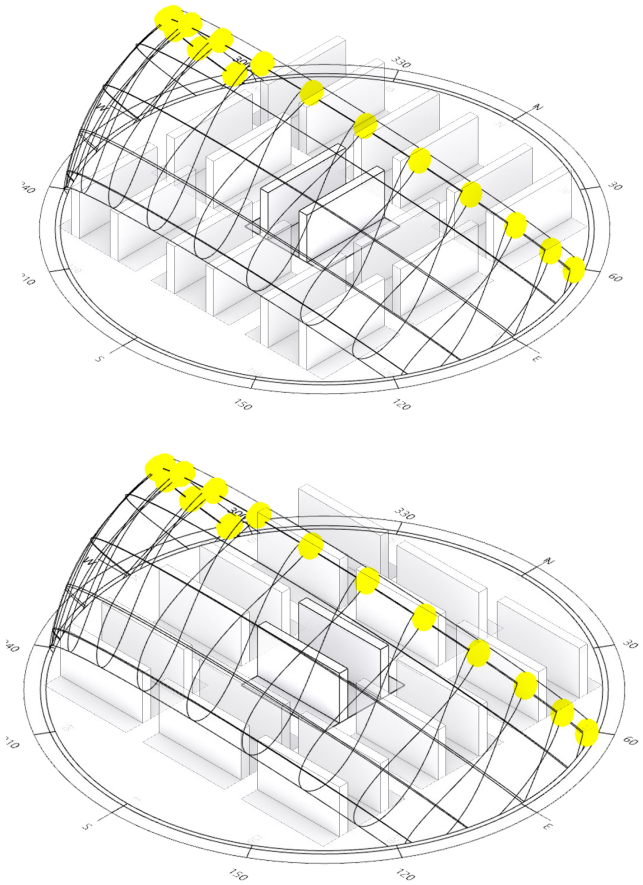

Fig. 126 Sunpatch for N-S (Top) and (E-W) orientation (July 15th-21st)

Everything that have been stated in the previous paragraphs regarding the building orientations could be verified in the above picture, showing the sun-path, for the extreme hot week in the two possible scenarios (the 2 bar type has been arbitrary chosen).

UTCI (Extreme Hot Week) vs Solar Potential (Full Year)

The image of the previous page shows the dispersion chart including all the values obtained for the bar type for the UTCI and the Solar Radiation in order to show where the main types are located in respect to each others comparing both values. The text on the right indicates where are the main groups located in terms on UTCI.

In the two graphs of the following page, orientations have been further subdivided in order to understand how base dimension are affecting the position of each simulated case. In each graph the magnitude of the dots indicated the base dimensions of each module composing the type (e.g. for the 3 bars case the 25x100 indicates that all the 3 bars have a base

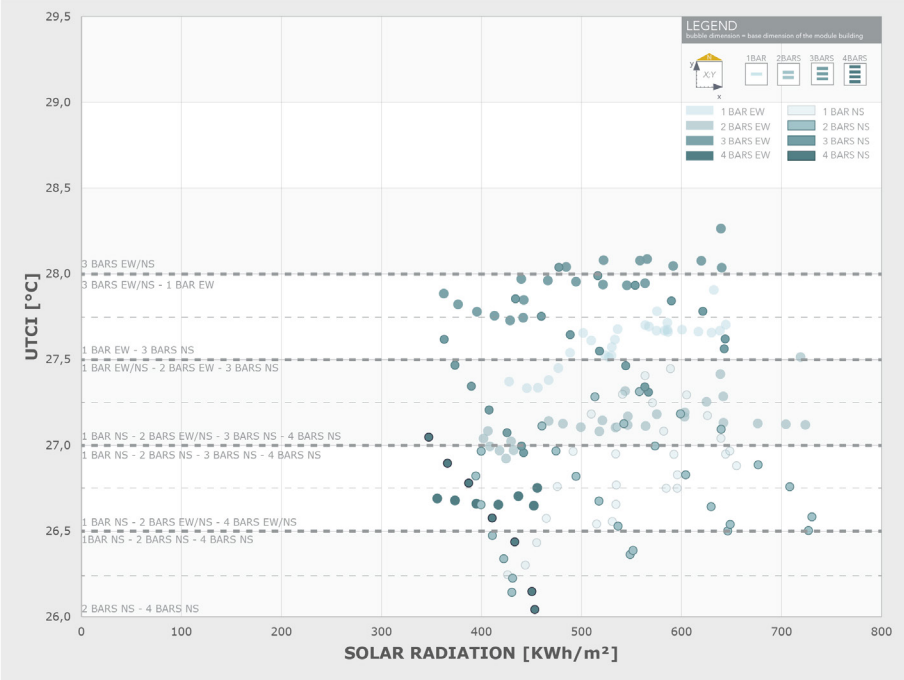

Fig. 125 UTCI (Extreme Hot Week) vs Solar Potential (Full Year), overall results for the bar type.

area of 2500). Moreover the arrows are showing the direction of increase of the base dimensions of the buildings.

In the left graph (N-S orientation) it is possible to see the distinction of the three main groups with common x dimension (the shorter) where a decrease of the UTCI is parallel to an increase of the base dimensions and increase of the solar potential. Moreover, combining all the groups trends it is evident that as far as base dimensions are increasing the UTCI increases but the solar potential also does.

The right graph (the E-W) shows a similar behavior with increasing solar potential parallel to an increase of the base dimension from left to right. The only difference with the N-S orientation is that here there is not a very neat UTCI gap between the y dimension's group of the same type. It is possible to state that, in general, the UTCI inside the same type does not change more than 0.5 °C. Moreover, the 4 types are more independent in terms of both UTCI and solar potential from each other compared to the ones of the other orientation that were registering more overlapping zones of values.

In the next graph (left in the next page) the data have been classified in the same "zones" of UTCI and solar radiation identified in the Towers' Chapter. For the sake of simplicity (in order to be later on able to compare all typologies), the levels of both parameters will be the same for all the analyzed categories.

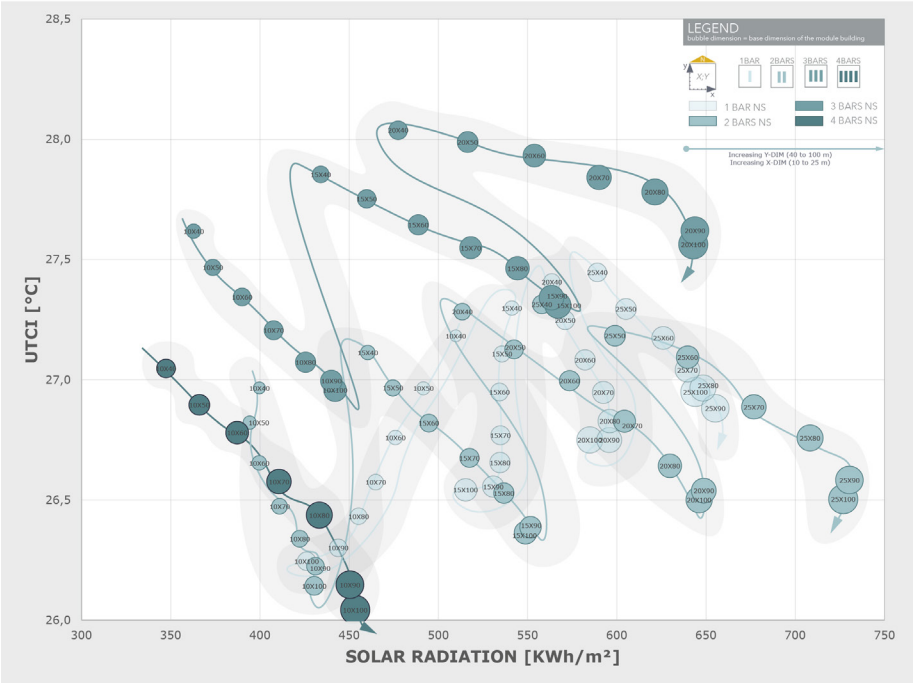

Fig. 127 Chart X: N-S orientation, UTCI (Extreme Hot Week) vs Solar Potential (full year) and relationship with base dimensions..

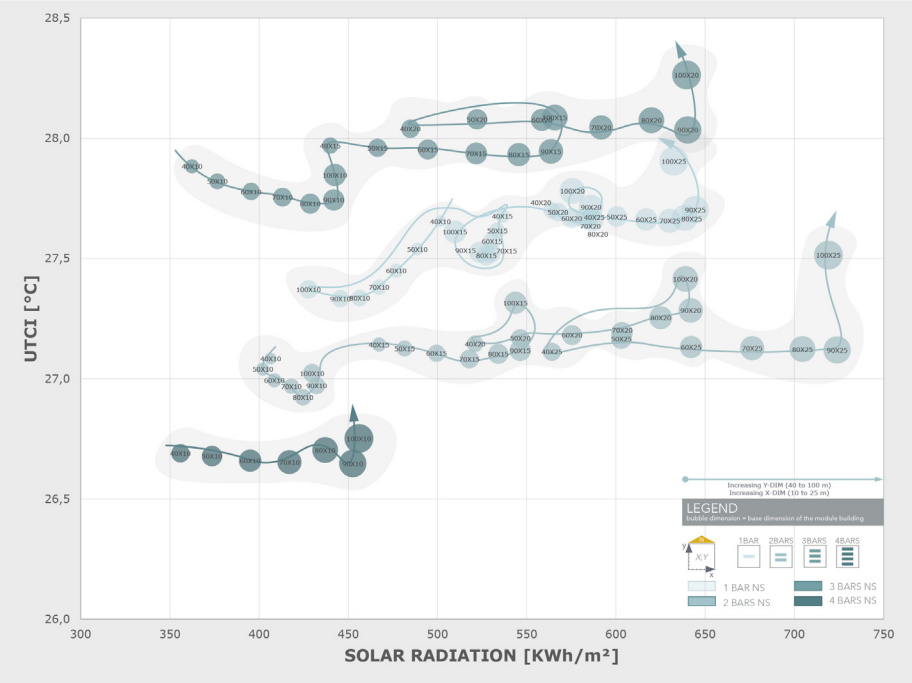

Fig. 128 Chart X: E-W orientation, UTCI (Extreme Hot Week) vs Solar Potential (full year) and relationship with base dimensions..

Table e. Evaluation of the different classification zones

Color	*Solar Potential*	*UTCI*	*Result*
White	High	Medium-Low/Low	Good summer outdoor comfort and high yearly solar potential
Lower Light Grey	Medium-Low	Medium-Low/Low	Good summer outdoor comfort and medium-low yearly solar potential
Upper Light Grey	High	High/Very High	Poor summer outdoor comfort and high yearly solar potential
Dark Grey	Medium-Low	High/Very High	Poor summer outdoor comfort and low solar potential

In the last graph, which is combining the best cases identified in the previous one, is possible to notice that on the right are mostly present those cases showing a N-S orientation, but also some E-W oriented are still present. Moreover, for the N-S orientation cases with smaller x dimensions (shorter side,10-15 m) are mainly located in the left part of the graph, while those with bigger ones (20-25 m) on the right (higher s.r.). In each group of common x the lower values for UTCI are reached by bigger base dimensions. The tendency is reversed for the E-W orientation.

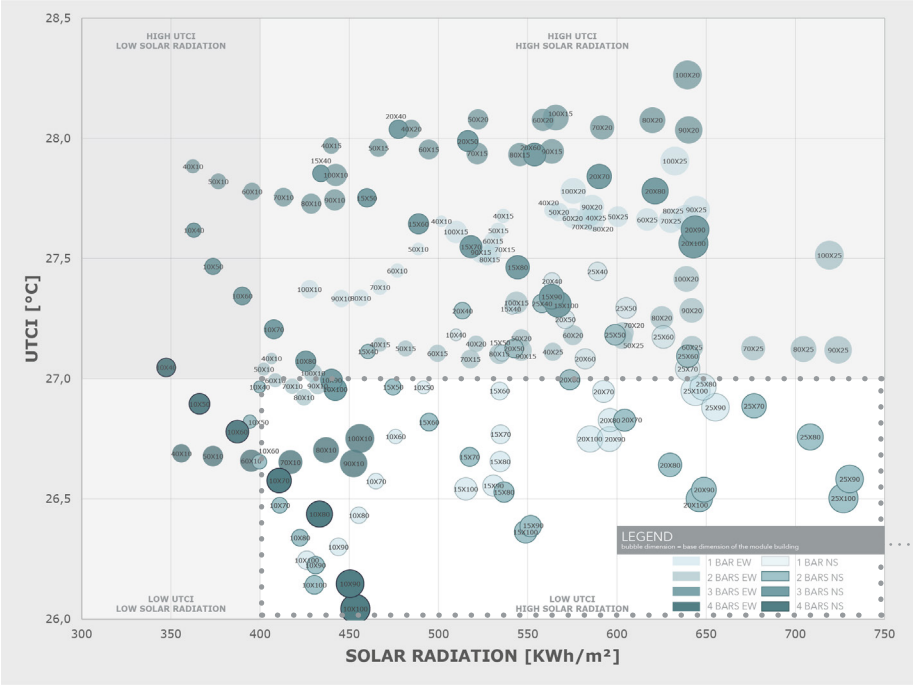

Fig. 129 Chart X: N-S orientation, UTCI (Extreme Hot Week) vs Solar Potential (full year) and relationship with base dimensions..

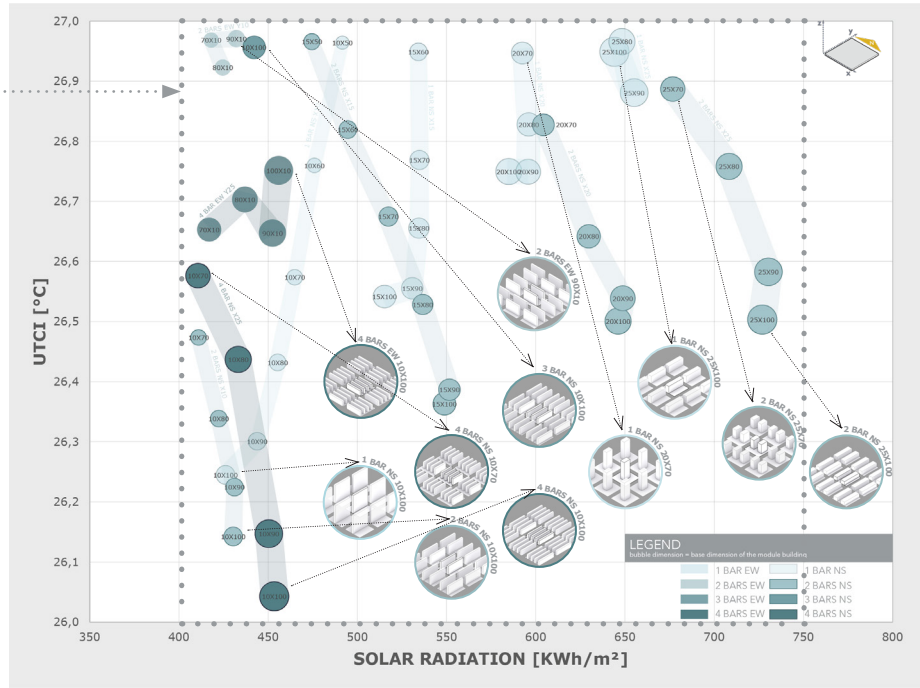

Fig. 130 Chart X: N-S orientation, UTCI (Extreme Hot Week) vs Solar Potential (full year) and relationship with base dimensions..

Courtyard Typology

Average UTCI (Extreme Hot Week)

In the bar chart on the left the average values of UTCI for each courtyard type have been plotted, while on the right is possible to see the UTCI distribution on the ground for a selected case of each type. For the sake of clarity in the comparison, it has been chosen a constant depth equal to 10 m for the No Divisions types (both No Divisions pure and No Divisions with fixed courtyard and variable setback from the street) and for the 1 and 2 Divisions.

By looking at them, it is possible to see that the 2 Divisions case N-S oriented is showing the lower values overall, while the highest values are reached by No Division case with variable sidewalk. In the first mentioned case the reason behind these lower values is pretty evident by looking at the UTCI map which shows generally lower temperature inside the three courtyards. This case is, in fact, the one where the interior courtyards have the smaller dimension; circumstance that leads to an increase of the shadow effect. The E-W orientation is displaying sightly higher values due to the most favored orientation in respect to the sun path.

On the contrary the case with fixed inner courtyard has a very small inner patio but the low temperature inside is, on the other hand, compensated by the higher peaks reached in the "frame" of land around the building adjacent to the street.

Generally, it is possible to state that as far as the building depth increases from 10 to 25 m the UTCI also does. The reason is due to the lower building height which, because of the constant FAR, is lower for buildings with higher floor areas. The decrease of the temperature inside the courtyard is related to the lack of shadow effect of shortest cases.

Another interesting consideration could be formulated using as a comparison metrics the number of inner courts. Intuitively, the higher the number of courts created in a same dimension perimeter gets, the lower will be the width of the courtyard itself. As far as the courtyard becomes long

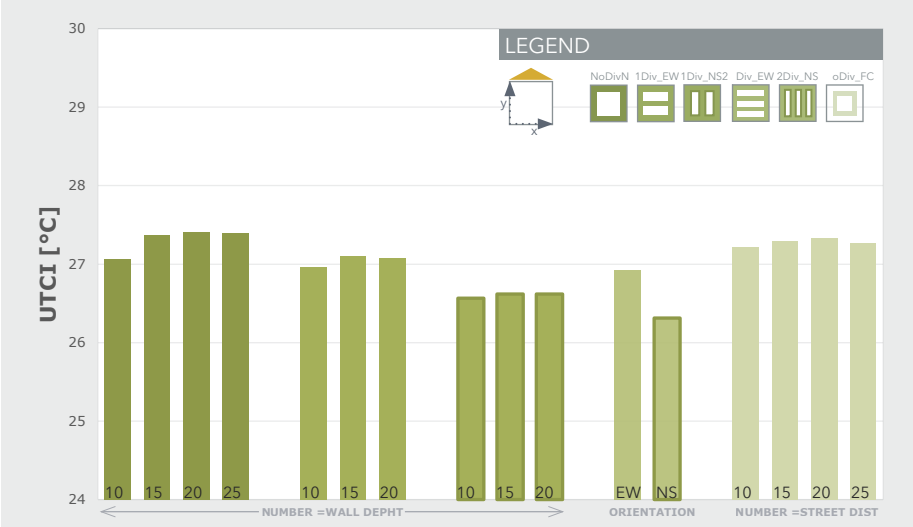

Fig. 132 Fig. X. Courtyard Typology: UTCI values for the Extreme Hot Week.

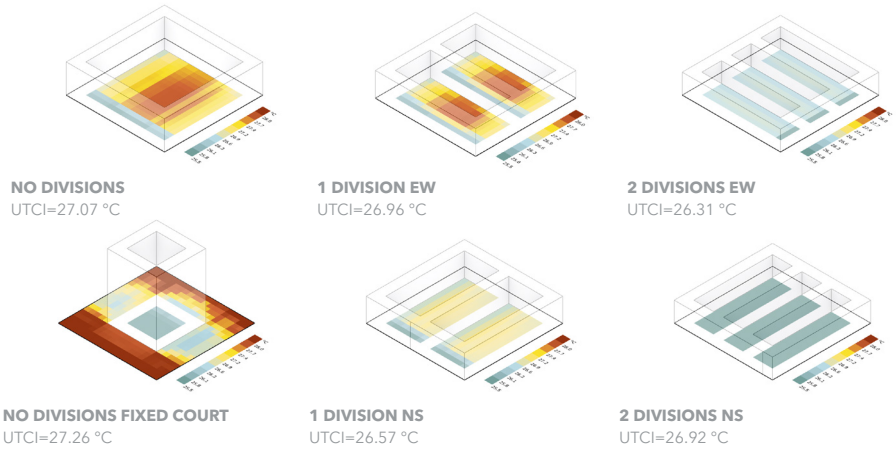

Fig. 131 Fig. X: UTCI maps for a selection of courtyard types having common 10 m wall depth (Weather Station: New York; LaGuardia AP_NY_USA; Period:1 JAN 1:00 - 31 DEC 24:00).

and "thin" the sun rays have difficulties in reaching ground. For this reason to higher number of patios correspond lower UTCI levels.

Solar Potential

In the bar chart on the left the average values of solar potential for each courtyard type have been plotted, while on the right is possible to see the Solar Irradiance distribution on the surface of each of the selected cases. For the sake of comparison, it has been chosen a constant depth equal to 10 m for the No Divisions types (both No Divisions pure and No Divisions with fixed courtyard and variable setback from the street) and for the 1 and 2 Divisions.

From the bar chart it is possible to understand the general trend of increasing solar potential alongside with the increase of base dimensions from 10 to 25 m. This tendency has been already seen, for instance, in the case if the bar. Similarly, in this typology the roof is the surface of the envelope which is more exposed to the sun-rays and so is the one which is able to collect more energy. As a consequence, the cases which are showing bigger base dimensions (an so the roof ones) are those which are presenting higher values.

Moving to the specific analysis of the radiations maps, it is generally verified that big changes in the solar potential values do not exist when there is a change in the orientation from N-S to E-W. In fact, the main surface, the roof indeed, shows the same area in both cases and the contribute brought by the other surfaces (both exterior or interior walls to the courtyard) can be considered negligible. On the other hand, is possible to see an increase in the amount of solar radiation as far as the number of inner patios increases, which could be still devoted to an increase in the percentage of "roof surfaces" incremented by the addition of a central one or more wings.

After these considerations, it possible to adfirm that the best scenario overall in terms of solar potential is represented by the No Divisions case, especially by the 25 m building depth case while the lower one by the 10 m depth case for the No Divisions with fixed patio dimensions' case.

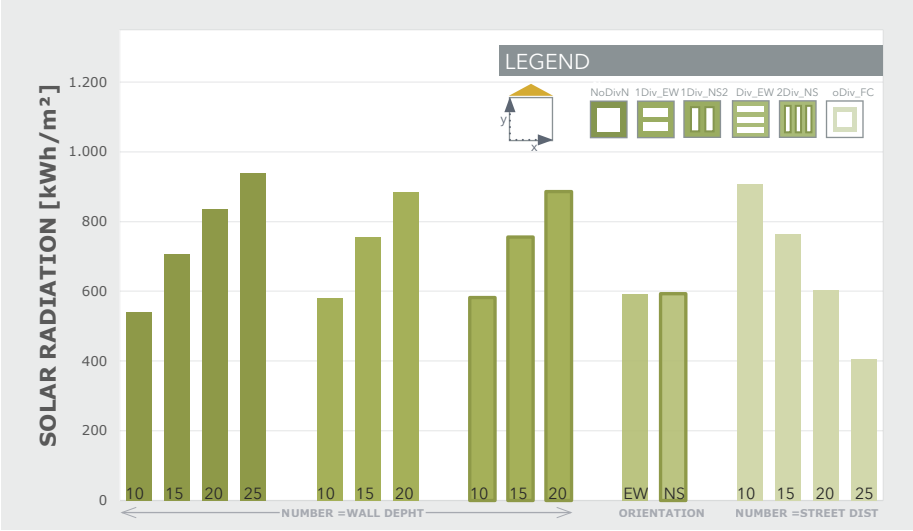

Fig. 134 Solar Potential (kWh/m²year) for the Full Year on the envelope.

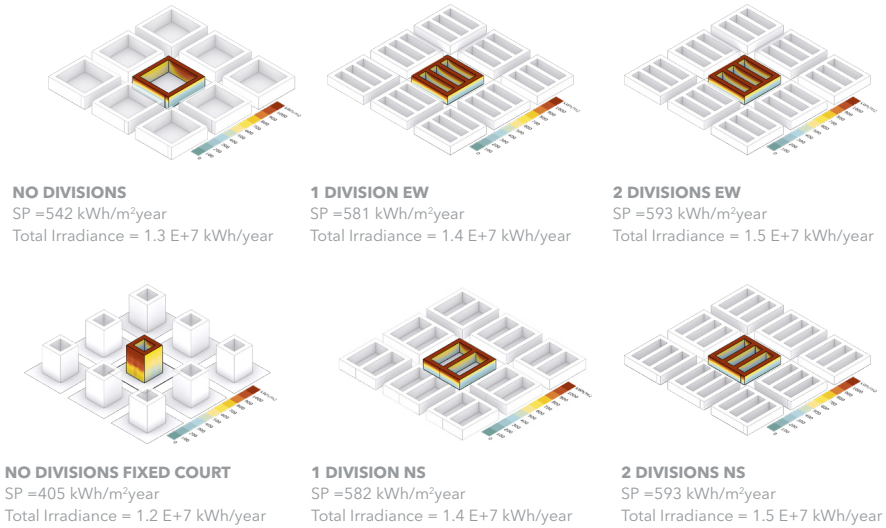

Fig. 133 Solar Potential maps for a selection of courtyard types having common 10 m wall depth.

UTCI (Extreme Hot Week) vs Solar Potential (Full Year)

In the following graphs the data of UTCI and Solar Potential have been plotted together in a dispersion chart. Moreover, the dimension of each bubble is scaled according to the base dimensions of each case. This means that, bigger bubbles will have bigger base and, as a consequence, higher Building Coverage Ratio and smaller building's height.

Having this in mind, it is generally possible to notice that the bigger base dimensions cases owe higher values of solar potential in respect to the smaller ones, but at the same time highet UTCI. Secondly, comparing the different orientations N-S cases are generally located in lower UTCI ranges compared to the E-W ones.

Considering the solar radiation it is verifiable that the this typology, compared to the other two of the Toer and Bar, cover higher levels of solar radiation because almost all the cases are located above the 400 kWh/m^2 value.

Furthermore, considering the UTCI, it is possible to define a "denser area" which includes most of the cases and is located in a UTCI range 27-28 °C. In the below graph, a selection of the best performing cased in terms of both values has been identified in the white-dotted line area and includes all the 1 Division cases, the 2 divisions E-W ans N-S oriented and the 10 m depth case of the 1 Division E-W oriented case. These will be considered the "champion cases" of these last building typology and will be compared in the final analysis with the other one from the previous typologies.

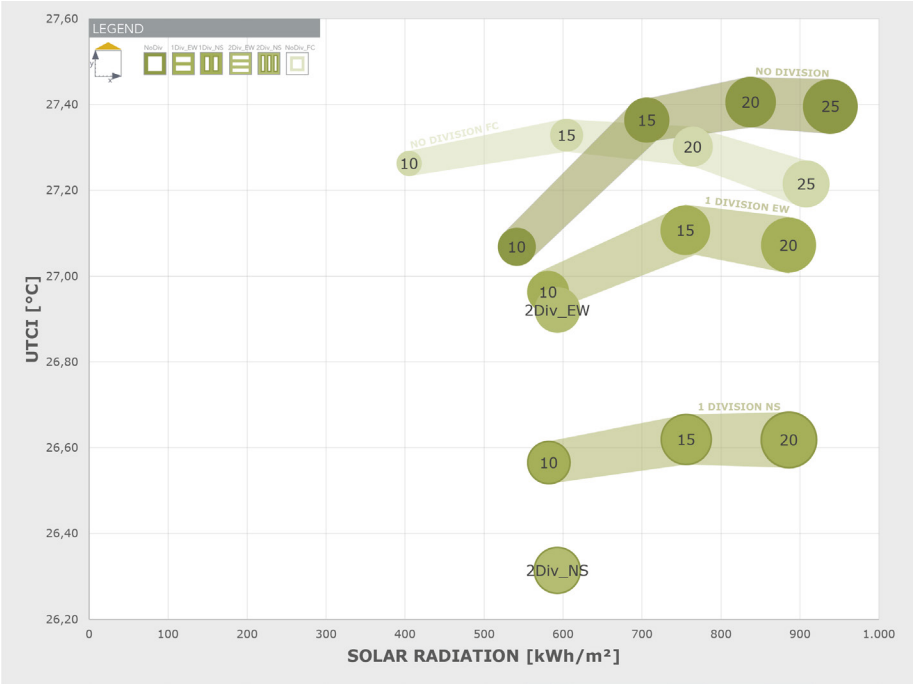

Fig. 135 UTCI (Extreme Hot Week) vs Solar Potential (full year) and relationship with base dimensions..

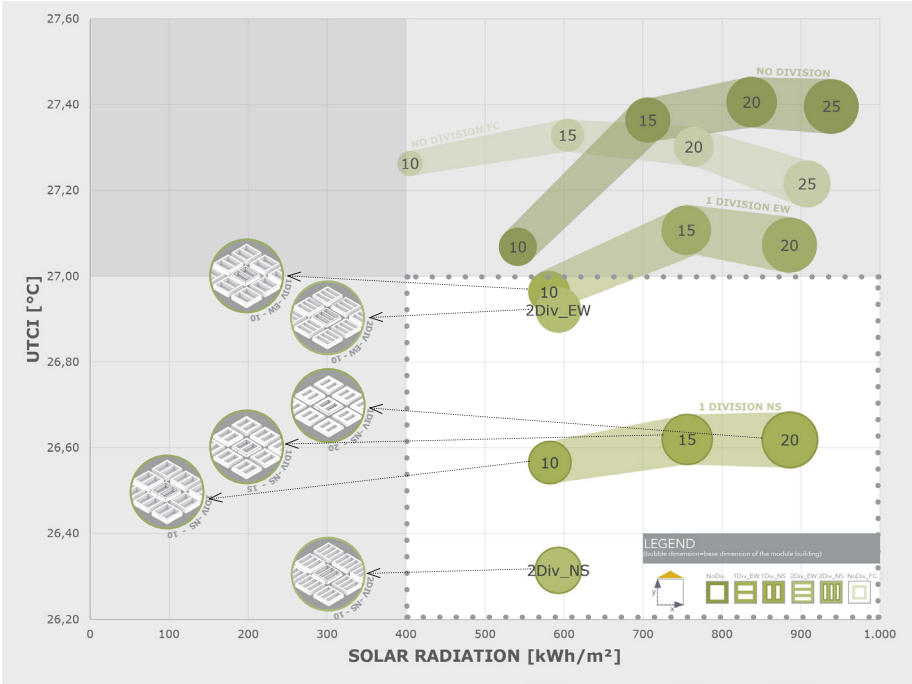

Fig. 136 UTCI (Extreme Hot Week) vs Solar Potential (full year): selection of the best cases..

5 Selection of the Champions

The following chapter will be divided into two different sections. In the first, the data collected for UTCI and Solar Potential will be compared in cumulative scattered diagram. In particular, in the diagram we will compare the cases of all three types that have "passed" the selection that saw imposed as thresholds that of 26°C-27°C as temperature range and 400 kWh/m^2 as minimum solar radiation. The second part will be devoted to a detailed analysis of the UTCI comfort maps, in order to "skim" the list of champions that have passed the previous selection. The selection criterion will be described in details later on in this chapter. First, in order to remind the reader which cases were selected, the following summary tables, with selected cases of each typology are provided with relative values of avarage UTCI and SR.

Table f. Election of the best cases among all typologies according to UTCI and Solar Potential comparison.

TYPOLOGY	*DIMENSIONS* [m]*	*HEIGHT [m]*	*BCR [%]*	*UTCI [°C]*	*S.I. [[kWh/m^2]*
COURTYARD					
1 Div. E-W	10	24	44	26,96	581
1 Div. N-S	10	24	44	26,57	582
	15	17	62	26,62	756
	20	14	76	26,62	886
2 Div. E-W	10	20	52	26,92	593
2 Div. N-S	10	20	52	26,31	593

**Dimensions are referred in case of Towers and Bars to the X and Y respectively, while in the case of Courtyards the represen-*

the building depth.

Table g. Selection of the best cases among all typologies according to UTCI and Solar Potential comparison.

	DIMENSIONS [m]*	*HEIGHT [m]*	*BCR [%]*	*UTCI [°C]*	*S.I. [[kWh/m^2]*
TOWER					
2X2	25X25	42	25	26,83	529
	25X20	53	20	26,81	481
	25X15	70	15	26,85	430
	20X25	53	20	26,76	481
	20X20	66	16	26,79	447
	20X15	88	12	26,79	412
	15X25	70	15	26,65	429
	15X20	88	12	26,66	411
2X3	25X20	35	30	26,78	474
	25X15	47	23	26,66	421
	20X20	44	24	26,67	435
2X4	25X10	53	20	26,66	427
	20X10	66	16	26.70	411
3X2	20X25	35	30	26,94	470
	20X20	44	24	26,94	431
	15X25	47	23	26,65	418
3X3	20X20	29	36	26,80	435
3X4	20x10	44	24	26,66	425

**Dimensions are referred in case of Towers and Bars to the X and Y respectively, while in the case of Courtyards the represent*

the building depth.

Table h. Selection of the best cases among all typologies according to UTCI and Solar Potential comparison.

TYPOLOGY	*DIMENSIONS* [m]*	*HEIGHT [m]*	*BCR [%]*	*UTCI [°C]*	*S.I. [[kWh/m²]*
BAR					
2 BARS E-W	*90X10*	17	18	26,97	432
	80X10	19	16	26,92	425
	70X10	21	14	26,97	418
	60X10	25	12	26,99	408
4 BARS E-W	*100X10*	8	40	26,75	456
	90X10	8	36	26,65	452
	80X10	9	32	26,70	437
	70X10	11	28	26,65	417
1 BAR N-S	*25X100*	12	25	26,95	644
	25X90	13	23	26,88	655
	25X80	15	20	26,97	648
	20X100	15	20	26,75	585
	20X90	17	18	26,75	596
	20X80	19	16	26,83	596
	20X70	21	14	26,95	592
	15X100	20	15	26,54	515
	15X90	22	14	26,56	531
	15X80	25	12	26,66	535
	15X70	28	11	26,77	535
	15X60	33	9	26,95	534
	10X100	8	10	26,25	426
	10X90	8	9	26,30	444
	10X80	9	8	26,43	455
	10X70	11	7	26,57	465
	10X60	13	6	26,76	476
	10X50	15	5	26,96	492

TYPOLOGY	*DIMENSIONS* [m]*	*HEIGHT [m]*	*BCR [%]*	*UTCI [°C]*	*S.I. [[kWh/m²]*
BAR					
2 BARS N-S	25X100	6	50	26,50	727
	25X90	7	45	26,58	730
	25X80	8	40	26,76	708
	25X70	9	35	26,89	677
	20X100	8	40	26,50	646
	20X90	8	36	26,54	649
	20X80	9	32	26,64	630
	20X70	11	28	26,83	604
	20X60	13	24	27,00	574
	15X100	10	30	26,36	549
	15X90	11	27	26,39	552
	15X80	13	24	26,53	537
	15X70	14	21	26,67	517
	15X60	17	18	26,82	495
	15X50	20	15	26,97	475
	10X100	15	20	26,14	430
	10X90	17	18	26,22	431
	10X80	19	16	26,34	422
	10X70	21	14	26,47	411
3 BARS N-S	10X100	10	30	26,96	442
	10X90	11	27	27,00	440
4 BARS N-S	10X100	8	40	26,04	453
	10X90	8	36	26,15	450
	10X80	9	8	26,44	433
	10X70	11	7	26,58	411

**Dimensions are referred in case of Towers and Bars to the X and Y respectively, while in the case of Courtyards the represent the building depth.*

The following scattered chart is combining the three typologies according to the obtained results for both evaluated parameters. Furthermore, the dimension of the "bubbles" of the diagram are also sized according to the percentage of occupied area. For instance, the smaller sizes represent cases such as the Towers or the 1 Bar types, while the bigger ones, instead, bigger numbers of buildings or base areas which are more developed in extension on the ground rather than in height, such as the Courtyard cases. As a consequence, to bigger base dimensions, because of the constant FAR, correspond a lower height and vice-versa for smaller ones.

It possible to clearly recognize an area denser than the others correspondent to the 400-500 kWh/m^2 range of solar potential. This zone is including almost all the tower cases (exception is made for the 2X2_25X25 case) and the E-W oriented cases from the Bar type, which were also identified before to perform badly if compared to the N-S ones. Moreover, the same area could be also identified as the one which is having the higher values of UTCI and so performing the worst in terms of both parameters. Conversely, the right part of the chart (with a S.R. higher than 500 kWh/m^2) displays a predominance of the Bar/Courtyard types. For the Bar, the categories which are mainly present are the 1-2 bars N-S oriented.

It is possible to deduce from this graph that, for all typologies, cases with bigger base dimensions are advantaged not only for UTCI but also for the capability of collecting solar energy. In fact, the best case overall in terms of solar potential is constituted by the Courtyard type N-S oriented with 1 Division and a building depth equal to 20 m. The case itself, but also the others of the same typology, is showing in general quite low values of UTCI (around 26,5 °C). On the contrary, considering the UTCI, the best case in these terms is represented by the 4 bars type N-S oriented 10x100.

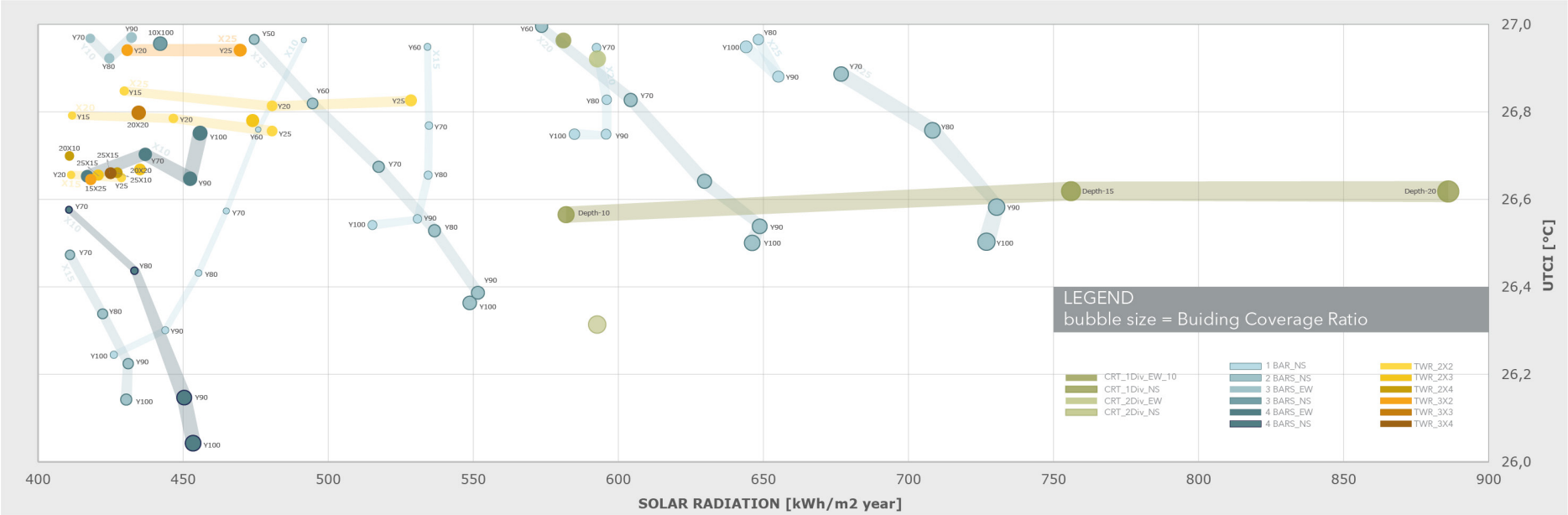

Fig. 137 UTCI vs Solar Radiation, comparison of the three typologies according to the results of the previous phase.

Detailed UTCI analysis of the identified champions

In this last section, the best cases of all types, that have been previously identified in the diagram of the previous page (i.e. those with average UTCI values between 26°C and 27°C and annual solar irradiance larger than 400 kWh/m2) will be further screened using the method described below.

The UTCI values that have been used so far as to identify the best cases were average values. The zoning lot described in the chapter about the "Massing" was in fact divided into a 5x5 meters grid. The software calculates for each "test point", or sensor, located at the center of each "patch" resulting from the division of the grid, the UTCI for each hour of the selected period (in this case "Extreme Hot Week") and makes an average, which will then be the value reported in the point. The values used so far for the UTCI evaluation are then the average of the values obtained on all patches weighted by the number of patches.

As it has already been mentioned in the chapter on the UTCI comfort maps this average value can be used to give a general description of the outdoor comfort for each typology, but it can also be misleading without taking into account the thermal asymmetries that can result from combinations of base dimensions, geometries and number of buildings. In order to make a more precise analysis of each case, an additional method has been identified. It consists in detecting, for each of the winning arrangements, the temperatures of each sensor located in each patch of the ground subdivision and subsequently to group them into the following thermal levels:

- UTCI < 25°C
- 25 °C<UTCI<26°C
- 26 °C<UTCI<27°C
- 27 °C<UTCI<28°C
- 28 °C<UTCI<29°C
- UTCI>30°C

This makes it possible to have the precise number of patches located in a specific "thermal comfort/discomfort band". In the following example the methodology is explained using as an example the Tower type 2x3.

Table i. Numbers of ground patches falling into each temperature range for the 2x3 type.

Temperature Range [°C]	*25x25*	*25x20*	*25x15*
X<25	0	0	0
25<X<26	0	0	0
26<X<27	135	73	51
27<X<28	170	135	143
28<X<29	14	173	144
29<X<30	0	71	49
X>30	0	0	0
TOTAL N. OF PATCHES	319	452	387

Since, however, the number of patches into which the land is divided depends on the base size of the arrangements, it is not possible to obtain a comparative unique graph for all types, unless the data are not converted into percentages.

Table j. Percentages of ground patches falling into each temperature range for the 2x3 type.

Temperature Range [°C]	*25x25*	*25x20*	*25x15*
X<25	0%	0%	0%
25<X<26	0%	0%	0%
26<X<27	42%	16%	13%
27<X<28	53%	30%	37%
28<X<29	4%	38%	37%
29<X<30	0%	16%	13%
X>30	0%	0%	0%

Combining the informations of the previous tables it is possible to obtain the bar chart on the top right, where columns are representing the number of patches falling into the temperature ranges and the text the percentages dividing each value by the total.

After these preliminary steps data have been plotted into a cumulative frequency chart. A cumulative frequency plot is a way to display cumulative information graphically. It shows the number, percentage, or proportion of observations that are less than or equal to particular values. In a data set, the cumulative frequency for a value x is the total number of scores that are less than or equal to x. To construct the graph the number of patches relative to a specific temperature range is added to the previous value, the data converted to percentage values and finally represented as in the graph on the right.

According to the UTCI Assessment Scale seen in the first chapters, temperatures from 26°C to 32°C belong to the "Moderate Heat Stress" category and those between 9°C and 26°C to the "No Thermal Stress" one. Beginning from this assumption will be considered more performant those cases that will have the greater number of patches pertaining to this category (i.e. the points on the curves positioned higher in correspondence of the vertical line of the 26 °C). This means that the considered case has an higher percentage of values which are lower than 26 °C. For instance, in the above chart, for the 25x20 case the 43% of the patches has a temperature lower than 26 °C.

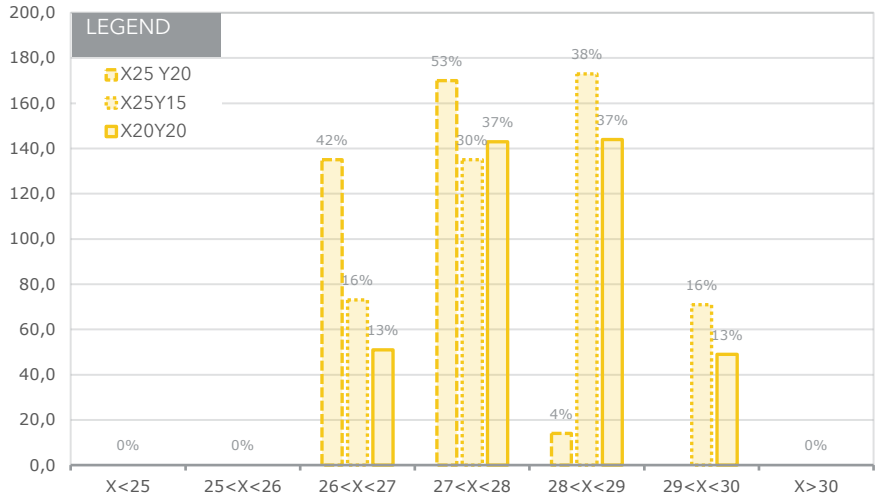

Fig. 139 Absolute and percentage number of patches for each temperature level

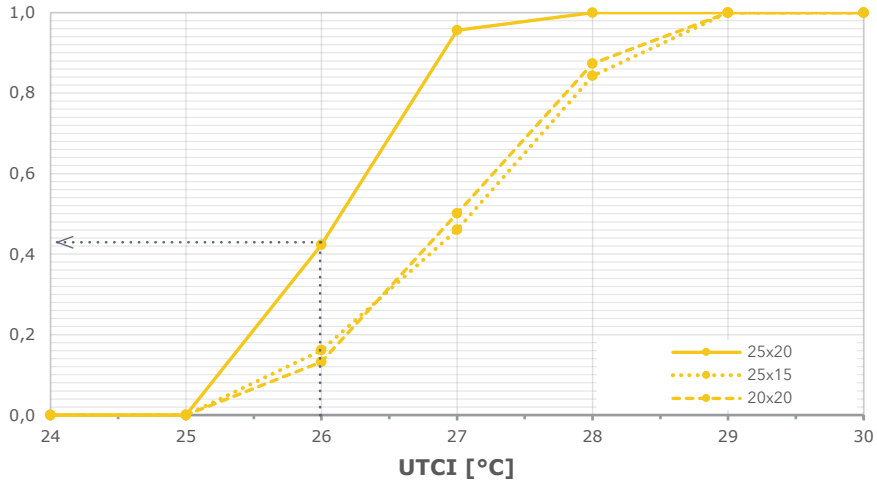

Fig. 138 Cumulative Frequency Chart for the 2x3 Tower Type.

Tower Typology: Cluster Two, Case 2x2

The "Cluster Two", belonging to the tower typology, among the other Tower's types, the one that has the most cases that passed the selection of the previous chapters. In order to represent the data clearly, the graphs for the different base sizes referring to the x dimension (25, 20 and 15 m) have been separated. Thanks to this separation of data, it was possible to identify trends common to all three graphs regarding the curves representing each analyzed case.

In the images on the right, where the three cases with equal dimension X25 are represented, it is possible to see that they have a very similar pattern of temperatures' distributions. The lines that representing them have in fact similar slopes and values. Among them, the cases with greater dimensions of the y (25 and 20 m) are advantaged in terms of comfort, showing a greater number of "patches" of the grid with temperature below 26 ° C. The highest value is the one of the case 25x20 m.

Please note that the types represented are those with greater base area and consequently lower heights (given constant FAR) than all other arrangements of the type 2x2. As can be seen from the UTCI Comfort Maps, the distribution of UTCI on the ground is very similar. Temperatures are higher in the median band and in those immediately located at the North and South of the buildings. These three bands are wider in the case at 25x15 m because, going to "thin" the y dimension, these bands will be accentuated in size and therefore will be more affected by solar radiation. It is no coincidence that this case is located in the lowest zone in the break in the values of UTCI and consequently will be the first to be discarded. On the contrary the other two cases have very similar values.

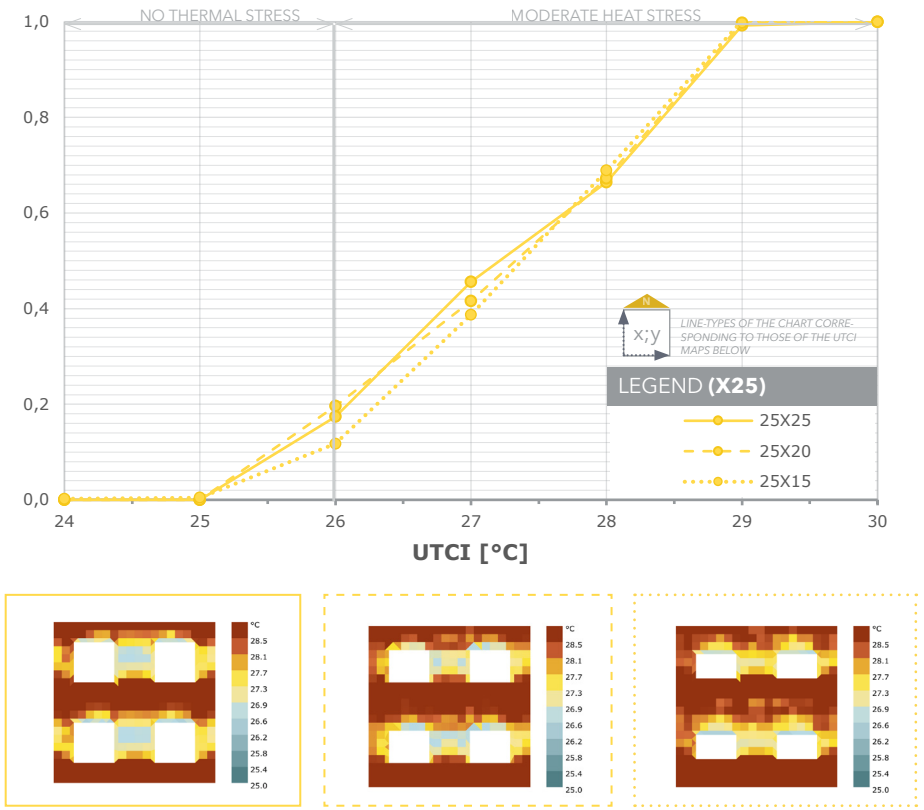

Fig. 140 Up: Cumulative Frequency Chart for Cluster Two, Type 2x2, X25. Down: UTCI Comfort Maps for the three selected base dimensions iterations.

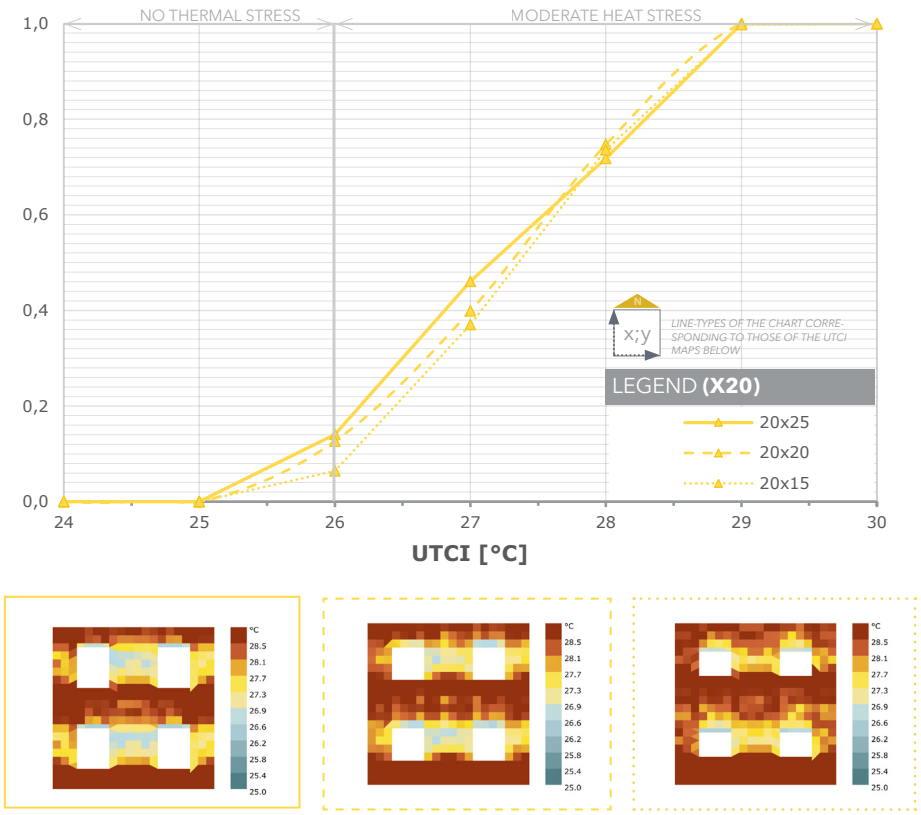

Fig. 142 Up: Cumulative Frequency Chart for Cluster Two, Type 2x2, X20. Down: UTCI Comfort Maps for the three selected base dimensions iterations.

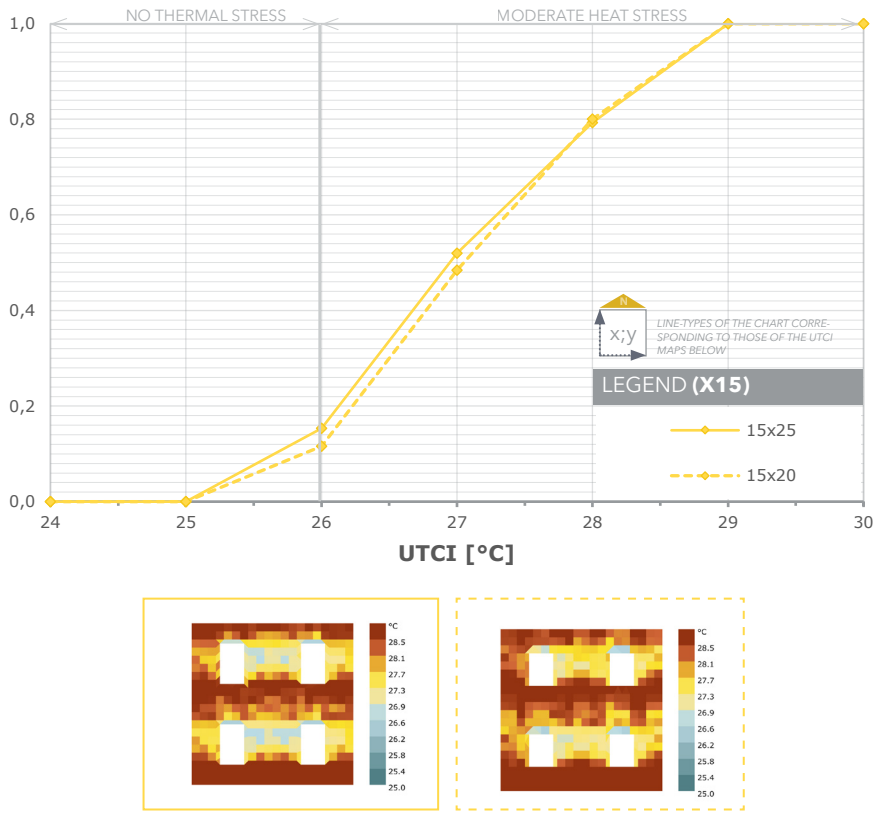

Fig. 141 Up: Cumulative Frequency Chart for Cluster Two, Type 2x4, X15. Down: UTCI Comfort Maps for the two selected base dimensions iterations.

Even for the case of the above figure (for x equal to 20) the same rule as illustrated for the previous case seems valid. The case with smaller size of the y (15 m) always remains the most disadvantageous in terms of comfort. The same could be stated also for the last case, with x equal to 15 m: higher dimensions of y generates better comfort conditions. In addition, comparing the 15x20 case with the 20x15 and the 15x25 with the 25x15 it could be said that with a N-S orientation (that of the larger side) in these cases (with equal height and base dimensions) is favored because deeper buildings in the y-directing helps in decreasing the high thermal bands that created in the South, central and North zones of the building lot. Going back to the 20x25 and 25x20 cases of the previuos cases, it is possible tnotice the same tendency, with the former one (N-S orented building) showing lower temperature levels.

Tower Typology: Cluster Two, Case 2x3 and 2x4

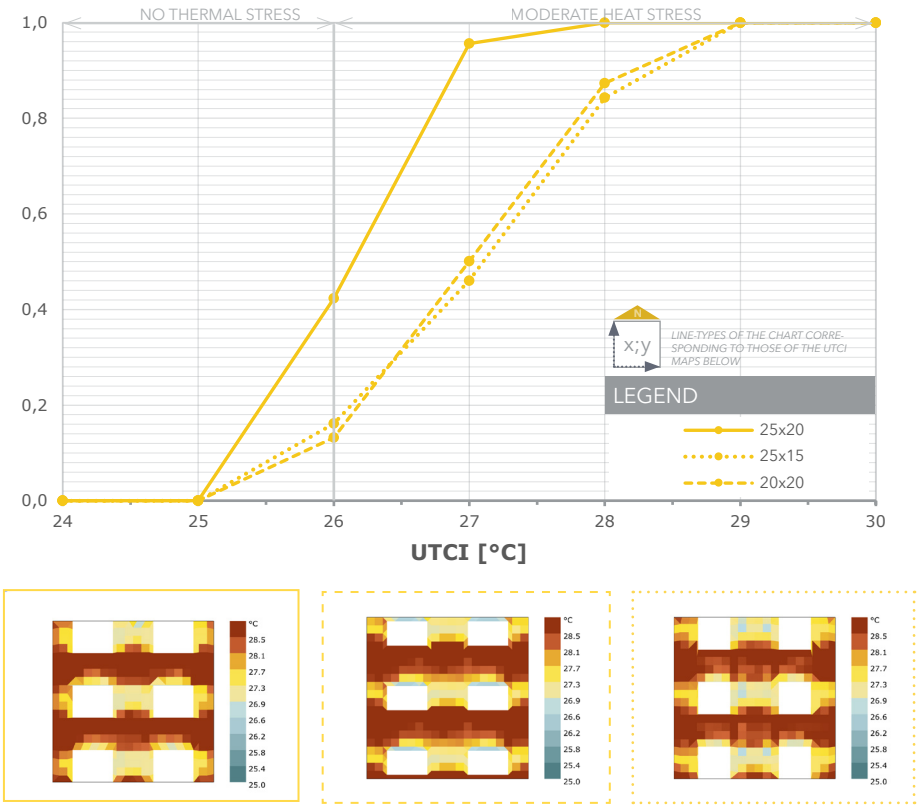

Fig. 143 Up: Cumulative Frequency Chart for Cluster Two, Type 2x3, X25-20. Down: UTCI Comfort Maps for the three selected base dimensions iterations.

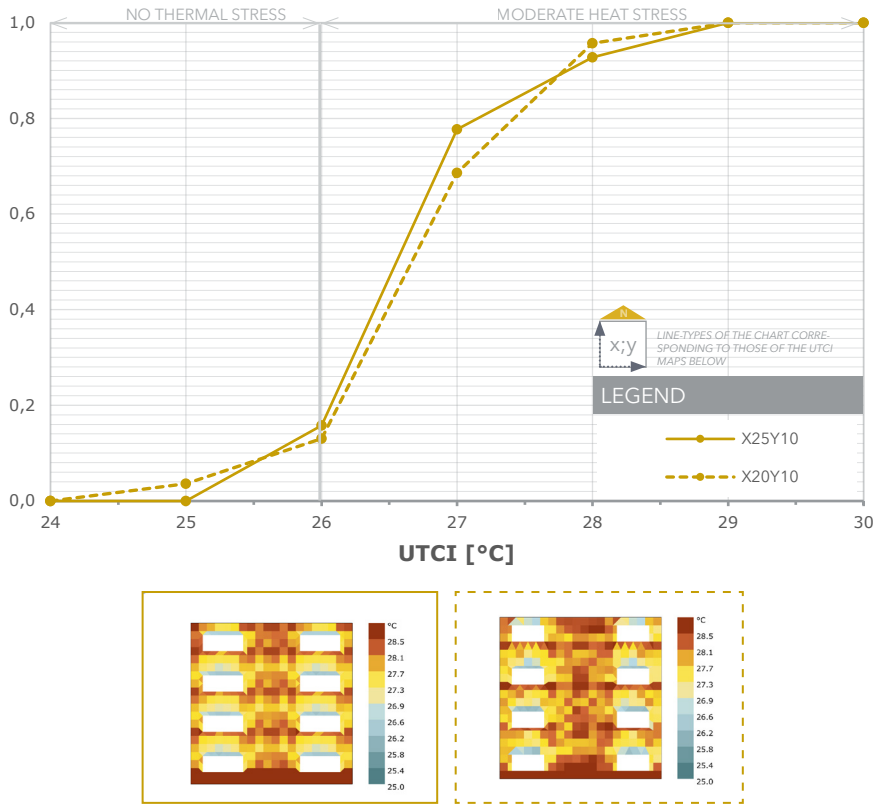

Fig. 144 Up: Cumulative Frequency Chart for Cluster Two, Type 2x3, X25-20. Down: UTCI Comfort Maps for the two selected base dimensions iterations.

Also with regard to the 2x3 type, the dynamics are the same as exposed for the 2x2 case. In fact, we can see the same alternation of "bands" of a darker red color, with the difference that in this case they are located between the different "rows" of buildings. Always respecting what previously exposed, also in this case, between the two cases with X25 it is possible to notice how the one with greater dimension y (25x20) is with the greater number of patches localized in the line of 26°C. Furthermore, also an increase of the x-dimension (case 25x20 compared to 20x20) brings further advantages in terms of comfort.

Finally, analyzing the type 2x4 both trends can be considered quite similar with a slight advantage of the case 25x10, for the greater size of the x dimension, as already defined above.

Tower Typology: Cluster Three, Case 3x2, 3x3 and 3x4

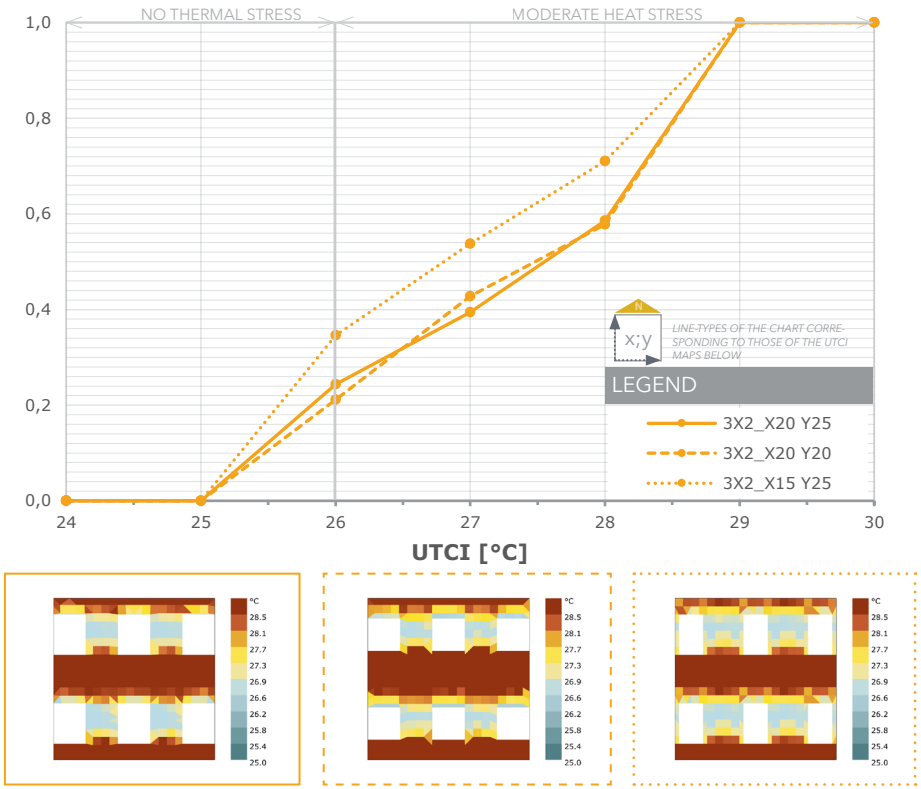

Fig. 145 Up: Cumulative Frequency Chart for Cluster Three, Type 3x2, X20-15. Down: UTCI Comfort Maps for the three selected base dimensions iterations.

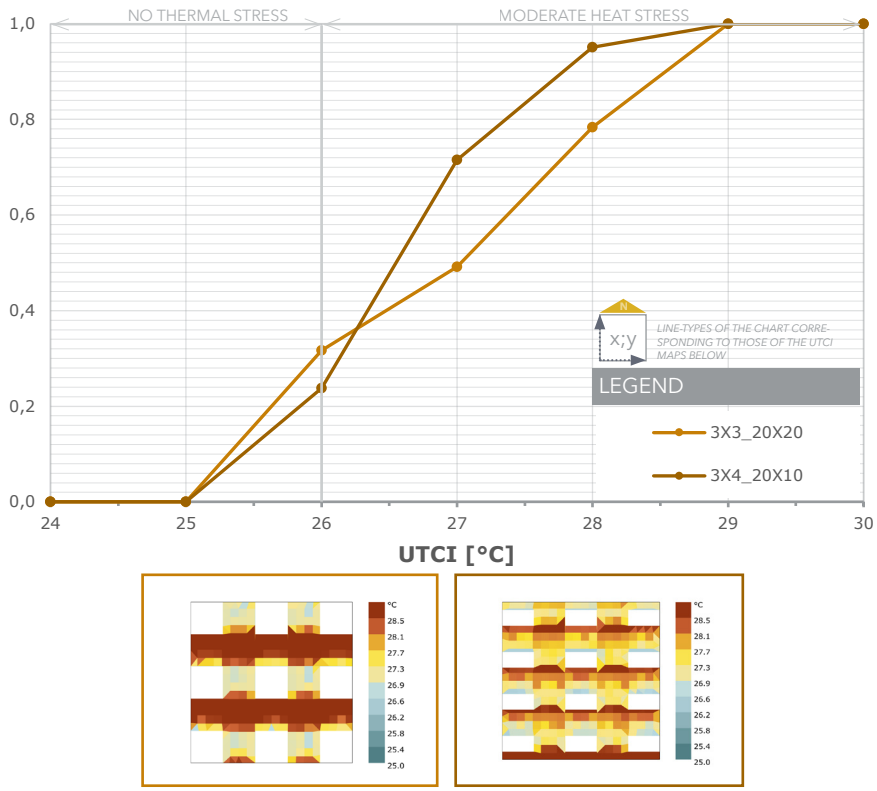

Fig. 146 Up: Cumulative Frequency Chart for Cluster Three, Types 3x3 and 3x4, X20. Down: UTCI Comfort Maps for the two selected base dimensions iterations.

In this case, it is possible to affirm that the 3x2_15x25 case has the highest percentage of patches belonging to this category compared the others. Looking at the comfort maps, it is possible to note a confirmation of the fact that rectangular plan dimensions are preferable to square ones, guaranteeing greater solar screening of the lot. The novelty that can be seen from this arrangement is that, with the same y dimension for cases with rectangular base dimensions with privileged N-S development, cases with a smaller x dimension are generally performing better. In fact, since, generally, the lower temperature zones are those located in the spaces between the "long" sides of the buildings, when they tend to reduce, as in the transition from the size 20x25 to 15x25, the number of lower temperature zones also tend to decrease.

Lastly, comparing case 3x3 and 3x4, in the former one the percentage of "red areas" is higher, but at the same time the one of lighter ones is. Conversely, the 3x4 has more uniform temperatures (almost 70% under 27 °C) but less under the 26°C threshold.

Bar Typology: 1 Bar N-S oriented

Regarding the 1 Bar NS oriented typology, in the comparative graph "UTCI vs Solar Radiation" of the previous chapter it is possible to see how the four groups classified according to the common dimension of the side aligned to the x axis (25, 20, 15 and 10 m) are homogeneously distributed in the range of temperatures and radiations considered. In order to decide which will be the best scenario, it was decided to analyze the "limit" cases, i.e. the extremes (x corresponding to 10 and 25 m). It was verified that both cases with the x placed in the middle between these two dimensions (15 and 10 m) show a behavior included between the limit values. The same assumption has been made for the y dimension: also in this case, if more y-iteration were present, only the smaller and the bigger were considered in the analysis, assuming those in the middle to have an average behavior between the extremes.

In the cases analyzed, it is evident that the best situation is represented by the 1-bar case with base dimensions equal to 10x70. This solution is privileged with respect to the others given the smaller base dimensions and greater height. It should be noted, however, that the 1-bar case presents a slightly different behavior with respect to the cases of the same typology but with greater number of Buildings (2, 3 And 4 bars) . Here, in fact, a fundamental role is played by the context, since there is only one main building in the arrangement. it is clear that in the case where the buildings making up the context are taller, the greater the influence on the contralateral lot. To this we owe in fact the facilitated condition of the 10x70 case. We will see later on in this chapert that in the cases with more bars, the privileged cases will be those consisting of longer bars (10x100) just because of the conditions that will be created in the areas between them, alias the "urban canyons".

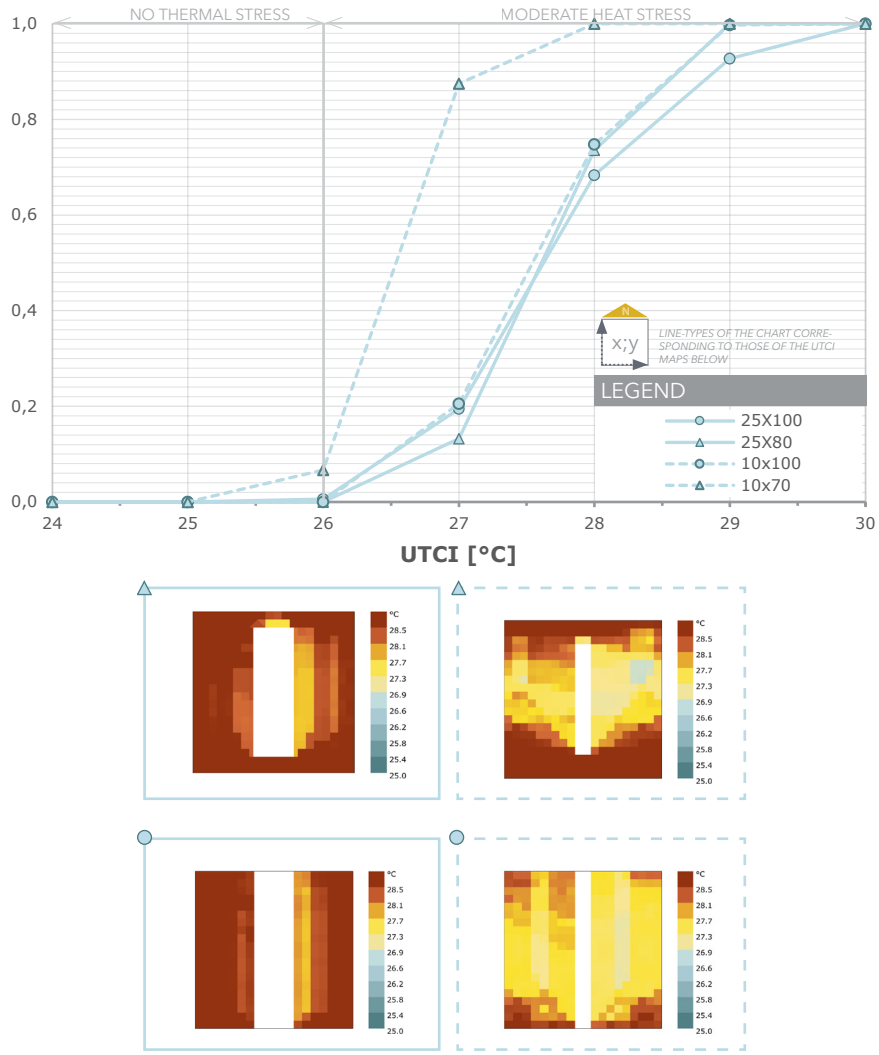

Fig. 147 Up: Cumulative Frequency Chart for 1 Bar Type, Depth 25-10 m. Down: UTCI Comfort Maps for the four selected base dimensions iterations.

Bar Typology: 2 Bars N-S oriented

The 2 bar case, along with the one-bar case, has the most cases resulting from the "UTCI vs Solar Radiation" Comparison performed before. Again, the technique of selecting extremes in terms of largest and smallest base sizes was adopted. Thus, cases with x equal to 10 and 25 m were selected for the smaller base sizes in the NS orientation and the 10 m case for the E-W (the only one with this orientation that may be considered from the previous analysis).

From the lines of the graph it is possible to notice a very similar behavior characterizing both 25x100 case and 10x100 one, which have in common the same y dimension. Similarly, the curve corresponding to the 10x70 case looks similar to the 25x70 one. Among these pairs of values, the 10x100 size is preferred to the 25x100 size, and similarly, the 10x70 case is better than the 25x70 case, because of the higher amount of patches showing temperatures lower than the 26°C comfort limit. The reason that justify this trend could be searched in the comfort maps below the chart.

In cases with a common length of 70 m, by looking at the colorful plans, it is possible to identify two different zones: a central corridor at lower temperatures and an outer "frame" at much higher temperatures, which tends to greatly affect the overall comfort of the arrangement. However, it should be kept in mind that the temperatures created in both cases in the "canyon" between the buildings are lower than in the 100 m long cases. Given in fact the smaller base dimensions of the Y70 cases compared to the Y100 ones, this will result in a higher height (due to the constant FAR), and this height will result in greater shading. It is, in fact, due to the lower temperatures of the inner "canyon" that the 10x70 and the 10x100 could be considered the best among the four types. The 10x70 it is particulary standing out due to the smaller base dimensions and consequent height.

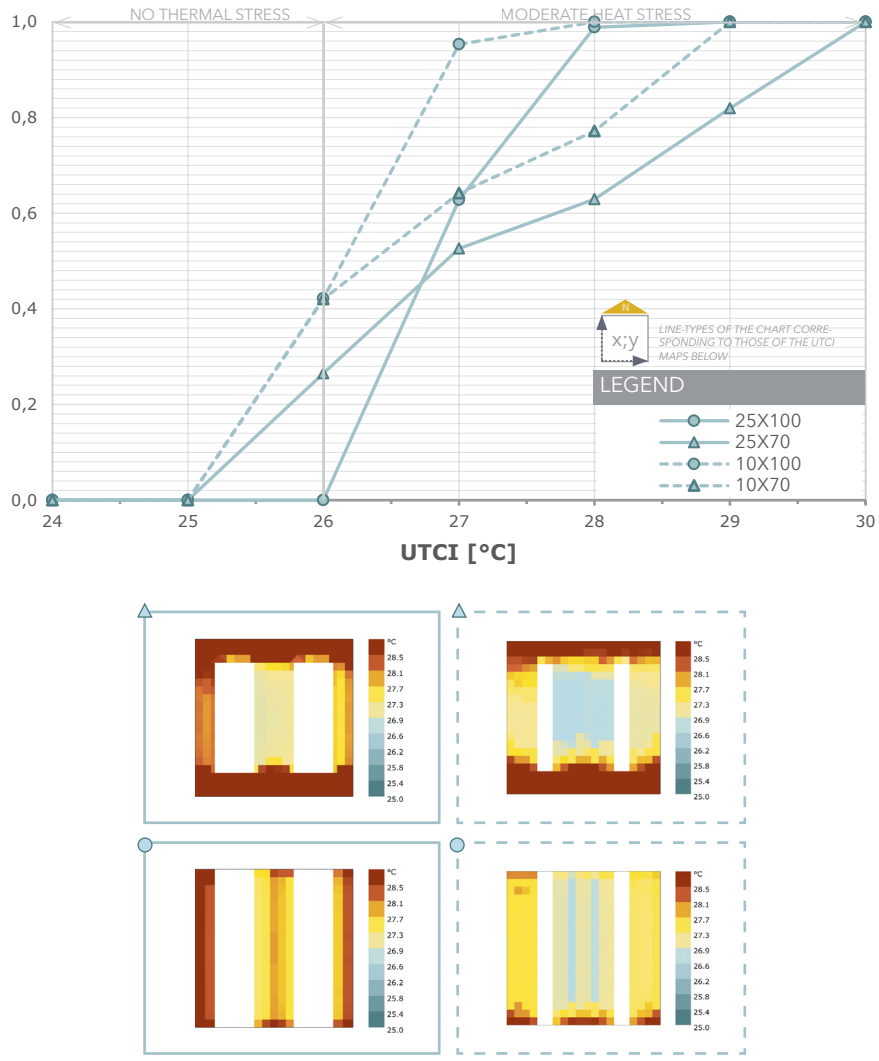

Fig. 148 Up: Cumulative Frequency Chart for 2 Bars Type N-S, Depth 25-10 m. Down: UTCI Comfort Maps for the four selected base dimensions iterations.

Bar Typology: 2 Bars E-W oriented

In the next two cases, however, it is possible to appreciate the difference with the cases seen previously for the 2 bars, generally oriented in N-S direction (reference is always made to the preferred orientation of the largest dimension of the bar). In the case of the E-W orientation shown in the figures, it is possible to witness a general raising of temperature levels. Incidentally, the effect of orientation plays such a fundamental role that the effects of size changes are minimized. This can be appreciated by looking at the curves that are created in the "cumulative frequency chart", which have almost the same slope, until they overlap at 29 °C.

Buildings arranged in this way, i.e. parallel to the path of the sun from West to East during the day, are not able to completely shield solar radiation. In addition to this, solar radiation from the south does not generate high temperature zones in the strip facing the southernmost building and, between the buildings, in the strip immediately in front of the northernmost building in the complex. Obviously, the case with larger dimensions (i.e. 90x10) will be the one slightly more performing because it is able to constitute a superior solar screen in the central "canyon" between the two bars.

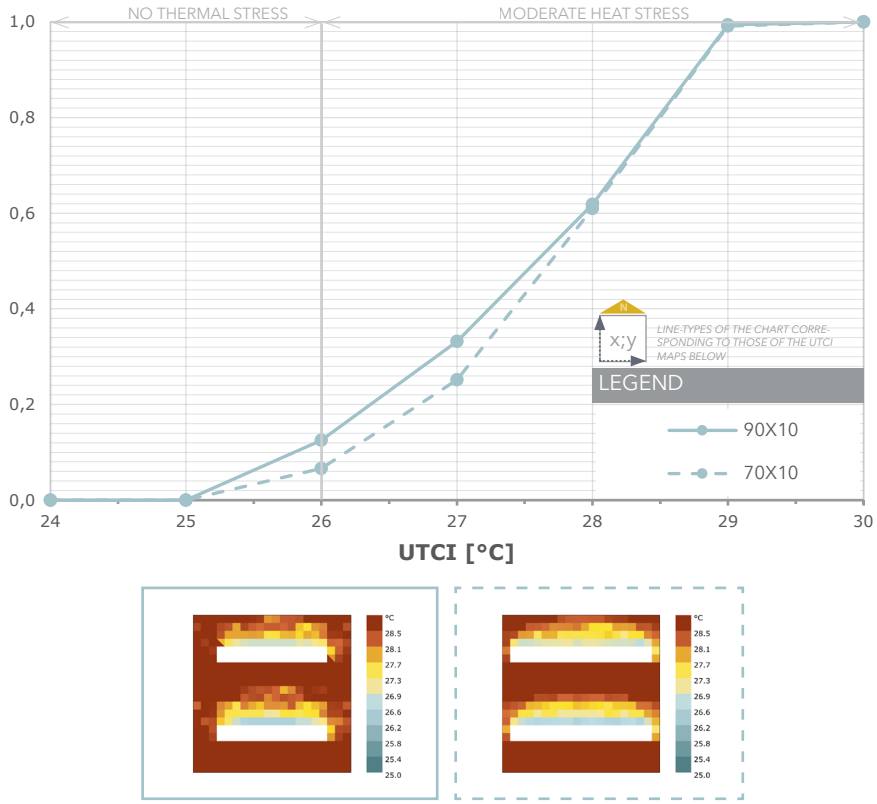

Fig. 149 Up: Cumulative Frequency Chart for 2 Bars Type N-S, Depth 10 m. Down: UTCI Comfort Maps for the two selected base dimensions iterations.

Bar Typology: 4 Bars N-S oriented

The last case considered for the bar typology is the 4 bars. Also in this case from the previous selection phase, according to UTCI and solar radiation, both orientations have been selected, N-S and E-W. Equally as before, considering this case it is possible to notice two different trends that configure the curves.

Regarding the E-W orientation, similarities can be appreciated with the previous case, that of the 2 bars E-W oriented. Also in this case the two curves referred to two different base dimensions are very similar to each other and presenting an almost linear trend from 25 to 27°C and then slightly separate at 28°C. Also in this case, it is possible to notice an outher "frame" at higher temperatus, more pronouncd on the small base dimensions (70x10). The number of patches with lower temperature of the E-W case, which are reaching the 20% of the whole plot area, are indeed higher than those of the 2 bars type due to the presence of more buildings providing more shading.

On the other hand, for N-S orientations, the trend is similar to the 2 bars types, with the 10x100 case performing the best ove the 10x70. Same considerations could be formulated regarding the length, which is higher than then 70 m one and so performing better for shading purposes.

The 4 bars case is also the one that among the other bar types is recording the higher number of patches corresponding to the comfort limit. This is due to the higher number of building. It has been previously described how much this number is able to affect the general UTCI, decresing the amount of areas available on the ground and at the same time providing the higher shading effect.

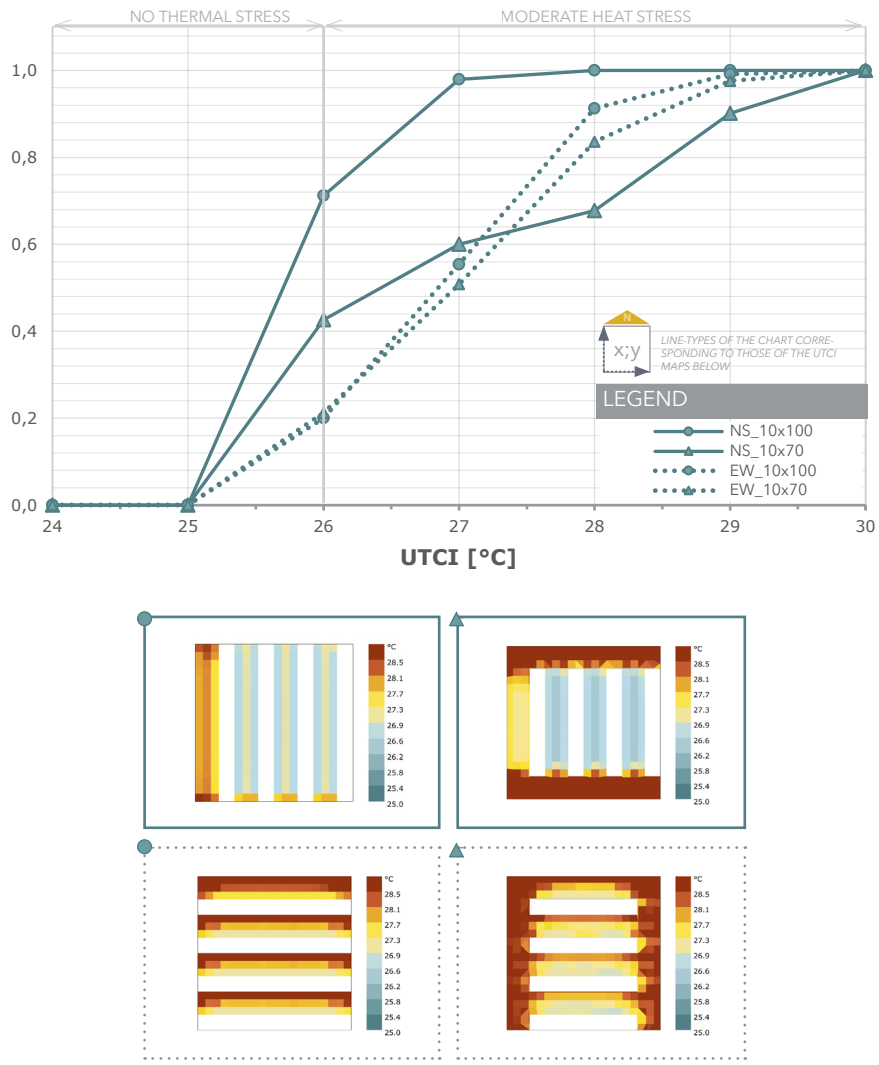

Fig. 150 Up: Cumulative Frequency Chart for 4 Bars Type N-S/E-W, Depth 10 m. Down: UTCI Comfort Maps for the four selected base dimensions iterations.

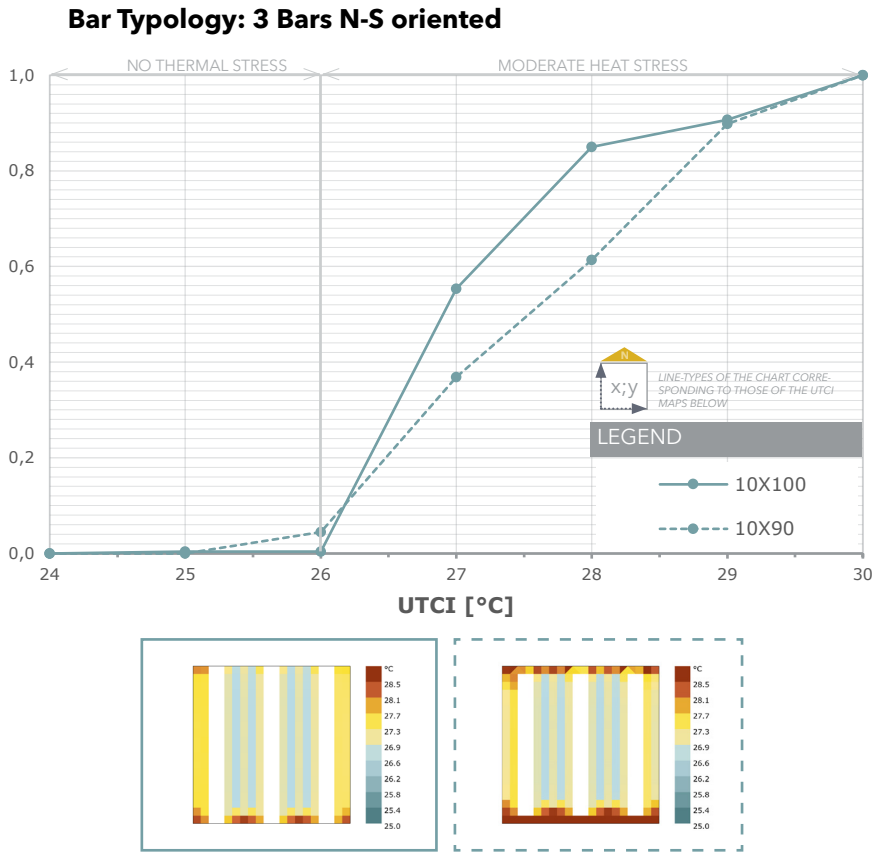

Fig. 151 Up: Cumulative Frequency Chart for 3 Bars Type, Depth 10 m. Down: UTCI Comfort Maps for the two selected base dimensions iterations.

Regarding the 3-bar case, not many considerations can be made without causing a repetition of what has been said up to this point. The type turns out in fact to have a median condition with respect to the 2 and 4 bars types. In short, we again see a clear preference for cases with longer bar lengths, in N-S orientation. The preferred case is again the one with 100 m length compared to 90 m and less. In fact, the more the buildings decrease in y-axis size, the more the surrounding "frame" will be at a higher temperature.

Courtyard Typology: 1 Division N-S/E-W Oriented

The last type to be analyzed are the courtyards. First of all, the cases selected in the previous phase have been divided into two sub-graphs: one for the typology with a single internal subdivision and therefore with two internal courtyards (1 Division); the other one for the typology with two internal subdivisions and three resulting courtyards (2 Divisions). With regard to the first typology, for a matter of clarity, both orientations, N-S and E-W, have been included in the same graph.

Among the 1 Division cases with N-S orientation, the one with a depth of 10 m, however, records a higher percentage of areas with temperatures below 26 °C and 25 °C and is therefore considered the best of the three cases showing a preferable N-S orientation. This case is having also the 100% of the cases with temperature lower than 27°C. A special mention also deserves the case with a depth of 20 m that totals the highest amount of areas below 25 °C and will be therefore counted among the "winning" cases. Finally, considering the typology with E-W orientation, it presents a much more linear trend compared to the above cases but with many more individual areas at higher temperatures such as 28°C.

Considering the thermal maps what stated previously is very clear. At first, the 10 m depth case of the N-S is showing the best conditions in the inner patios. This feature is surely related to the higher height of the type (due to lower base dimensions) compared to the other two. Moreover, under the architectural point of view this bigger dimension of the inner patio allow to have a bigger livable space which is indeed pretty confined in the other two cases. For the reasons see before in other cases, such as the 2 bars one, the E-W orientation is definitely the less advantaged due to the alignment with the sun path during the day.

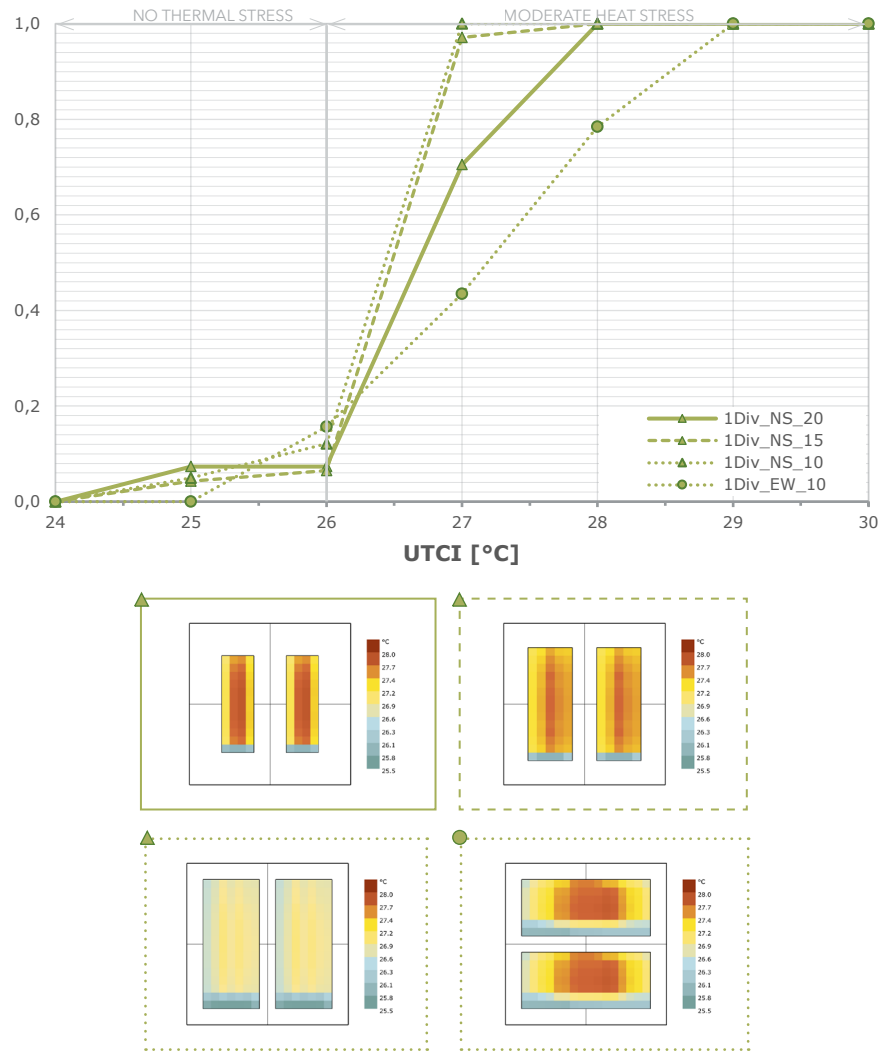

Fig. 152 Up: Cumulative Frequency Chart for Courtyard Type 1 Division N-S/E-W, Depth from 10 to 25 m. Down: UTCI Comfort Maps for the four selected base dimensions iterations.

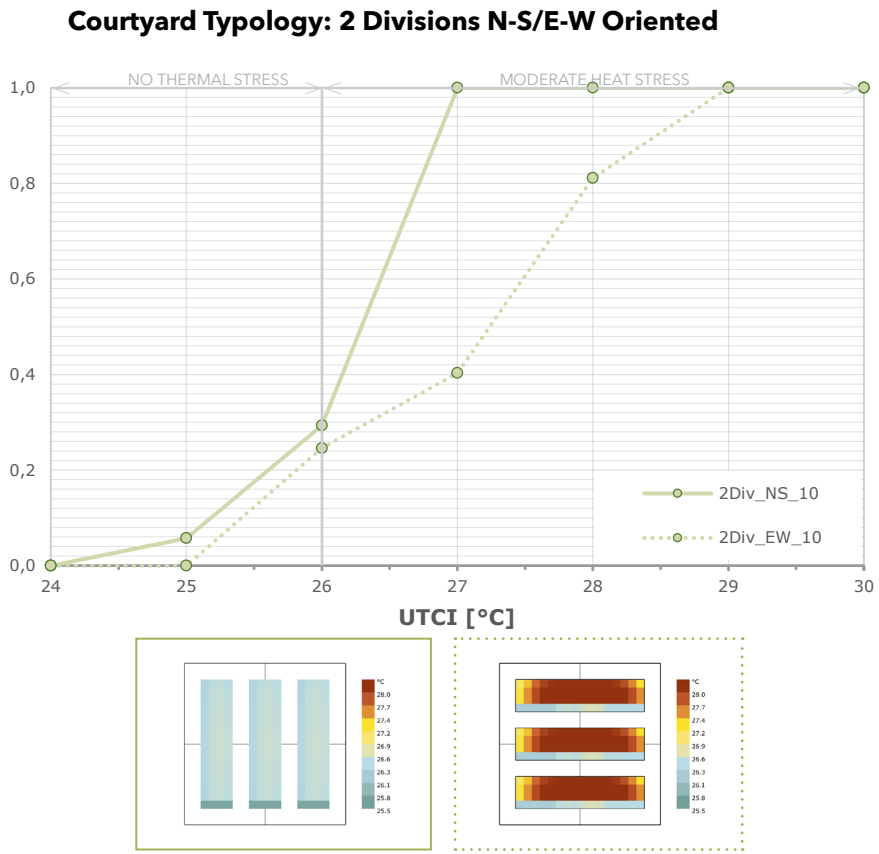

Fig. 153 Up: Cumulative Frequency Chart for Courtyard Type, 2 Divisions N-S/E-W, Depth from 10 to 25 m. Down: UTCI Comfort Maps for the four selected base dimensions iterations.

Referring to the N-S orientation, firstly, it is possible to notice a very similar trend for the 1 Division cases with depths of 10 and 15 meters and the 2 Division one with same orientation; both of them showing almost the totality (95% -100%) of the patches located below 27 °C. The trend of the N-S orientation can be therefore considered as winning. It also shows low temperature levels and many values belonging to the known comfort range of 25-26 °C. The confirmation of the chart trends could be found in the lower comfort maps, with the E-W orientation showing definitely darker colors.

Champions for the Tower Typology

The following two diagrams pertain to the tower type. Inside them, all the cases analyzed singularly have been represented together to give an overall picture of the whole typology. For each type (2x2, 2x3, 3x2, 3x3, 3x4) the best cases have been selected. To follow, an interpretation of the data collected will be give, deciding which case or cases are working better. However, it should be kept in mind that all the provided cases have high performance. It was decided to select a case for each typology in order to leave the designer with a wider range of possible solutions and greater flexibility in choosing the number of buildings that could potentially be used.

The best result in general is the one obtained for the 2x3 typology followed by the 3x2. It is immediately evident that, besides having the same base dimensions, these two typologies have in common the number of buildings on the lot. Analyzing the plans, it is also possible to suppose an improvement in performance when the preferential direction of arrangement of the buildings is N-S (case 2x3), meaning by this the direction of the axis which has the greatest number of buildings (in this case the y, which is North oriented).

The impact of the number of buildings is also evident when considering the succession of values on the 26 °C vertical axis. The 6 buildings of the above-mentioned cases are followed by the 9 buildings of the 3x3 case and the 12 of the 3x4 case. Lastly, certainly evident in this final selection, the height of the buildings. It can be said that a medium-low height of buildings is more favorable from the point of view of low UTCI comfort ranges. This implies, as a consequence, a higher percentage of Building Coverage Ratio.

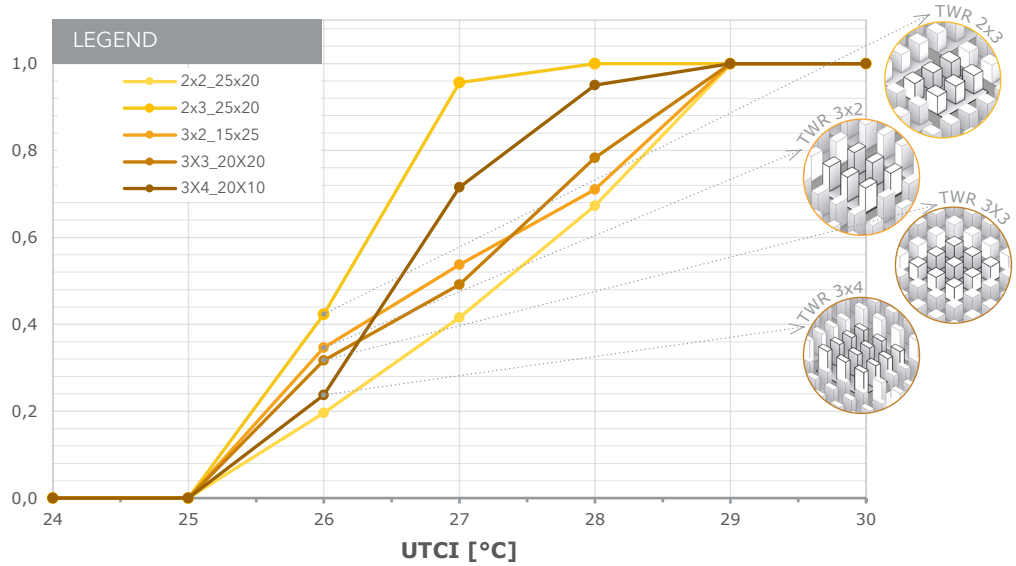

Fig. 154 Cumulative Frequency Chart for the best cases selected for the Tower Typology

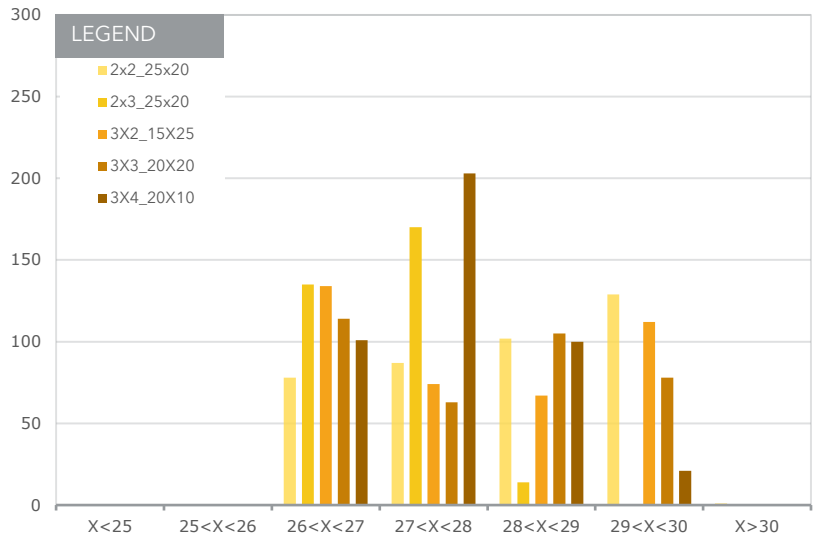

Fig. 155 Percentage of patches showing different temperature levels for bast cases of the Tower Typology.

Champions for the Bar Typology

The same type of reasoning followed for the case of Towers will also be applied referring to the Bar type. Again, a significant influence of the Building Coverage Ratio could be seen affecting the results. The case of the 4 bars is the privileged, with the highest number of patches reporting a temperature below 26 °C. The definitely surprising factor is the difference between the 4-bar case and the 3-bar case, which occupies the last position among the best cases. This inconsistency could be due to the interrelation between height and BCR. Given in fact the constant FAR ratio, the 4-bar case will have a lower distance between the buildings ensuring the beneficial effects of shading. Always considering the constant FAR factor the 2-bar buildings will be consequently higher but also more distant from each other, ensuring better conditions of comfort in the hot season. It could be said that the three-bar case lies exactly in the median situation between these two cases and that the relationship between building distance and building height is not favorable to obtain optimal comfort conditions.

Differently from Tower typology, it is possible to see that the base dimensions are more relevant. It is enough to see that in terms of basic dimensions, solutions with a longer side between 90-100 m and a shorter one equal to 10 m are preferred. The only difference lies in the case of the 1 bar, in which the dimensions of the longer side have an average length between 50 and 100 m (minimum and maximum available) for iterations. In the first case in fact, as has been seen in detail in the chapter dedicated to UTCI comfort maps, the temperature at the extremes would be more influenced by solar radiation; conversely, the second case would be much more affected by a greater thermal asymmetry between the two sides (East and West) of the bar.

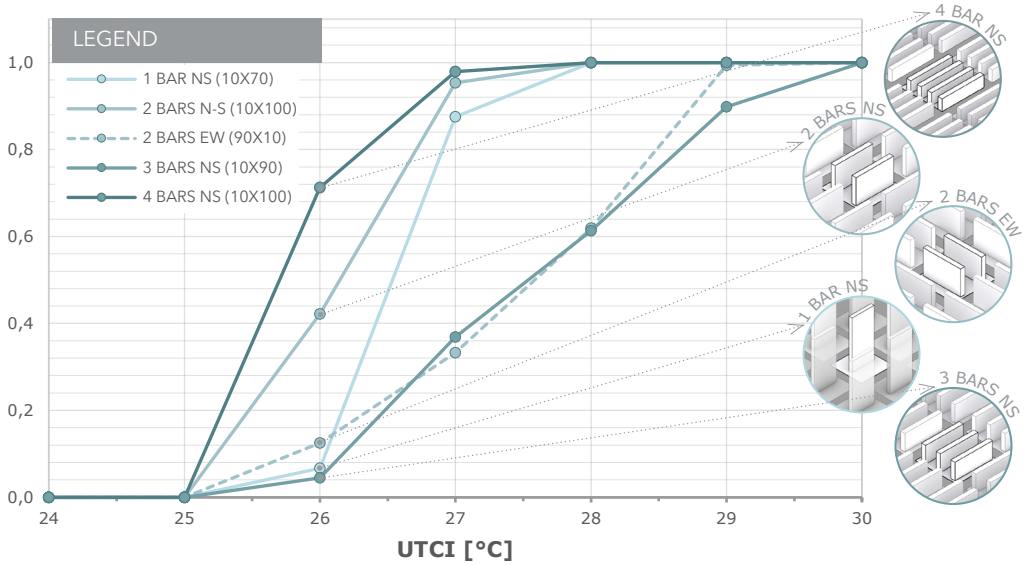

Fig. 156 Cumulative Frequency Chart for the best cases selected for the Tower Typology

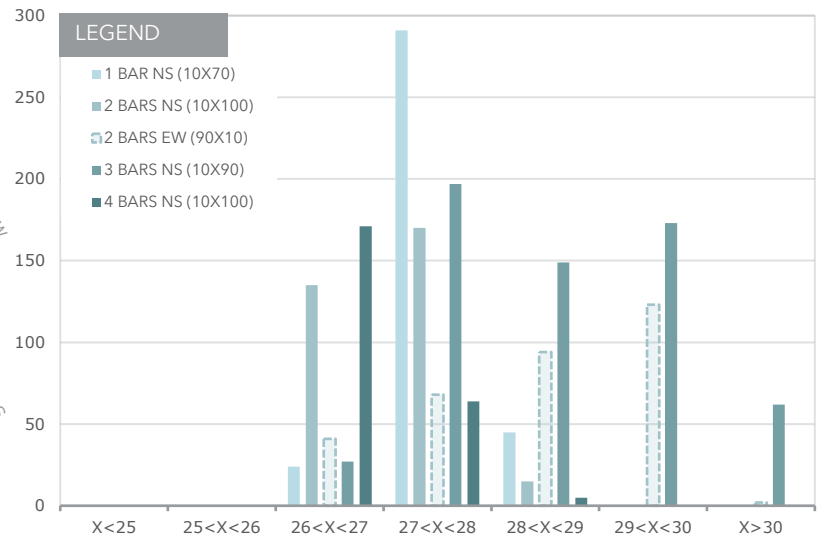

Fig. 157 Percentage of patches showing different temperature levels for bast cases of the Tower Typology.

Champions for the Courtyard Typology

In the previous chapter the courtyard shape has been considered the most performing one and from the following diagrams it is possible to find a confirmation of this statement. In this case it is necessary to pay attention not only to the vertical line of 26°C, but also to two other main points.

Firstly, the courtyard is the only one of the three arrangements capable of providing temperatures below 26°C; it is enough to see the percentage, albeit not very high, of patches between 25 and 26°C. Secondly, it is possible to note that the number of patches at temperatures between 28 °C and 30 °C is lower when compared to the other two types. This peculiarity of the courtyard configuration is determined by the protected nature of the inner courtyards, which enjoy ideal shading conditions for the hottest season.

Having this in mind, it is now possible to move on to more detailed considerations on the examined cases. The best scenario is represented by the 2 divisions case both N-S and E-W oriented. In this case, in fact, the restricted nature of the inner patio is affected by the beneficial effect of shading, more than in the cases with only one division (and therefore two patios), which are located immediately below. It is certainly interesting to note the similarity of the curves representing both cases oriented N-S but with two and one division. The curves, as can also be seen in the bar chart on the right (where they represent the "highest" columns), join the 27°C vertical line, with most of the inner patches recording a UTCI below 27°C.

Lastly, the type with one division, N-S oriented and with 20 m depth il located in the last position. In fact, due to constant FAR this case is providing greater base area and so lower height. This means that, being lower the surrounding walls, the patio will be more affected by solar radiation causing higher temperatures in general.

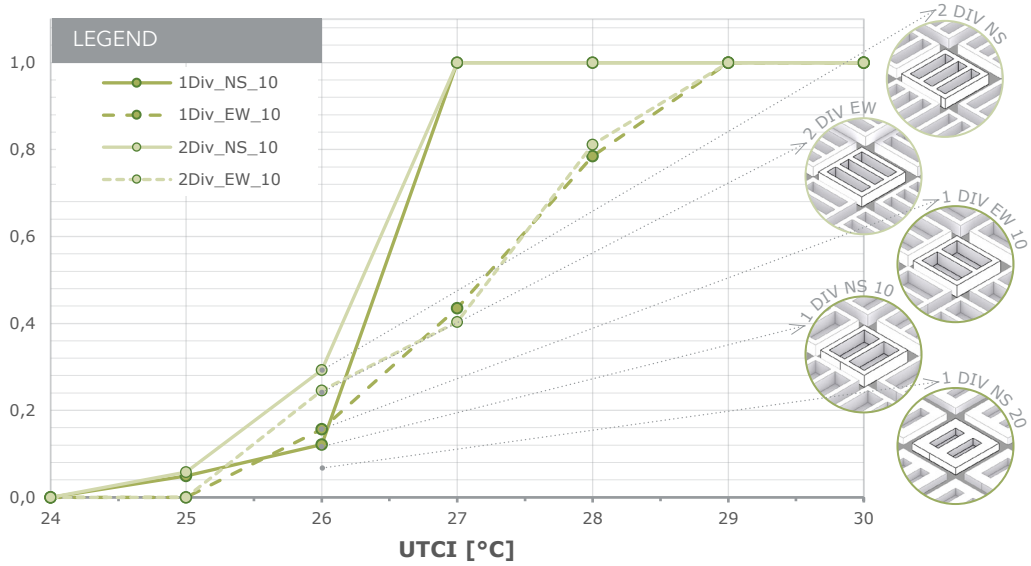

Fig. 158 Cumulative Frequency Chart for the best cases selected for the Tower Typology

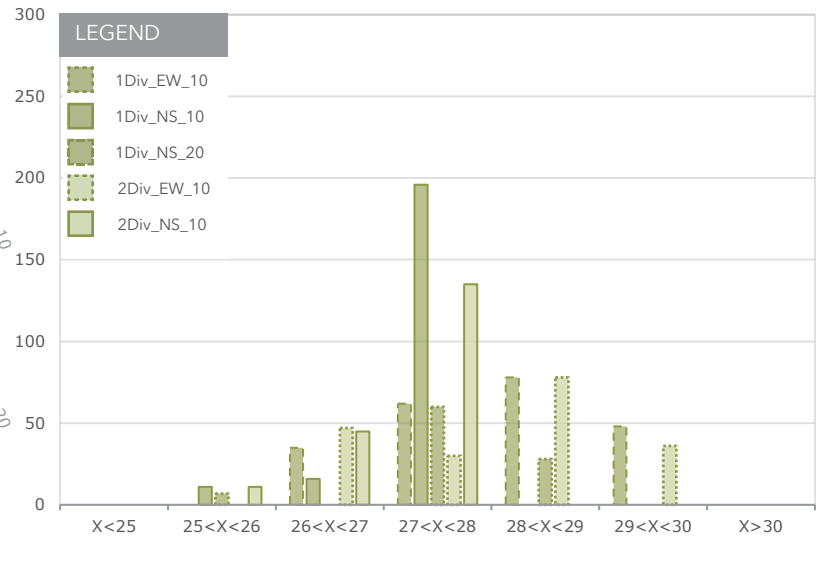

Fig. 159 Percentage of patches showing different temperature levels for bast cases of the Tower Typology.

6 Results

Concluding the study, it is possible to draw the following conclusions for the three typologies.

Courtyards

The courtyard type has the lowest average UTCI values and the highest average solar radiation values. It would therefore seem to be, at first analysis, the best typology. Conversely, considering the UTCI comfort maps punctually it is possible to note, for the best case identified (i.e. the one with two divisions and yards oriented N-S) that the number of patches of land with a temperature below 26 °C is around 30%. In any case it is possible to find, in this preferred case, a number of patches with UTCI below 27 °C equal to 100%. This second datum therefore justifies the decidedly lower average UTCI values compared to the other types analyzed. For this first analyzed typology a rather uniform UTCI value will therefore be recorded, but fewer comfort zones. However, generally better preferences are obtained for N-S orientation and small depths of the perimeter wall (10 m), which, without altering the solar potential, maximize the benefits of shading in the interior patio, providing a more extensive solar pattern to the solar path from West to East. This feature is due to the bigger height of the type, which is generated by the constant FAR ratio, being smaller the base dimensions.

Fig. 160 Summary graphic representation of the best criteria for Courtyard Selection

Bars

The bar, as has been previously discussed, represents the typology with the widest distribution of cases in the UTCI/Solar Radiation spectrum and ranges analyzed. The type is also the one that records, in its best case, that is 4 BARS NS 10X100, among all the types analyzed, the highest percentage of "patches" below the thermal stress limit identified at 26 °C, with 70% of them below this threshold. Together with the 4-bar type, also the 2-bar type obtained a remarkable result. It is therefore possible to say that an even number of bars have a greater possibility of controlling the external summer temperature. Also in this case, it is possible to notice an increase in performance for the N-S orientations compared to the E-W cases. Finally, there are greater benefits from a longitudinal development of the base dimensions, and therefore lengths of 100-90 m will be preferred compared to the minimum of 40-50 m. The only exception to this statement is constituted by the 1 bar case which is showing better performances with smaller length (70 m) and due to the highest shading potential of its hegiht. Also with regard to depth, smaller solutions of 10-15 m are preferable to those of 25-20 m.

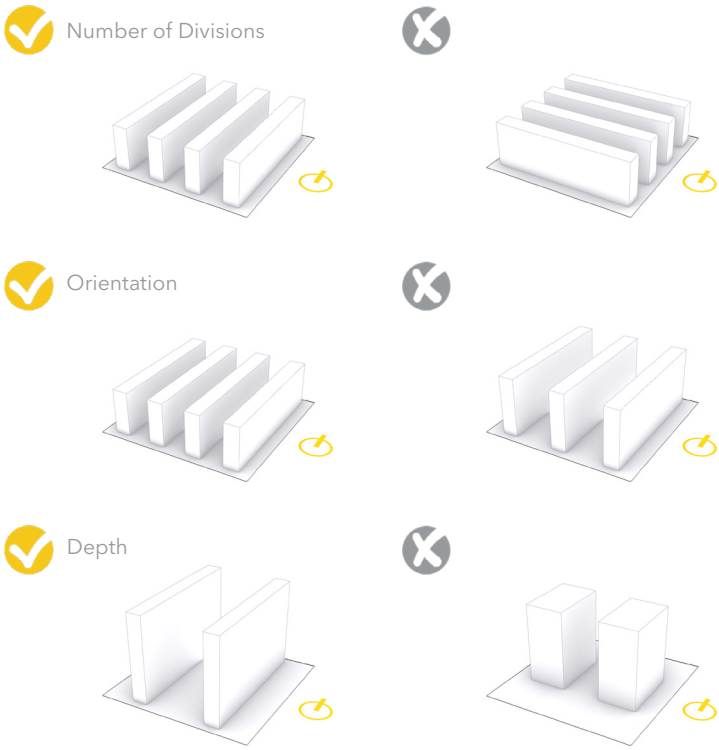

Fig. 161 Summary graphic representation of the best criteria for the Bar Selection

Towers

Lastly, as far as the tower type is concerned, it has been verified as having the lowest performance under both indicators analyzed.

For this typology, it seems that the characteristic that most influences the results in terms of UTCI values is the land cover index. In fact, in the case of a lower number of buildings (e.g. 2x2), higher base dimensions are preferred. On the contrary, in the case of arrangements with more buildings (e.g. 2x4, 3x4) smaller base dimensions are preferred.

In addition, for Cluster Two, for the types 2x3 and 2x4 the selected cases appear to have a preferred orientation direction E-W, with the longer side of the buildings aligned along the x axis, Among the arrangements that report this particular development, larger sizes of y are preferred. Conversely, for type 2x2, base dimensions are way more relevant that the orientation, not showing preferable cases between E-W and N-S. For Cluster Three, however, an N-S orientation appears to be better. In this case, the arrangements with greater x-dimension have a better performances. From the figures on the right it is possible to understand that the best arrangements are those which are able to have shielded corridors N-S oriented and, more in general, an homogeneous distribution of buildings on the available zoning lot.

Fig. 162 Summary graphic representation of the best criteria for the Tower Selection

7 Further Work

As this study is part of a broader research that happens in collaboration between Pratt Institute (NY, USA) and Politecnico di Milano (Milan, IT), a lot of the topics on building performance and optimisation, with focus on solar capture, that were not covered in this thesis were already or will be dealt by other colleagues.

As matter of fact, in parallel to this study, the thesis "Building Massing and Performance: guideline for early-stage design analysing energy demand, daylighting and solar potential" is being developed by the colleague Rafaella Monteiro, also a MSc student from the Building and Architectural Engineering program at Politecnico di Milano. In her research, indoor comfort on the same typology case studies is analysed, following the same principles used for the present study. It deals with an entire set of indicators different from the ones applied here, due to the fact that this research focused on buildings and their outdoor comfort levels. Meanwhile, the work from Rafaella studies the effect on the same buildings but for Indoor conditions.

Her research started from the statement that the Building Sector is one of the responsible sectors for climate change, a consequence of population growth and the evolving forms of society's housing and living. Even though it contributes up to 30% of global annual GHG emissions and consumes up to 40% of all energy, it has a great potential for delivering significant and cost-effective mitigation measures. High-performance buildings can play a crucial role also in reducing energy use, by applying energy-saving strategies. To contribute to the growing knowledge on building massing at early-stage design, the goal of her research is to study building typologies and evaluate the resulting energy performance, to answer for environmental and regulations requirements, but considering at the same level of importance daylighting levels, which impacts greatly on several buildings aspects, such as its comfort and the electricity demand for lighting.

In her study, case studies from towers, courtyards, and bars with the same floor-to-area ratio are analysed, but in regards to daylighting conditions, solar potential, and energy demand, all the three indicators ranked equally. As the research finds some answers, the study is further detailed in order to reach a final answer and understand each typology's strengths and weaknesses. It has been proved that, for instance, high-rise towers have a high energy requirement while also a high solar production, which can be an interesting trade-off, considering the great daylight performance in the slender cases. Courtyards can be slightly limited in their daylight conditions while presenting a very low energy requirement. Bars seem to be the least performing typology among the three, presenting a considerably higher energy requirement with low solar capture and some daylighting limitations, mainly due to overshadowing. It is then proved that even if other passive strategies are applied on the envelope, the limitations from the massing decision follow along all the design process, and they must be carefully chosen at the early-stage to avoid resulting in poor building performance.

To have this wide knowledge on indoor and outdoor parameters is intended to provide a global scenario, joining forces from both of the researches towards the improvement of building massing knowledge.

Appendix

The following appendix includes the climate analysis of the analyzed site, that is, a series of preliminary analyses previously used for the climatic framework of the area under consideration. This information has been included here, at the end of the document, in order not to burden the previous dissertation. The data collected concern those parameters most useful for the calculation of the indicators evaluated, more properly: dry bulb temperature, relative humidity, wind speed and solar radiation.

Location

Due to the genesis of this study, held in collaboration with Pratt Institute of New York City, the location that will be considered for this study is precisely the same. New York City (NYC) is the most populous city in the United States. With an estimated 2019 population of 8,336,817 distributed over about 302.6 square miles (784 km2), New York City is also the most densely populated major city in the United States. Located at the southern tip of the State of New York, the city is the center of the New York metropolitan area, the largest metropolitan area in the world by urban landmass.

Therefore, for this study it was used the climate file for New York (same ones that have been used by the students of the Pratt Institute Course mentioned before), more specifically, data measured at La Guardia Airport. The coordinated of the airport are 40.7769° N, 73.8740° W and is located at 6 m above the sea level. In the next paragraphs we will analyze the climatic conditions of the site in question with reference to the significant parameters for the calculation of UTCI.

In order to calculate the exact climatic conditions of the site it has been used Ladybug, the famous Grasshopper plugin for Rhino. First, the climate file was downloaded on the basis of which the climate conditions were calculated. This weather file, that has been downloaded from "OneBuilding" website, ranges from 2004 to 2016. EPW (Energy Plus Weather format) files are synthesized from real recorded data from different years in a given climate. This is done to ensure that, for each month, the selected data is statistically representative of the average monthly conditions over the 18+ years of recording the data. Different EPW files have been synthesized from different years depending on whether they are TMY (Typical Meteorological Year), TMY2, TMY3, AMY (Actual Meteorological Year) or other.

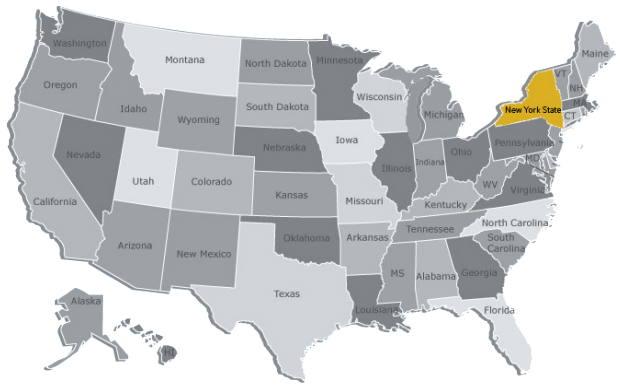

Fig. 163 Identification of the Case Study location on the general USA's countries map.

Dry Bulb Temperature

The first parameter that will be analyzed is the Dry Bulb Temperature. The Dry Bulb temperature (in Celsius degree), usually referred to as "air temperature", is the most used air property. The Dry Bulb Temperature refers basically to the ambient air temperature. It is called "Dry Bulb" because the air temperature is indicated by a thermometer not affected by the moisture of the air. It is measured using a normal thermometer freely exposed to the air but shielded from radiation and moisture. The following graph plots the annual recorded temperatures for the selected location.

The data have been collected on an annual basis, hour by hour, from the weather station. Secondly, they have been averaged by the author on a monthly basis in order to plot the final bar chart on the top-right. The chart on the bottom-right is indeed calculated by the Ladybug default component directly in Grasshopper canvas.

In the bottom-right chart, the Dry Bulb Temperature data have been plotted according to a color scale on an annual basis. Moreover, on the horizontal axis, the values are classified by month while on the vertical one they are divided according to different time ranges of the day. It is immediately evident that the hottest period of the year ranges from June to September and the peak hours belong to the 12 pm-6 pm time slot. Conversely, the coldest season includes months from December to March, while April, May, and October can be considered mild. According to the top-right bar chart, the averagely hottest month can be considered July, that, alongside with August, is also registering the highest temperature peak of 35°C. It is possible to see that very high temperature peaks are registered also in those months which are generally considered "mild". An example is the 34 °C peak reached in September and the 30°C one for May. The lowest average temperature is reached in January, which is also presenting the lowest temperature (-10°C) together with February and March.

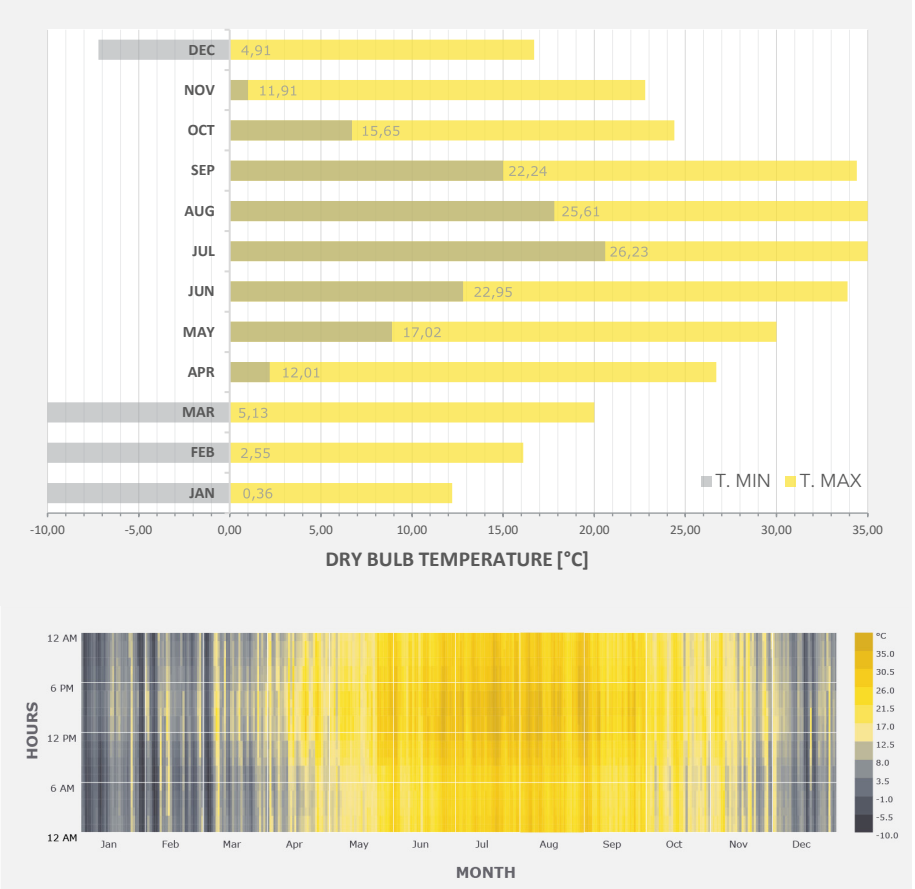

Fig. 164 Dry Bulb Temperature [°C], hourly data (Weather Station: New York LaGuardia AP_NY_USA; Period:1 JAN 1:00 - 31 DEC 24:00).

Relative Humidity

The relative humidity is the ratio of the current absolute humidity to the highest possible absolute humidity (which depends on the current air temperature). A reading of 100 percent relative humidity means that the air is saturated with water vapor and cannot hold anymore, creating the possibility of rain.

Relative Humidity is very important in human perception of outdoor weather. The process of sweating is the body's attempt to keep cool and maintain its current temperature. If the air's RH is equal to 100%, sweat will not evaporate into the air. As a result, humans feel much hotter than the actual temperature when RH is high. Conversely, if the relative humidity is low, the feeling is colder than the actual temperature because our sweat evaporates easily, cooling us off. For instance, if the air temperature is 24°C and the relative humidity is 0%, the air temperature feels like 21°C to our bodies; while, if the relative humidity is 100%, human perception ranges around 27°C. People usually feel more comfortable at a relative humidity of between 30% and 50%.

The graph on the right shows the relative humidity values in percentage (on the vertical axis) yearly and months are highlighted on the horizontal axis. Values have been obtained hour by hour for all the days of each month (24 RH values for each day), then averaged daily and finally plotted together in the chart.From the graph, it is possible to understand the general trend of relative humidity around the year. The lowest peak is reached in March (22%), while the highest one in May (94%). The months that have more days where RH is in the comfort range (30%-50%) are February (average RH 50%), followed by December (average RH 55%), January (average RH 56%), and July (average RH 58%)

Conversely, the months which are presenting fewer days in the comfort range are May and October (average monthly RH respectively equal to 69% and 64%). It is also interesting to notice that the other summer months (June, August, and September) generally present fewer values of RH belonging to the comfort range compared with winter ones since values are generally higher than 50%.

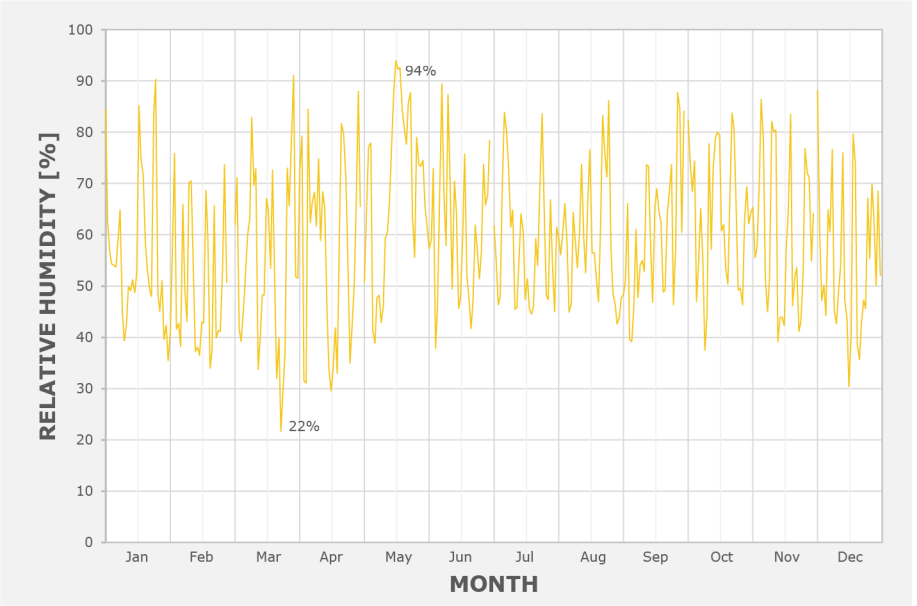

Fig. 165 Relative Humidity [%], daily data. (Weather Station: New York; LaGuardia AP_NY_USA; Period:1 JAN 1:00 - 31 DEC 24:00).

Wind Speed

The image on the top-right is representing the Wind Rose Diagram of the selected site. A "Wind Rose Diagram" is a tool that graphically displays the distribution of wind speeds and wind directions over a period of time. The diagrams comprise 16 radiating spokes, which represent wind directions in terms of the cardinal wind directions (North East South West) and their intermediate ones. In this case, the rose shows wind directions and the relative wind speeds (in m/s) yearly. The wind speed for the selected direction can be read in the colored legend on the right. Each 'Spoke' indicates how often the wind blows from each direction and how often the wind blows within each pre-defined wind speed range (bins). This is shown by the color bands on each spoke. A wind rose diagram uses a polar coordinate system, whereby data is plotted a certain distance away from the origin at an angle relative to north. By reading the diagram it is possible to understand that the wind is mostly blowing from the S-Direction with an average speed ranging from 3.50 m/s to 10.50 m/s. Instead, the maximum average wind speed was 14.00 m/s from NW direction and, in a minor part from WNW direction.

Considering that wind speed can undergo several hourly variations along the same day, in the following chart the hourly data have been categorized applying the "Beaufort Wind Force Scale" which classify the different types of wind according to their speed (in m/s). It is evident that the biggest sector (35%) belongs to the Gentle Breeze category (from 1.6-3.3 m/s), followed by the Moderate Breeze (5.5-7.9 km/h) and thirdly by the Light Breeze (1.6-3.3 m/s). Strong Breeze/Almost Stormy/Stormy events occurs only the 1% of the hours toward the whole year.

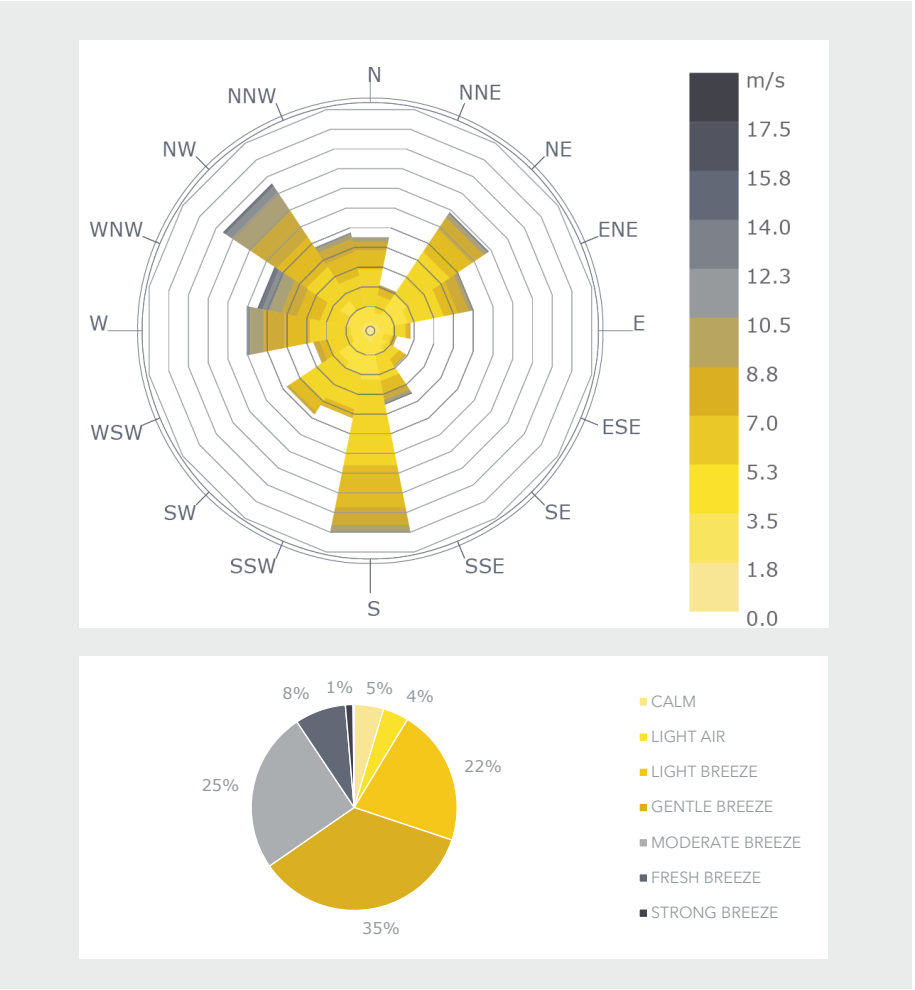

Fig. 166 Wind Rose representing Wind Speed (m/s): calm for 4.59% of the time = 402 hours; each closed polyline shows frequency of 1.3% = 113 hours; (Weather Station: New York; LaGuardia AP_NY_USA; Period:1 JAN 1:00 - 31 DEC 24:00).
Fig. 167 Annual Wind Speeds Classified according to Beaufort Wind Force Scale (Weather Station: New York; LaGuardia AP_NY_USA; Period:1 JAN 1:00 - 31 DEC 24:00).

Global Horizontal Irradiance

The Global Horizontal Irradiance (GHI), in W/m2, is the total irradiance from the sun on a horizontal surface on Earth. It is the sum of direct irradiance and diffuse horizontal irradiance. It is usually calculated using the following formula:

$$GHI = DNI + DHI \times \cos(z)$$

Where:

- DNI is the Direct Normal Irradiance
- DHI is the Diffuse Horizontal Irradiance
- Z is the solar zenith angle of the sun.

The Direct Normal Irradiance is measured at the surface of the Earth at a given location with a surface element perpendicular to the Sun. It excludes diffuse solar radiation (radiation that is scattered or reflected by atmospheric components). Losses depend on time of day (length of light's path through the atmosphere depending on the solar elevation angle), cloud cover, moisture content and other contents. The irradiance above the atmosphere also varies with time of year (because the distance to the sun varies), although this effect is generally less significant compared to the effect of losses on DNI. Conversely, the Diffuse Sky Radiation is the radiation at the Earth's surface from light scattered by the atmosphere. It is measured on a horizontal surface with radiation coming from all points in the sky excluding circumsolar radiation (radiation coming from the sun disk).

Looking at the Radiation Rose it can be seen that most of the radiation (mostly consisting of the Direct component) comes from the South-West. This data can be very useful to the designer with regard to the analysis of the "solar benefits", which will then take care to place solar panels / photovoltaic roofs or facades exposed in this direction, or to place on this side the rooms that might need more light and heat. On the contrary, the North-facing side will be the one that will be less affected by the direct component of solar radiation, being able to count on almost a quarter of the amount of radiation of the South orientation.

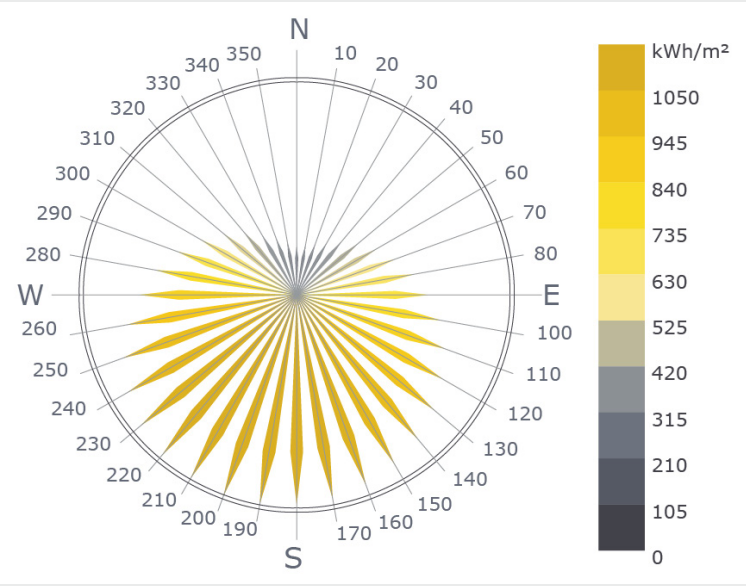

Fig. 168 Radiation Rose representing Solar Radiation for selected location, yearly data (Weather Station: New York; LaGuardia AP_NY_USA; Period:1 JAN 1:00 - 31 DEC 24:00).

References

[1] E. M. Fischer and C. Schär, "Consistent geographical patterns of changes in high-impact European heatwaves," Nat. Geosci., vol. 3, no. 6, pp. 398–403, 2010, doi: 10.1038/ngeo866.

[2] T. C. M. de Nijs, R. de Niet, and L. Crommentuijn, "Constructing land-use maps of the Netherlands in 2030," J. Environ. Manage., vol. 72, no. 1–2, pp. 35–42, 2004, doi: 10.1016/j.jenvman.2004.03.015.

[3] "the-average-summer-season-intensity @ www.eea.europa.eu." [Online]. Available: https://www.eea.europa.eu/data-and-maps/figures/the-average-summer-season-intensity.

[4] "urban-heat-islands @ www.usgs.gov." [Online]. Available: https://www.usgs.gov/media/images/urban-heat-islands.

[5] L. W. A. van Hove, C. M. J. Jacobs, B. G. Heusinkveld, J. A. Elbers, B. L. Van Driel, and A. A. M. Holtslag, "Temporal and spatial variability of urban heat island and thermal comfort within the Rotterdam agglomeration," Build. Environ., vol. 83, pp. 91–103, 2015, doi: 10.1016/j.buildenv.2014.08.029.

[6] T. R. Oke, "The energetic basis of the urban heat island," Q. J. R. Meteorol. Soc., vol. 108, no. 455, pp. 1–24, 1982, doi: https://doi.org/10.1002/qj.49710845502.

[7] J. A. Voogt and T. R. Oke, "Thermal remote sensing of urban climates," Remote Sens. Environ., vol. 86, no. 3, pp. 370–384, 2003, doi: https://doi.org/10.1016/S0034-4257(03)00079-8.

[8] A. M. RIZWAN, L. Y. C. DENNIS, and C. LIU, "A review on the generation, determination and mitigation of Urban Heat Island," J. Environ. Sci., vol. 20, no. 1, pp. 120–128, 2008, doi: https://doi.org/10.1016/S1001-0742(08)60019-4.

[9] I. D. Stewart and T. R. Oke, "Local climate zones for urban temperature studies," Bull. Am. Meteorol. Soc., vol. 93, no. 12, pp. 1879–1900, 2012, doi: 10.1175/BAMS-D-11-00019.1.

[10] K. E. Trenberth, "Climate and Climate Change: Intergovernmental Panel on Climate Change," Encycl. Atmos. Sci. Second Ed., pp. 90–94, 2015, doi: 10.1016/B978-0-12-382225-3.00492-8.

[11] D. Scherer and W. Endlicher, "Editorial: Urban climate and heat stress - Part 1," Erde, vol. 144, no. 3–4, pp. 175–180, 2013, doi: 10.12854/erde-144-13.

[12] K. M. A. Gabriel and W. R. Endlicher, "Urban and rural mortality rates during heat waves in Berlin and Brandenburg, Germany," Environ. Pollut., vol. 159, no. 8, pp. 2044–2050, 2011, doi: https://doi.org/10.1016/j.envpol.2011.01.016.

[13] R. S. Kovats and S. Hajat, "Heat stress and public health: A critical review," Annu. Rev. Public Health, vol. 29, pp. 41–55, 2008, doi: 10.1146/annurev.publhealth.29.020907.090843.

[14] A. J. Arnfield, "Two decades of urban climate research: A review of turbulence, exchanges of energy and water, and the urban heat island," Int. J. Climatol., vol. 23, no. 1, pp. 1–26, 2003, doi: 10.1002/joc.859.

[15] P. Höppe, "Different aspects of assessing indoor and outdoor thermal comfort," Energy Build., vol. 34, no. 6, pp. 661–665, 2002, doi: 10.1016/S0378-7788(02)00017-8.

[16] C. Ketterer and A. Matzarakis, "Urban Climate Human-bio-meteorological assessment of the urban heat island in a city with complex

topography – The case of Stuttgart , Germany," vol. 10, pp. 573–575, 2014.

[17] "temperature-download3-2016 @ www.epa.gov." [Online]. Available: https://www.epa.gov/sites/production/files/2016-10/temperature-download3-2016.png.

[18] J. C. Caro, T. Armour, M. Fernandez, T. Armour, and M. Fernandez, "Madrid + Natural."

[19] B. Givoni, "Climate considerations in building and urban design," 1998.

[20] V. Cheng, K. Steemers, M. Montavon, and R. Compagnon, "Urban form, density and solar potential," PLEA 2006 - 23rd Int. Conf. Passiv. Low Energy Archit. Conf. Proc., no. January, 2006.

[21] S. Berkovic, A. Yezioro, and A. Bitan, "Study of thermal comfort in courtyards in a hot arid climate," Sol. Energy, vol. 86, no. 5, pp. 1173–1186, 2012, doi: 10.1016/j.solener.2012.01.010.

[22] S. Thorsson, F. Lindberg, J. Björklund, B. Holmer, and D. Rayner, "Potential changes in outdoor thermal comfort conditions in Gothenburg, Sweden due to climate change: The influence of urban geometry," Int. J. Climatol., vol. 31, no. 2, pp. 324–335, 2011, doi: 10.1002/joc.2231.

[23] M. Pijpers-van Esch, R. Looman, and G. Hordijk, "The effects of urban and building design parameters on solar access to the urban canyon and the potential for direct passive solar heating strategies," Energy Build., vol. 47, pp. 189–200, 2012, doi: 10.1016/j.enbuild.2011.11.042.

[24] M. Taleghani, L. Kleerekoper, M. Tenpierik, and A. Van Den Dobbelsteen, "Outdoor thermal comfort within five different urban forms in the Netherlands," Build. Environ., vol. 83, pp. 65–78, 2015, doi: 10.1016/j.buildenv.2014.03.014.

[25] T.-P. Lin, "Thermal perception, adaptation and attendance in a public square in hot and humid regions," Build. Environ., vol. 44, no. 10, pp. 2017–2026, 2009, doi: https://doi.org/10.1016/j.buildenv.2009.02.004.

[26] M. Nikolopoulou and S. Lykoudis, "Thermal comfort in outdoor urban spaces: Analysis across different European countries," Build. Environ., vol. 41, no. 11, pp. 1455–1470, 2006, doi: https://doi.org/10.1016/j.buildenv.2005.05.031.

[27] L. Chen and E. Ng, "Outdoor thermal comfort and outdoor activities: A review of research in the past decade," Cities, vol. 29, no. 2, pp. 118–125, 2012, doi: https://doi.org/10.1016/j.cities.2011.08.006.

[28] R. F. Goldman, "Assessment of Thermal Comfort," ASHRAE Trans., vol. 84, no. 1, pp. 1–6, 1978.

[29] J. Pickup and R. D. Dear, "an Outdoor Thermal Comfort Index (Out-Set*) -Part I –the Model and Its Assumptions," 15th ICB ICUC, no. January 1999, pp. 1–7, 2000, [Online]. Available: https://www.researchgate.net/publication/268983313.

[30] K. Blazejczyk and B. Krawczyk, "The influence of climatic conditions on the heat balance of the human body," Int. J. Biometeorol., vol. 35, pp. 103–106, 1991, doi: 10.1007/BF01087485.

[31] P. Höppe, "The physiological equivalent temperature – a universal index for the biometeorological assessment of the thermal environment," Int. J. Biometeorol., vol. 43, no. 2, pp. 71–75, 1999, doi: 10.1007/s004840050118.

[32] N. A. Kenny, J. S. Warland, R. D. Brown, and T. G. Gillespie, "Part A: Assessing the performance of the COMFA outdoor thermal comfort model on subjects performing physical activity," Int. J. Biometeorol., vol. 53, no. 5, p. 415, 2009, doi: 10.1007/s00484-009-0226-3.

[33] P. Bröde, G. Jendritzky, D. Fiala, and G. Havenith, "The universal thermal climate index UTCI in operational use," Proc. Conf. Adapt. to Chang. New Think. Comf. Wind. 2010, no. April, pp. 9–11, 2010.

[34] G. Jendritzky, A. Maarouf, and H. Staiger, "Looking for a universal thermal climate index UTCI for outdoor applications," no. January 2001, pp. 353–367, 2015.

[35] K. J. K. Buettner, "Physical Aspects of Human Bioclimatology," in Compendium of Meteorology: Prepared under the Direction of the Committee on the Compendium of Meteorology, T. F. Malone, Ed. Boston, MA: American Meteorological Society, 1951, pp. 1112–1125.

[36] G. Jendritzky, G. Havenith, P. Weihs, E. Batchvarova, and R. DeDear, "The Universal Thermal Climate Index UTCI Goal and State of COST Action 730," Environ. Ergon. XII2, no. 1, pp. 509–512, 2007.

[37] P. Bröde, E. L. Krüger, and F. A. Rossi, "Assessment of Urban Outdoor Thermal Comfort By the Universal Thermal Climate Index UTCI," XIV Int. Conf. Environ. Ergon. Stylianos Kounalakis Maria Koskolou (Eds), Greece 2011, no. 2003, 2011.

[38] K. Błazejczyk et al., "An introduction to the Universal thermal climate index (UTCI)," Geogr. Pol., vol. 86, no. 1, pp. 5–10, 2013, doi: 10.7163/GPol.2013.1.

Web Sources

[1] "8efda62e48d3d62b41f81b1792fc2896276a3ba0 @ hydrashare.github.io." [Online]. Available: https://hydrashare.github.io/hydra/?keywords=microclimate.

[2] "index @ grasshopperdocs.com." [Online]. Available: http://grasshopperdocs.com/.

[3] "solar-radiation-absorbed-materials-d_1568 @ www.engineeringtoolbox.com." [Online]. Available: https://www.engineeringtoolbox.com/solar-radiation-absorbed-materials-d_1568.html.

[4] "utci_doku @ www.utci.org." [Online]. Available: http://www.utci.org/utci_doku.php.

[5] "urban-heat-can-white-roofs-help-cool-the-worlds-warming-cities @ e360.yale.edu." [Online]. Available: https://e360.yale.edu/features/urban-heat-can-white-roofs-help-cool-the-worlds-warming-cities.

[6] "what-is-a-biosolar-roof-and-how-could-it-change-city-living-b2c71215d646 @ medium.com." [Online]. Available: https://medium.com/@green_wood/what-is-a-biosolar-roof-and-how-could-it-change-city-living-b2c71215d646.

[7] "nyc-coolroofs @ www1.nyc.gov." [Online]. Available: https://www1.nyc.gov/nycbusiness/article/nyc-coolroofs.

[8] "the-crown-estate-ecology-masterplan @ www.arup.com." [Online]. Available: https://www.arup.com/projects/the-crown-estate-ecology-masterplan.

[9] "article @ task63.iea-shc.org." [Online]. Available: https://task63.iea-shc.org/article?NewsID=341.

[10] "2764bbac87b81f81fddb54cc3a9a69db2c3121d7 @ www.berlin.de." [Online]. Available: https://www.berlin.de/sen/uvk/en/nature-and-green/landscape-planning/baf-biotope-area-factor/.

[11] "5202 @ csis.myclimateservice.eu." [Online]. Available: https://csis.myclimateservice.eu/node/5202.

[12] "new-york-city-painted-6-million-square-feet-of-rooftop-white-2018-8 @ www.businessinsider.com." [Online]. Available: https://www.businessinsider.com/new-york-city-painted-6-million-square-feet-of-rooftop-white-2018-8?IR=T.

[13] "sustainable-design @ www1.nyc.gov." [Online]. Available: https://www1.nyc.gov/site/ddc/about/sustainable-design.page.

[14] "the-average-summer-season-intensity @ www.eea.europa.eu." [Online]. Available: https://www.eea.europa.eu/data-and-maps/figures/the-average-summer-season-intensity.